Electronic Thesis and Dissertation Repository

4-29-2014 12:00 AM

Physical Sulphate Attack on Concrete

Ahmed Ramadan Suleiman
The University of Western Ontario

Supervisor
Moncef Nehdi
The University of Western Ontario

Graduate Program in Civil and Environmental Engineering
A thesis submitted in partial fulfillment of the requirements for the degree in Master of
Engineering Science
© Ahmed Ramadan Suleiman 2014

Follow this and additional works at: https://ir.lib.uwo.ca/etd

Part of the Civil Engineering Commons, and the Structural Engineering Commons

PHYSICAL SULPHATE ATTACK ON CONRETE

(Thesis format: Integrated Article)

by

Ahmed Ramadan <u>Suleiman</u>

Graduate Program in Engineering
Department of Civil and Environmental Engineering

A thesis submitted in partial fulfillment
of the requirements for the degree of
Master of Science

The School of Graduate and Postdoctoral Studies
Western University
London, Ontario, Canada

ABSTRACT

Field experience with concrete exposed to sulphates has often shown that concrete can suffer from surface scaling above the ground level caused by physical sulphate attack. This type of attack has been ignored and, in some instances, confused with chemical sulphate attack. In addition, current standards that evaluate the performance of concrete under sulphate attack, only deal with the chemical aspects of sulphate attack. This lack of information has led to confusion and contradictory views regarding the mechanisms of concrete deterioration due to physical sulphate attack.

In the current thesis, the performance of concrete exposed to environments prone to physical sulphate attack was investigated. The effects of mineral additives, water-to binder (w/b) ratio, along with various curing conditions on the performance of concrete exposed to physical sulphate attack was studied. In addition, the effectiveness of different surface treatment materials in mitigating physical sulphate attack on concrete was explored.

Results show that concrete can experience dual sulphate attack. The lower immersed portion can suffer from chemical sulphate attack, while the upper portion can be vulnerable to physical attack. Lowering the w/b ratio and moist-curing the concrete reduced surface scaling above the solution level since the volume of pores was decreased. Although partial replacement of cement with pozzolans also decreased the pore volume, surface scaling increased due to the increased proportion of small diameter pores and the associated growth of capillary suction and surface area for evaporation.

Epoxy- and silane-based surface treatment materials were found to be adequate for protecting both cured and non-cured concrete exposed to physical sulphate attack. However, it was found that adequate curing of the concrete before coating is important to eliminate the separation of the surface treatment based on bitumen and to enhance the resistance of concrete to physical sulphate attack. Using a water-based solid acrylic polymer resin did not provide adequate protection of concrete against physical sulphate attack.

Keywords: *Surface; Physical; Sulphate attack; Capillary; Pore; Structure; Treatment; Crystallization; Chemical, Pozzolans.*

Co-Authorship Statement

This thesis has been prepared in accordance with the regulation of integrated-article format stipulated by the Faculty of Graduate Studies at Western University. Substantial parts of this thesis have been submitted for publication to peer-reviewed technical journals. All experimental work, data analysis, and writing of the initial versions of publications listed below were carried out by the candidate. The research advisor and any other co-author provided guidance and supervision, and helped in the development of the final versions of publications:

1- Suleiman, A. R., Soliman, A., and Nehdi, M. "Investigation of concrete exposed to dual sulphate attack." *Cement and Concrete Research*, Under review.

2- Suleiman, A. R., Soliman, A., and Nehdi, M. "Effect of surface treatment materials on durability of concrete exposed to physical sulphate attack.", *ACI Materials Journal,* Under review.

3- Suleiman, A. R., Soliman, A., and Nehdi, M. "Effect of supplementary cementitious materilas on durability of concrete exposed to physical sulphate attack." To be submitted for peer review.

To: My Beloved Mother Naima,

My Father Ramadan,

My Beloved Sisters Sondos, and Lujain

and My Brother Tarik.

ACKNOWLEDGMENTS

TABLE OF CONTENTS

LIST OF TABLES

LIST OF FIGURES

NOTATIONS

ASTM	American Society for Testing and Materials
ACI	American Concrete Institute
C	Existing solute concentration
C_S	The saturation concentration
CSA	Canadian Standards Association
dV	Increase of crystal volume
EN	European Standards
ESEM	Environmental Scanning Electron Microscopy
FA	Fly Ash
HS	High Sulphate resistance cement
k_{CL}^{E}	Curvature of the crystal end (hemispherical)
k_{CL}^{S}	Curvature of the cylindrical side
Mi	Initial mass of the cylinder
MIP	Mercury intrusion porosimtry
Mt	Mass of the cylinder at time
OPC	Ordinary Portland Cement
P	Pressure exerted by growing crystals
P_l	Pressure in the liquid
P_S	Pressure in the solid (in atmospheres)
Q^{E}	Solubility product
Q^{S}	Lower solubility product

R	Gas constant
r_e	Radius of the pore small entries
RH	Relative Humidity
r_l	Radius of the large pore
r_p	Radius of the pore
r_s	Radius of the small pore
SF	Silica Fume
$\grave{T}$	Absolute temperature
(t)	Time
V_S	Molar volume of solid salt
XRD	X-Ray Diffraction
δ	Solution film thickness between the crystal and the pore wall
σ	Interfacial tension between the crystal face and its saturated solution
σdA	The increase of crystal surface area
M_i	Initial mass of cylinder
M_t	Mass of cylinder at time t

CHAPTER ONE

INTRODUCTION

1.1   Background

Since the 19th century, stone deterioration in historical monuments due to salt crystallization has been a subject of investigation (Goudie and Viles, 1997). Several studies have investigated the related deterioration mechanisms and how such a problem can be mitigated, since it is considered as a major threat to historical monuments and building stones.

However, concrete deterioration due to salt crystallization, or the so called physical sulphate attack on concrete, has been ignored and confused in some occasions with chemical sulphate attack (Haynes *et al.*, 1996; Haynes *et al.*, 2008; Mehta, 2000). According to Scherer (2004), concrete can be vulnerable to damage when salt crystals grow from a supersaturated solution in its pores. This process was described as physical attack on concrete since, unlike chemical sulphate attack, it does not involve any chemical interaction between the sulphate ions and the concrete hydration products (Haynes *et al.,* 1996).

Moreover, the consequences of physical sulphate attack are different from those of chemical sulphate attack since it leads to surface degradation similar to that caused by cycles of freezing and thawing, while chemical sulphate attack results in expansion and cracks due to the formation of ettringite ($Ca_6Al_2(SO_4)_3(OH)_{12} \cdot 26H_2O$) and gypsum ($CaSO_4 \cdot 2H_2O$) (Mehta, 2000). Using the "sulphate attack" terminology in-situ to describe concrete deterioration due to sulphates may lead to confusion between physical and chemical attack (Haynes *et al.*, 1996).

Field experience regarding concrete exposed to sulphates has shown that concrete often suffers from surface scaling caused by physical sulphate attack, which is limited to the above-ground portion, while the portion embedded in sulphate rich

soil (exposed to chemical sulphate attack) has mostly been found in intact condition (Yoshida *et al.,* 2010; Stark, 1989; Irassar *et al.*, 1995). The damaging process involves capillary rise and evaporation of ground water containing sulphates at the above ground concrete surface, resulting in crystal growth in concrete pores and damage (Irassar *et al.*, 1995; Haynes *et al.*, 1996).

Nevertheless, current standards that evaluate the performance of concrete under sulphate attack, such as ASTM C1012 (Standard Test Method for Length Change of Hydraulic-Cement Mortars Exposed to a Sulphate Solution), only cover the chemical aspects of sulphate attack and ignore physical attack, since it evaluates the concrete performance when it is fully immersed in a sulphate solution (Aye and Oguchi, 2011; Santhanam *et al.,* 2001). This may serve to more confusion in assessing the deterioration of concrete due to sulphates under field exposure.

Previous studies have shown that adding pozzolanic minerals to concrete had significantly improved its durability under chemical sulphate attack (Al-Amoudi, 2002; Hooton, 1993; Al-Akhras, 2006; Nehdi and Hayek, 2005). Indeed, pozzolanic minerals reduce the porosity in concrete and consume calcium hydroxide, which is a cement hydration product that is vulnerable to chemical sulphate attack. Moreover, reducing the w/c ratio improves the concrete durability to sulphate exposure since it decreases the volume of voids in the hydrated cementitous matrix and limits sulphates penetration into concrete (Mehta and Monteiro, 2006).

However, the general lack of information in the open literature and limitations of current standards regarding physical sulphate attack on concrete have led to contradictory views. For instance, some researchers have suggested that low w/c ratio concrete with fine pores may become more vulnerable to damage by physical sulphate attack since the small pores can be disrupted before the larger pores by salt crystal growth (Hime, 2003; Haynes and Bassuoni, 2011). Conversely, other experimental studies have shown that lowering the w/c ratio of concrete exposed to physical sulphate attack enhanced its durability (Yoshida *et al*., 2010; Hartell *et al*., 2011).

Furthermore, Aye and Oguchi (2011) reported higher surface scaling damage in blended cement mortars having small pore sizes than that for the control plain cement mortar. Thus, it is argued that from the limited available literature, the role of

the w/c ratio and pozzolanic minerals in concrete exposed to physical sulphate attack is still controversial.

Regarding the performance of stones under physical salt attack, several studies have shown that the vulnerability of stones to damage depends on their pore structure (Angeli *et al.,* 2008; Scherer, 2004; Buj and Gisbert, 2010). For instance, stones that include high percentages of micro-pores connected with larger pores are the most vulnerable to damage by salt crystallization (Wellman and Wilson, 1965; Angeli *et al.,* 2008; Navarro and Doehne, 1999). The presence of micro-pores increases the capillary rise and the surface area of the evaporation, leading to high supersaturation of the pore solution and subsequent damage (Navarro and Doehne, 1999). Hence, pore connectivity seems to be an important factor for the deterioration of stones due to physical salt attack.

Buj and Gisbert (2010) tested fifteen samples of stones that are similar to those commonly used in the cultural and architectural heritage. They found that stones with low porosity and high amount of small pores with low connectivity are less vulnerable to damage than stones with high porosity and higher average pore radius. Thus, the previous suggestion regarding the poor performance of concrete with low w/c ratio under physical sulphate attack is questionable.

1.2   Research Objectives

Despite the current knowledge and specifications on concrete deterioration due to sulphate attack, there is only limited information and studies regarding the damage of concrete due to physical sulphate attack. According to Haynes *et al.* (2008), in certain environmental conditions, physical sulphate attack can cause serious damage to concrete. This was reported in several field investigations for concrete structures in partial contact with sulphates. For instance, in southern California, Novak and Colville (1989) investigated the causes of damage in concrete floor slabs of 20-30 year-old homes located on sulphate rich soil. They proposed that damage was mainly due to salt crystallization since none of the chemical sulphate products such as ettringite and gypsum were identified, yet salt minerals such as thenardite (Na_2SO_4) and mirabilite ($Na_2SO_4.10H_2O$) were found within the cracks.

Another field study by Stark (1989) showed extensive damage that was limited to the upper portions of concrete beam specimens half embedded in sulphate rich soil, whereas the portion embedded in soil was found in intact condition. Similar cases of deterioration were reported in other places including the Arabian Gulf region, Japan, and Australia (Al-Amoudi, 2002; Yoshida *et al.,* 2010; Hime *et al.,* 2001). Since there is lack of information on the behaviour of concrete under physical sulphate attack in the open literature, the main scope of the present thesis is to investigate the effects of various parameters that influence the performance of concrete exposed to physical sulphate attack.

1.3   Original Contributions

This research investigates the behaviour of concrete exposed to environments prone to physical sulphate attack. It explores several factors that could improve the durability design of concrete in sulphate laden environments. Specific original contributions of the current thesis include:

1- Studying the effects of the concrete pore structure on the durability of concrete under physical sulphate attack, since previous studies have shown that the vulnerability of stones exposed to salt weathering depended on their pore structure.

2- Evaluating the effectiveness of coating the concrete surface with different types of treatment materials when exposed to physical sulphate attack, since the durability of coated concrete has been mainly studied under chemical sulphate attack.

3- Investigating the impact of using supplementary cementing materials in concrete exposed to physical sulphate attack since previous studies have shown that using supplementary cementing materials can improve the overall performance of concrete, particularly under chemical sulphate attack.

1.4   Thesis Structure

The present thesis has been structured and organized according to the guidelines of the Faculty of Graduate Studies at Western University. It includes seven chapters that focus on the performance of concrete under physical sulphate attack.

Chapter two provides a state-of-art review of the existing knowledge on concrete deterioration due to physical sulphate attack. Previous field and laboratory investigations have been reviewed and discussed. In addition, previous theories regarding crystallization within porous materials have been briefly presented.

Chapters three and four focus on the behaviour of concrete partially immersed in sulphate solutions and exposed to cyclic temperature and relative humidity. The mechanisms of damage above and below the solution level have been investigated. In addition, several factors that affect the concrete pore structure including mineral additives, w/b ratio along with various curing conditions have been examined under physical sulphate attack.

Chapter five explores the effects of using different types of surface treatment materials that may mitigate the surface deterioration of concrete due to physical sulphate attack. Different types of commercially available surface treatment materials have been evaluated under environments prone to physical sulphate attack.

Chapter six examines the effects of using different types and percentages of supplementary commentating materials on concrete partially immersed in a sulphate solution.

Finally, general and specific conclusions drawn from the research study along with recommendations for future research have been included in Chapter seven.

1.5 References

Al-Amoudi, O. S. B., (2002), "Attack on plain and blended cement exposed to aggressive sulfate environment", *Cement and Concrete Composites*, Vol. 24, No. 3, pp. 305-316.

Al-Akhras, N. M., (2006), "Durability of metakaolin concrete to sulfate attack" *Cement and Concrete Research*, Vol. 36, No. 9, pp. 1727-1734.

Angeli, M., Benavente, D., Bigas, J., Menendez, B., Hebert, R., David, C., (2008), "Modification of the porous network by salt crystallization in experimentally weathered sedimentary stones", *Materials and Structures*, Vol. 41, No. 6, pp. 1091-1108.

ASTM C1012 (2012), "Standard Test Method for Length Change of Hydraulic-Cement Mortars Exposed to a Sulfate Solution", *American Society for Testing and Materials*, West Conshohocken, PA.

Aye, T., Oguchi, C. T., (2011), "Resistance of plain and blended cement mortars exposed to severe sulfate attacks", *Construction and Building Materials*, Vol. 25, No. 6, pp. 2988-2996.

Buj, O., and Gisbert, J., (2010), "Influence of pore morphology on the durability of sedimentary building stones from Aragon (Spain) subjected to standard salt decay tests", *Environment Health Sicence*, Vol. 61, No. 7, pp. 1327-1336.

Flatt, R. J., (2002), "Salt damage in porous materials: how high supersaturations are generated", *Journal of Crystal Growth*, Vol. 242, No. 3-4, pp. 435-454.

Goudie, A., and Viles, H., (1997), Salt Weathering Hazards, *John Wiley & Sons*, England, 241 p.

Hartell, J. A., Boyd, A. J., and Ferraro, C. C., (2011), "Sulfate attack on concrete: Effect of partial immersion", *Journal of Materials in Civil Engineering*, Vol. 23, No. 5, pp. 572-579.

Haynes, H., O'Neill, R., and Mehta, P. K. (1996), "Concrete deterioration from physical attack by salts", *Concrete International*, Vol. 18, No. 1, pp. 63-68.

Haynes, H., O'Neill, R., Neff, M. and Mehta, P. K. (2008), "Salt weathering distress on concrete exposed to sodium sulfate environment", *ACI Materials Journal*, Vol. 105, No. 1, pp. 35-43.

Haynes, H., and Bassuoni, M. T., (2011), "Physical salt attack on concrete", *Concrete International*, Vol. 33, No. 11, pp. 38– 42.

Hime, W. G., (2003), "Chemists should be studying chemical attack on concrete", *Concrete International*, Vol. 25, No. 4, pp. 82-84.

Hooton, R. D. (1993) " Influence of silica fume replacement of cement on physical properties and resistance of sulfate attack, freezing and thawing, and alkali-silica reactivity" ,*ACI Materials Journal*, Vol. 90, No. 2, pp. 143-151.

Irassar, E. F., Di Maio, A., and Batic, O. R., (1995), "Sulfate attack on concrete with mineral admixtures", *Cement and Concrete Research*, Vol. 26, No. 1, pp. 113-123.

Mehta, P. K., (2000), "Sulfate attack on concrete: Separating myths from reality", *Concrete International*, Vol. 22, No. 8, pp. 57-61.

Mehta, P. K., and Monteiro, P. J. M., (2006), "Concrete microstructure, properties, and materials", *The McGraw-Hill*, Third edition, 659 p.

Navarroa, C. R., and Doehnea, E., (1999), "Salt weathering: Influence of evaporation rate, supersaturation, and crystallization pattern", *Earth Surface Processes and Landforms*, Vol. 24, No. 3, pp. 191-209.

Nehdi, M., and Hayek, M., (2005), "Behavior of blended cement mortars exposed to sulfate solutions cycling in relative humidity", *Cement and Concrete Research*, Vol. 35, No. 4, pp. 731-742.

Novak, G. K., and Colville, A. A., (1989), "Efflorescent mineral assemblages associated with cracked and degraded residential concrete foundations in southern California", *Cement and Concrete Research*, Vol. 19, No. 1, pp. 1-6.

Santhanam, M., Cohen, MD., Olek, J., (2001), "Sulfate attack research − whither now?" *Cement and Concrete Research*, Vol. 31, No. 6, pp. 845-51.

Scherer, G. W., (2004), "Stress from crystallization of salt", *Cement and Concrete Research*, Vol. 34, No. 9, pp.1613– 1624.

Stark, D., (1989), "Durability of concrete in sulfate-rich soils", *Research and Development Bulletin, Portland Cement Association*, Vol. RD097.

Thaulow, N., Sahu, S., (2004), "Mechanism of concrete deterioration due to salt crystallization", *Materials Characterization*, Vol. 53, No. 2-4, pp. 123-127.

Yoshida, N., Matsunami, Y., Nagayama, M., and Sakai, E., (2010), "Salt weathering in residential concrete foundation exposed to sulfate-bearing ground", J*ournal of Advanced Concrete Technology*, Vol. 8, No. 2, pp. 121-134.

CHAPTER TWO

LITERATURE REVIEW

2.1 Introduction

Chemical sulphate attack on concrete structures has been considered as the predominant deterioration mechanism of concrete exposed to sulphate rich environments. However, under certain environmental conditions, concrete was found to suffer mainly from physical sulphate attack, which was generally ignored in the literature. This lack of information has led to contradictory views and confusion regarding the deterioration of concrete due to physical sulphate attack. According to Mehta (2000), cases of concrete damage due to physical sulphate attack have been confused with chemical sulphate attack. For instance, for the case of concrete damaged by salt weathering, a number of researchers supported the separation of physical sulphate attack from chemical attack. They argued that salt weathering is a purely physical phenomenon, which has the same appearance as surface scaling caused by cycles of freezing and thawing (Haynes *et al.*, 1996; Mehta; 2000).

Moreover, the consequences of physical sulphate attack are different from those of chemical attack (Neville, 2004). Physical attack mainly induces surface scaling in the concrete above the ground level, while chemical sulphate attack generally involves chemical interactions between the sulphate ions and the cement paste components, leading to loss of adhesion of the cement hydration products and formation of ettringite, gypsum, and/or softening due to the formation of thaumasite (Mehta, 2000). Conversely, Skalny *et al. (*2000; and 2002) suggested that complete separation of physical and chemical sulphate attack is probably a wrong assumption and serves to more confusion. They also criticized the idea of characterizing the repeated expansion and contraction by the term physical. Hence, they suggested that the main process is hydration and dehydration of sodium sulphate, similar to ettringite or gypsum formation, which is a physicochemical process.

In this chapter, a state-of-the-art review of the existing knowledge on concrete deterioration due to physical sulphate attack is presented. Previous field and laboratory investigations regarding the deterioration of concrete due to physical sulphate attack are also highlighted.

2.2   Sources of Sulphates

According to Skalny *et al.* (2002), there is more than one source of salt weathering or sulphate attack on concrete structures. These include sulphates from natural sources that are either present in soils or dissolved in ground water. For instance, sulphates those originate from agricultural waste-water are chemically aggressive (e.g. ammonium sulphates that enter the ground-water after it had been used as fertilizer) (Skalny *et al.*, 2002). The coal and metallurgical industry are considered to be another source of sulphates (Skalny *et al.*, 2002). Also, atmospheric pollution may lead to increased sulphate concentration in the soil and ground-water (Skalny *et al.*, 2002; Goudie and Viles, 1997).

2.3   Mechanisms of Physical Sulphate Attack

There is more than one theory proposed to identify the mechanism of concrete deterioration due to physical sulphate attack: (1) Solid volume change, (2) Salt hydration distress, and (3) Crystallization pressure (Thaulow and Sahu, 2004).

2.4   Solid Volume Change Theory

This theory proposes that concrete damage is a result of an increase in the salt volume. For instance, sodium sulphate can increase by 314% in volume when anhydrous sodium sulphate (Na_2SO_4, thenardite) transforms to the hydrous form ($Na_2SO_4.10H_2O$, mirabilite) as shown in **Equations 2.1** and **2.2** (Scherer, 2004, Thaulow and Sahu, 2004, and Skalny *et al.*, 2002). When it occurs, this process leads to fatigue and loss of cohesiveness of the cement paste within a concrete matrix (Skalny *et al.*, 2002).

$$2Na^+ + SO_4{}^{2-} \xrightarrow{\hspace{3cm}} Na_2SO_4.10H_2O \qquad (2.1)$$

Solution   Evaporation   Solid

$$Na_2SO_4.10H_2O \xleftarrow{\hspace{3cm}} Na_2SO_4 \qquad (2.2)$$

Mirabilite   Repeated recrystallization   Thenaride
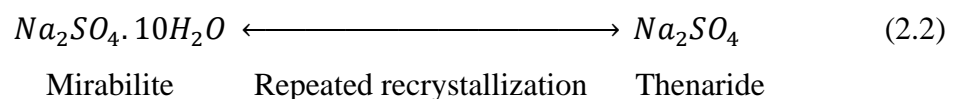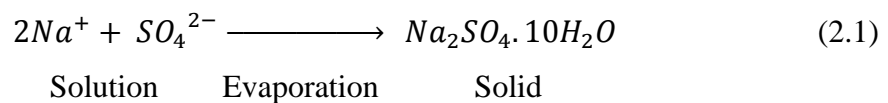
Even though this mechanism seems to be the most accepted theory of concrete damage due to salt crystallization, it ignores the volume of the water in the net calculations (Thaulow and Sahu, 2004). When the volume of water is included in the net volume calculations, the total solid volume decreases (Thaulow and Sahu, 2004). In addition, thenardite does not continually absorb water since it hydrates and expands (Scherer, 2004). Moreover, this theory does not explain the scaling of concrete due to other salts that do not have anhydrous forms (Thaulow and Sahu, 2004).

2.5   Salt Hydration Distress Theory

The salt hydration distress theory defines the deterioration mechanism of concrete exposed to physical salt attack as a result of pressure generated against the concrete pore walls due to the salt hydration process. This mechanism occurs when the concrete surface is exposed to cyclic relative humidity, or when a portion of the concrete is wet while an immediate adjacent portion is relatively dry (Hime *et al*., 2001). Thus, salt undergoes solid-state hydration. However, formation of hydrous or anhydrous salt cannot occur just only by moisture absorbing and hydration (Thaulow and Sahu, 2004). In other words, the salt does not undergo solid-state hydration. Instead, through solution hydration occurs as thenardite dissolves and generates a highly supersaturated solution with respect to mirabilite, which exerts crystallization pressure on the concrete pore walls (Thaulow and Sahu, 2004, Tsui, *et al.* 2004, Folliard and Sandberg, 1994).

2.6   Salt Crystallization Theory

According to Thaulow and Sahu (2004), the salt crystallization pressure theory is the actual mechanism of concrete damage due to salt weathering. In this theory, salt crystals can grow from a supersaturated solution and exert sufficient pressure against the concrete pore walls, thus disrupting the cementitous matrix (Scherer, 2004; Thaulow and Sahu, 2004; Flatt, 2002; Tsui, *et al.* 2004). The process of damage due to salt crystallization is illustrated in **Figure 2.1**.

The supersaturation of a solution depends on several factors including the nature of the salt, the rate of the solution supply, and evaporation (Scherer, 2004). For instance, sodium sulphate is the most damaging salt in nature as it can reach to a very

high supersaturation degree through thenardite dissolution and evaporation (Scherer, 2004; Flatt, 2002; Tsui, *et al.* 2004; Thaulow and Sahu, 2004). Previous study by Scherer (2004) showed damage of stone specimens at the evaporation surface where the sodium sulphate concentration increased and precipitated in the subflorescence zone. In this zone, crystals can grow below the surface of a porous material when the evaporation rate is higher than the rate of water supply by capillary action, thus leading to damage. Such behaviour was observed by Irassar *et al.* (1995) and Stark (1989) where damage was only confined to the drying surface of the concrete partially immersed in sodium sulphate.
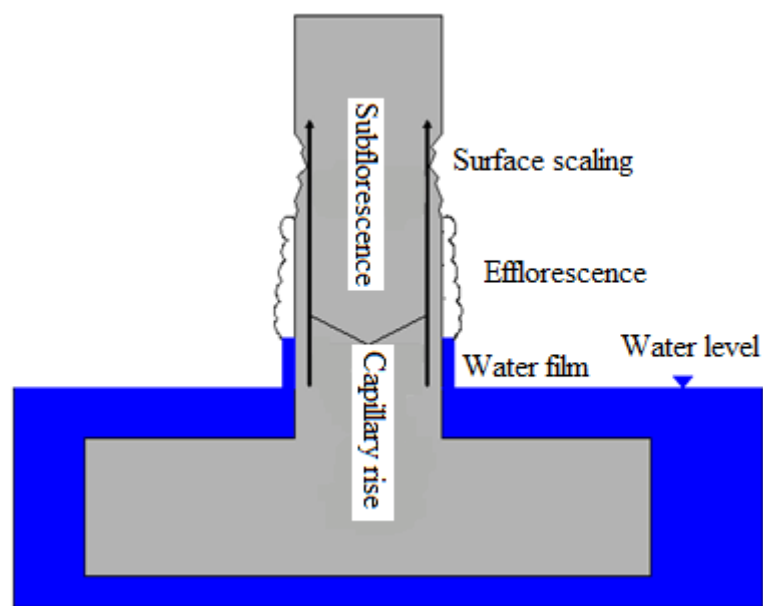
Figure 2.1: Schematic of capillary rise and concrete degradation in a foundation in contact with ground water that contains sodium sulphate.

2.7 Previous Field Investigations

Several previous field investigations have reported concrete deterioration due to physical sulphate attack. For instance, in southern California, Novak and Colville, (1989) investigated the cause of damage in concrete floor slabs of 20-30 year-old homes located on sulphate rich soil using X-Ray diffraction analysis. Salt minerals such as thenardite (Na_2SO_4) and mirabilite ($Na_2SO_4.10H_2O$) were found within the cracks. However, none of the chemical sulphate products such as ettringite and gypsum were identified. Novak and Colville (1989) proposed that the cause of

damage was primarily salt crystallization since none of the chemical sulphate products such as ettringite and gypsum were identified.

In 1989, a field study was conducted by the Portland Cement Association (Stark, 1989) to investigate the performance of concrete beam specimens partially embedded in sulphate rich soil and exposed to cyclic wetting and drying for five years. Extensive damage was only limited to the upper portions of the concrete beam specimens half embedded in the sulphate rich soil, whereas the embedded portion was found in intact condition. In addition, the damage escalated in the beam specimens that were made with a high w/c and when pozzolanic additives such as fly ash and slag were included in the concrete mixtures. Since the investigation was only based on visual inspection of the deteriorated beams, it was concluded that the damage was due to salt crystallization in concrete pores above the ground level.

Similar results were obtained by Irassar *et al.,* (1995) who monitored the performance of concrete cylinders partially buried in a soil containing 1% of sodium sulphate for five years. The performance of concrete was assessed according to several factors including visual inspection, compressive strength, modulus of elasticity, and X-Ray Diffraction (XRD). It was observed that the damage was only limited to the above ground portion of concrete, while the portion buried into the soil was found in intact condition. In addition, they found that using pozzolanic minerals in the concrete mixtures escalated the damage in the upper portion, while it improved the performance of the buried portion into the sulphate soil. Their compressive strength results indicated that the core of the concrete cylinders was in intact condition and the damage was limited to the concrete surface since the compressive strength increased in all cylinders. This outcome supports that the damage was mainly on the surface and caused by the physical sulphate attack.

Recently in Japan, an extensive field investigation was conducted by Yoshida *et al.,* (2010) to evaluate the deterioration of residential building foundations constructed on a sulphate-rich soil and experiencing surface scaling above the ground level. **Figure 2.2** shows cases of concrete foundation surface scaling above the ground level. It was reported that the damage started several months from the beginning of the construction to about fifteen years. Core samples were extracted from concrete foundations and analysed using different techniques such as XRD, XRF (X-Ray

fluorescence), DSC (differential scanning calorimetry), and EPMA (electron probe micro analyzing). In this work, analysis of results did not detect minerals such as ettringite and gypsum in the above ground concrete. Instead, sodium sulphate crystals were found.

Similar cases of deterioration were reported in other areas including the Arabian Gulf region and Australia (Al-Amoudi, 2002; Hime *et al.,* 2001). However, in the literature, only limited studies have focused on physical sulphate attack since chemical sulphate attack was the main interest (Haynes, 2008; Aye and Oguchi, 2011).

Figure 2.2: Concrete damage in field exposure to salt crystallization
(Yoshida *et al.,* 2010).

2.8 Previous Laboratory Studies on Physical Sulphate Attack

For decades, chemical sulphate attack on concrete was the main research interest, while physical sulphate attack has received little attention (Haynes, 2008; Aye and Oguchi, 2011). It is only recently that researchers started to focus on the performance of concrete under physical sulphate attack. However, there are contradictory views in the existing literature regarding concrete deterioration due to physical sulphate attack. **Table 2.1** summarizes previous lab studies on different concrete mixtures exposed to different environmental conditions.

2.8.1 Effect of w/c Ratio

Previous studies have suggested that concrete with low w/c ratio is more vulnerable to damage by physical sulphate attack since lowering the w/c ratio reduces the pore size diameter, which can behave similar to rocks with fine pores (Hime, 2003). However, a laboratory investigation by Folliard and Sandberg (1994) showed that concrete made with w/c = 0.30 had better performance than concrete made with w/c = 0.50 under an environment prone to physical sulphate attack. Yet, a study by Nehdi and Hayek (2005) showed that concrete mortars with an intermediate w/c = 0.45 had an extensive efflorescence formation compared with w/c = 0.30 and w/c = 0.60 as shown in **Figure 2.3**. Therefore, more research is needed to investigate the main role of the w/c in concrete exposed to physical sulphate attack.
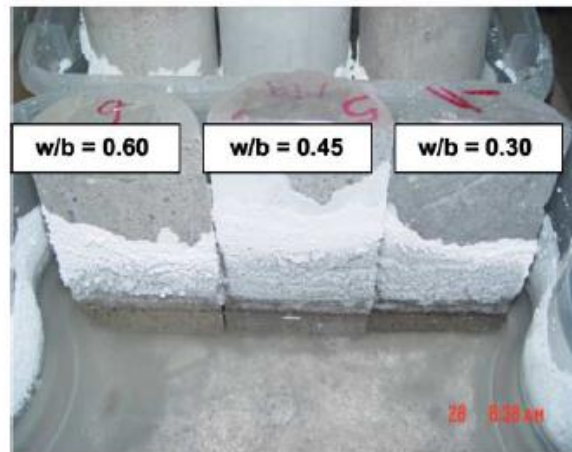
Figure 2.3: Salt efflorescence of concrete cylinders partially immersed in a sodium sulphate solution (Nehdi and Hayek, 2005).

2.8.2 Effect of Pozzolanic Minerals

Previous studies have shown that using pozzolanic minerals in cement mortar had significantly improved its durability under chemical sulphate attack (Al-Amoudi, 2002; Hooton, 1993; Al-Akhras, 2006; Nehdi and Hayek, 2005) since pozzolanic minerals reduce porosity and consume calcium hydroxide which is vulnerable to chemical sulphate attack. However, recent studies have shown that adding pozzolanic minerals to concrete mixtures exposed to physical sulphate attack escalated damage. For example, a study by Aye and Oguchi (2011) showed poor performance of blended cement mortars compared with that of plain cement mortars exposed to environments prone to physical sulphate attack.

Table 2.1: Previous lab investigations on concrete exposed to physical sodium sulphate attack

Authors	Concrete Matrix	Environment condition
Folliard and Sandberg, 1994	Concrete samples with w/c = 0.50 and 0.30	1-completely immeresed and subjected to rapid cooling from 30° to 5° C 2-Partially soaked and temperature was maintained at 25^oC 3-Partially soaked and subjected to temperature cycling between 30 and 5^oC 4-Fully immersed at 25° C and then dried until a constant weight at 110^0 C 5-Fully immersed at 35° C and then dried until a constant weight at 110^0 C
Nehdi and Hayek, 2005	Cement mortars having different w/c (0.30, 0.45, and 0.60) and binders (OPC, OPC + 8% silica fume, OPC + 25% class F fly ash, or OPC + 25% blast furnace slag	Partially immersed and exposed to cycled relative humidity consisting of consecutive sequences of 24 hours at RH > 95% followed by 24 hours at RH of 32 ± 3%
Haynes *et al.,* 2008	Concrete specimens made with Type II Portland cement and w/c = 0.65	Partially immersed and exposed to five environmental conditions a) 40 °C and 74% RH then 40 °C and 31% RH b) Cycled between 20 °C and 82% RH and 20 °C and 54% RH then 20 °C and 82% RH c) Cycled between 20 °C and 82% RH and 20 °C and 54% RH d) 20 °C and 54% RH then between 20 °C and 82% RH and 20 °C and 32% RH e) Cycled between 20 °C and 82% RH and 40 °C and 74% RH then between 20 °C and 82% RH and 40 °C at 31% RH
Hartell *et al.*, 2011	Concrete specimens made with Type II Portland cement and w/c = 0.40, 0.55, and 0.70	Stored in the laboratory under ambient conditions
Aye and Oguchi, 2011	Cement mortars with w/c = 0.45 and binders (OPC, sulphate resisting cement, OPC + 8% silica fume, OPC + 8% diatomaceous earth, and OPC + 25% fly ash)	a)-continuous full immersion at 20 °C b)-full immersion in sulphate solution at 20 °C for 94 h, oven drying at 50 °C for72 h, and cooling in air at 20°C for 2 h for one week cycle c) - partial immersion at 20 °C d) - partial immersion at 20 °C then oven drying at 50°C for72 h, and cooling in the air at 20°C for 2 h for one week cycle

2.8.3 Exposure Conditions

According to Thaulow and Sahu (2004), the most common salt found on scaled concrete surfaces exposed to environments prone to physical sulphate attack is sodium sulphate. Previous studies by Aye and Oguchi (2011) and Haynes *et al.,* (2008) showed high surface scaling when concrete was partially immersed in 5% sodium sulphate compared with exposure to other salts such as magnesium sulphate, soudium carbonate, and soudium chloride under the same expousre conditions (i.e exposure temperature, humidity, and salt concentration). However, the degree of degredation of concrete exposed to soudium sulphate mainly depends on the condition of the surrounding environment (i.e. RH and temperature).

Previous study by Folliard and Sandberg (1994) investigated the performance of concrete exposed to sodium sulphate under five ambient conditions. They found that concrete specimens deteriorated more readily when completely soaked in sodium sulphate and then exposed to cycles of rapid cooling from 30 °C (86 °F) to 5 °C (41 °F), which supports mirabilite formation. Another study by Haynes *et al.,* (2008) found that the most destructive damage occurred when concrete was exposed to an environment that supports the transition between thenardite and mirabilite rather than other environments that only support thenardite or mirabilite precipitation. Concrete specimens were partially immersed in sodium sulphate and exposed to cycling environmental conditions that changed biweekly between 20 °C (68 °F) at 82% relative humidity and 40 °C (104 °F) at 74% relative humidity for 406 days, and then exposed to 20 °C at 82% relative humidity and 40 °C (104 °F) at 31% relative humidity in bi-weekly cycles.

Similar observation was made by Aye and Oguchi (2011) when they examined mortar specimens under four different exposure conditions of sodium sulphate (i.e. continuous full immersion at constant temperature, full immersion under cyclic wetting and drying, continuous partial immersion at constant temperature, and partial immersion under cyclic wetting and drying). Extensive damage occurred when specimens were partially immersed and exposed to cyclic wetting and drying.

Similar observation was made by Aye and Oguchi (2011) when they examined mortar specimens under four different exposure conditions of sodium sulphate

(i.e. continuous full immersion at constant temperature, full immersion under cyclic wetting and drying, continuous partial immersion at constant temperature, and partial immersion under cyclic wetting and drying). Extensive damage occurred when specimens were partially immersed and exposed to cyclic wetting and drying.

In all previous cases, supersaturation was achieved leading to salt growth and damage. However, in the Folliard and Sandberg (1994) case, supersaturation of the sodium sulphate can be reached when the surrounding temperature dropped quickly from 30 °C (86 °F) to 5 °C (41 °F), leading to subsequent crystallisation of mirabilite, which generates pressure higher than the concrete tensile strength.

2.9 Theoretical Models of Crystallization Pressure

Several assumptions and theoretical models have been proposed to explain damage due to salt crystallization pressure. For instance, the mechanism of growth and dissolution of crystals was earlier discussed by Correns, (1949). **Equation 2.3** was proposed to calculate the pressure exerted by growing crystals,

$$P = \frac{RT^`}{V_S} \ln\left(\frac{C}{C_S}\right) \tag{2.3}$$

Where *P* is the pressure exerted by growing crystals,

R is the gas constant,

$T^`$ is the absolute temperature,

V_S is the molar volume of solid salt,

C is the existing solute concentration,

C_S is the saturation concentration.

A thermodynamic model was later developed to calculate salt crystallization pressure by (Wellman and Wilson, 1965) based on the assumption that the chemical free energy of solid increases with its surface. Therefore, larger crystals in the large pores will grow at the expense of the smaller crystals in small pores in a system having crystals in equilibrium with a saturated solution. The work required to extend the surface is equal to the work required during crystal growth on one face of the crystal, as shown in **Equation 2.4** (Wellman and Wilson, 1965)**:**

$$(P_i - P_s)dV = \sigma dA \tag{2.4}$$

Where P_i is the pressure in the liquid,

P_S is the pressure in the solid,

dV is the increase of crystal volume,

σdA is the increase of crystal surface area.

Wellman and Wilson (1968) also introduced the following **Equation 2.5** which estimates the crystallisation pressure in large pores:

$$\Delta P = 2\sigma \left(\frac{1}{r_l} - \frac{1}{r_s} \right) \tag{2.5}$$

Where r_l is the radius of the large pore,

r_s is the radius of the small pore,

σ is the interfacial tension between the crystal face and its saturated solution.

According to Wellman and Wilson (1965), the vulnerability of rocks to damage due to salt weathering depends on their pore structure. For instance, rocks that contain large pores connected by micro-pores are more venerable to damage. When a rock or a porous material is exposed to evaporation and its large and small pores are filled by a saturated salt solution, salt crystals will grow in the large pores at the expense of the smaller crystals in the small pores. This process will continue till damage occurs or $(P_l\text{-}P_S)/\sigma$ becomes greater than dA/dV (Wellman and Wilson, 1965). The damage depends on the size of the small pores and the interfacial tension between the crystal face and its saturated solution compared with the strength of the rock (Wellman and Wilson, 1965).

Scherer (2004) discussed the thermodynamics of crystallization within porous materials and the kinetic factors that affect stress development including capillary rise, evaporation, cement hydration, and cyclic drying and wetting. According to Scherer (2004), when a crystal precipitates in a cylindrical pore as shown in the **Figure 2.4**, the end of the crystal is hemispherical with a curvature given in **Equation 2.6**, whereas the cylindrical side has a curvature expressed in **Equation 2.7**. However, in the case a crystal growing in a large pore with small entries; the cylindrical side

becomes almost zero and the crystallisation pressure is determined by the curvature of the crystal in the pore entries.

$$k_{CL}^{E} = \frac{2}{(r_p - \delta)} \tag{2.6}$$

$$k_{CL}^{S} = \frac{2}{(r_e - \delta)} \tag{2.7}$$

Where δ is the solution film thickness between the crystal and the pore wall,

r_p is the radius of the pore,

r_e is the Radius of the pore small entries.
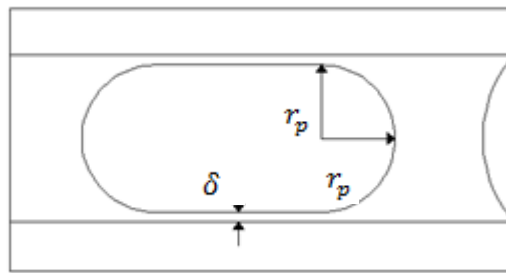
(a)
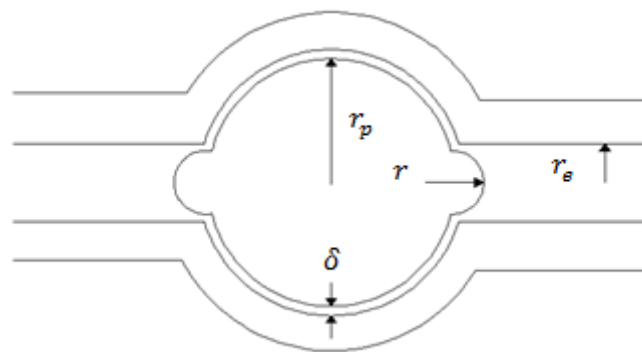
(b)

Figure 2.4: Crystal precipitating in a pore with radius r_p in the subflorescence zone: (a) pore is cylindrical; (b) crystal grows in a large pore with small entries (Scherer, 2004).

The subjected pressure from the pore wall on any other part of the crystal with curvature k_{CL}^{S} is given by **Equation 2.8,** which considers the exerted crystallisation pressure on the pore wall (Scherer, 2004):

$$P_w = k_{CL}^{E} - k_{CL}^{S} = \frac{RT}{V_c} ln \left(\frac{Q^E}{Q^S} \right)$$
(2.8)

Where P_w is the crystallisation pressure,

k_{CL}^{E} is the curvature of the crystal end,

k_{CL}^{S} is the curvature of the cylindrical side,

R is the gas constant,

T is the absolute temperature,

Q^E is the solubility product,

Q^S is the lower solubility product.

2.10 Standards and Specifications for Concrete Exposed to Sulphate Attack

Standards and specifications can offer guidelines for engineers to select appropriate materials and adequate construction operation processes. Regarding concrete exposed to sulphate attack, current standards and specifications such as ACI 318 (2011), CSA A23.1 (2009), and EN-206-1(2000) shown in **Table 2.2**, classify the severity of exposure based on the sulphate concentration in the ground water or soil and provide guidelines to select appropriate cementitious materials in concrete mixtures.

In addition, standard experiments such as ASTM C1012 and CSA A3004-C8 can be used to measure the expansion of concrete due to chemical reactions between the sulphate ions and the cement components. However, the reliability of the current standards and specifications has been criticized and questioned since it ignores the important parameters and factors that affect the performance of concrete in sulphate rich soil (Cohen and Mather, 1991; Skalny *et a.l,* 2002; Mehta, 1992).

According to Hooton (2008) current standard tests that evaluate the resistance of concrete to sulphate attack ignore the capillary rise or evaporative transport of sulphates into concrete. Concrete in the field can be exposed to wetting. Thus, faster

penetrability of sulphates can occur (Hooton, 2008). Change in temperature and relative humidity can lead to salt crystallization, which can cause degradation and scaling of the concrete surface. This typically occurs in foundations, slabs and partially embedded structures in sulphate rich soils, especially in dry weather and coastal areas. Currently, there is no standardized test that can address the concrete degradation due to physical sulphate attack. Hence, more research is required to establish specifications and standardized tests that can evaluate all aspects of sulphate attack.

Table 2.2: Requirements for concrete subjected to sulphate attack

Code	Severity	Condition		Maximum water-to-cementiting materials ratio	Cementitious materials
		Water-soluble sulphate (SO_4) in soil, percent by weight	Dissolved sulphate (SO_4) in water, ppm		
ACI 318 (2011)	Not applicable	$SO_4 < 0.10$	$SO_4 < 150$	N/A	No type restriction
	Moderate	$0.10 \leq SO_4 < 0.20$	$150 \leq SO_4 < 1500$	0.5	Moderate sulphate resistant Type (II)
	Severe	$0.20 \leq SO_4 \leq 2.00$	$1500 \leq SO_4 \leq 10000$	0.45	High sulphate resistant Type (V)
	Very severe	$SO_4 > 2.00$	$SO_4 > 10,000$	0.45	V + pozzolan or slag
CSA A23.1 (2009)	Moderate	$0.20 \leq SO_4 < 0.60$	$150 \leq SO_4 < 1500$	0.5	Type 20 or Type 50
	Severe	$0.60 \leq SO_4 \leq 2.00$	$1500 \leq SO_4 \leq 10000$	0.45	Type 50
	Very severe	$SO_4 > 2.00$	$SO_4 > 10,000$	0.4	Type 50
EN 206-1:2000	Slightly aggressive	$0.02 \leq SO_4 < 0.060$	$2000 \leq SO_4 < 3000$	0.55	Moderate sulphate resistant
	Moderately aggressive	$0.06 \leq SO_4 \leq 0.3$	$3000 \leq SO_4 \leq 12000$	0.5	Moderate or high sulphate resistant
	Highly aggressive	$0.30 \leq SO_4 \leq 0.60$	$12000 \leq SO_4 \leq 24000$	0.45	High sulphate resistant

2.11 References

Al-Amoudi, O. S. B., (2002), "Attack on plain and blended cement exposed to aggressive sulfate environment", *Cement and Concrete Composites*, Vol. 24, No. 3, pp. 305-316.

Al-Akhras, N. M., (2006), "Durability of metakaolin concrete to sulfate attack" *Cement and Concrete Research*, Vol. 36, No. 9, pp. 1727-1734.

Aye, T., Oguchi, C. T., (2011), "Resistance of plain and blended cement mortars exposed to severe sulfate attacks", *Construction and Building Materials*, Vol. 25, No. 6, pp. 2988-2996.

Flatt, R. J., (2002), "Salt damage in porous materials: how high supersaturations are generated", *Journal of Crystal Growth*, Vol. 242, No. 3-4, pp. 435-454.

Goudie, A., and Viles, H., (1997), "Salt weathering hazards", *John Wiley & Sons*, England, 241 p.

Hartell, J. A., Boyd, A. J., and Ferraro, C. C., (2011), "Sulfate attack on concrete: Effect of partial immersion", *Journal of Materials in Civil Engineering*, Vol. 23, No. 5, pp. 572-579.

Haynes, H., O'Neill, R., and Mehta, P. K. (1996), "Concrete deterioration from physical attack by salts", *Concrete International*, Vol. 18, No. 1, pp. 63-68.

Haynes, H., O'Neill, R., Neff, M. and Mehta, P.K. (2008), "Salt weathering distress on concrete exposed to sodium sulfate environment", *ACI Materials Journal*, Vol. 105, No. 1, pp. 35-43.

Haynes, H., O'Neill, R., Neff, M. and Mehta, P.K. (2010), "Salt weathering of concrete by sodium carbonate and soduim chloride", *ACI Materials Journal*, Vol. 107, No. 3, pp. 258-266.

Haynes, H., and Bassuoni, M. T., (2011), "Physical salt attack on concrete", *Concrete International*, Vol. 33, No. 11, pp.38– 42.

Hime, W. G., (2003), "Chemists should be studying chemical attack on concrete", *Concrete International*, Vol. 25, No. 4, pp. 82-84.

Hooton, R. D. (1993) " Influence of silica fume replacement of cement on physical properties and resistance of sulfate attack, freezing and thawing, and alkali-silica reactivity" *ACI Materials Journal*, Vol. 90, No. 2, pp. 143-151.

Hooton, R. D. (2008) "Bridging the gap between research and standards" *Cement and Concrete Research*, Vol. 38, pp. 247-258.

Irassar, E. F., Di Maio, A., and Batic, O. R., (1995), "Sulfate attack on concrete with mineral admixtures", *Cement and Concrete Research*, Vol. 26, No. 1, pp. 113-123.

Mehta, P. K., (2000), "Sulfate attack on concrete: Separating myths from reality", *Concrete International*, Vol. 22, No. 8, pp. 57-61.

Mehta, P. K., and Monteiro, P. J. M., (2006), "Concrete microstructure, properties, and materials", *The McGraw-Hill*, Third edition, 659 p.

Navarroa, C. R., and Doehnea, E., (1999), "Salt weathering: Influence of evaporation rate, supersaturation, and crystallization pattern", *Earth Surface Processes and Landforms*, Vol. 24, No. 3, pp. 191-209.

Nehdi, M., and Hayek, M., (2005), "Behavior of blended and cement mortars exposed to sulfate solutions cycling in relative humidity", *Cement and Concrete Research*, Vol. 35, No. 4, pp. 731-742.

Novak, G. K., and Colville, A. A., (1989), "Efflorescent mineral assemblages associated with cracked and degraded residential concrete foundations in southern California", *Cement and Concrete Research*, Vol. 19, No. 1, pp. 1-6.

Santhanam, M., Cohen, M. D., Olek, J., (2001), "Sulfate attack research – whither now?" *Cement and Concrete Research*, Vol. 31, No. 6, pp. 845-51.

Scherer, G. W., (1999), "Crystallization in pores", *Cement and Concrete Research*, Vol. 29, No. 8, pp. 1347-1358.

Scherer, G. W., (2004), "Stress from crystallization of salt", *Cement and Concrete Research*, Vol. 34, No. 9, pp.1613– 1624.

Stark, D., (1989), "Durability of concrete is sulfate-rich soils", *Research and Development Bulletin*, *Portland Cement Association*, Vol. RD097.

Thaulow, N., Sahu, S., (2004), "Mechanism of concrete deterioration due to salt crystallization", *Materials Characterization*, Vol. 53, No. 2-4, pp. 123-127.

Tsui, N., Flatt, R. J., and Scherer, G. W., (2003), "Crystallization damage by sodium sulfate", *Journal of Cultural Heritage*, Vol. 4, No. 2, pp. 109-115.

Wellman, H. W. and Wilson, A. T., (1965), "Salt weathering, a neglected geological erosive agent in coastal and arid environments", *Nature*, Vol. 205, pp.1097-1098.

Yoshida, N., Matsunami, Y., Nagayama, M., and Sakai, E., (2010), "Salt weathering in residential concrete foundation exposed to sulfate-bearing ground", *Journal of Advanced Concrete Technology*, Vol. 8, No. 2, pp. 121-134.

CHAPTER THREE

PERFORMANCE OF CONCRETE EXPOSED TO DUAL SULPHATE ATTACK

3.1 Introduction

Since the 19th century, concrete damage due to sulphates has received considerable attention. Several studies and investigations have focused on the deterioration mechanisms of concrete subjected to sulphates in sulphate bearing environments. It was mainly established that formation of ettringite and gypsum within the concrete matrix are responsible for the damage due to the sulphate attack (Tian and Cohen, 2000). Sulphate ions chemically react with calcium hydroxide and calcium aluminate hydrate to form gypsum and ettringite, which leads to expansion and strength loss of concrete (Roziere, *et al.,* 2009). This type of attack was described as a chemical sulphate attack on concrete.

However, field investigations reported that concrete partially embedded in sulphate rich soil can suffer from surface scaling above the ground level (Stark, 1989; Yoshida *et al.,* 2010). This type of deterioration was mainly ignored in the open literature since concrete was mainly studied when it is fully immersed in sulphate solutions. In addition, current standards that evaluate the performance of concrete under sulphate attack, such as the ASTM C1012 (Standard Test Method for Length Change of Hydraulic-Cement Mortars Exposed to a Sulphate Solution) and CSA A3004-C8 (Test Method for Determination of Sulphate Resistance of Mortar Bars Exposed to Sulphate Solution) only deal with the chemical aspects of sulphate attack (Aye and Oguchi, 2011; Santhanam *et al.,* 2001).

The damage process involves capillary rise and evaporation of the ground water containing sulphates at the above ground concrete surface, resulting in crystal growth in concrete pores and subsequent damage (Irassar *et al.,* 1995; Haynes *et al.,* 1996). Nevertheless, recent, study by *Liu et al.*, (2012) suggested that the damage above the solution level is more likely due to the chemical sulphate attack since high

sulphate concentration in the upper part of concrete partially immersed in sodium sulphate can be formed. Thus, according to the chemical reaction theory, a sulphate solution with a high concentration can lead to extensive chemical sulphate attack. This controversy in the literature may contribute to further confusion in the assessment of concrete deterioration due to sulphates under field exposure.

3.2   Need for Research

Durability of concrete exposed to sulphates has primarily been studied on specimens fully-submerged in sulphate solutions. However, field experience shows that concrete exposed to sulphates can suffer from surface scaling above the ground level due to physical attack. This damage has often been ignored and even confused with chemical sulphate attack. In this study, concrete partially-immersed in sulphate solutions and exposed to cyclic temperature and relative humidity was explored.

3.3   Experimental Program

3.3.1 Materials and Specimen Preparation

Concrete cylinders $100{\times}200$ mm ($4{\times}8$ in) in size were cast according to ASTM C192 (Standard Practice for Making and Curing Concrete Test Specimens in the Laboratory). Five binder types were used including: ordinary portland cement (OPC), high sulphate resisting cement (HS), OPC with 8% silica fume (SF), OPC with 25% class F fly ash (FA), and OPC with 8% metakaolin (MK). The physical and chemical properties of the cements, mineral additives, and aggregates are summarized in **Tables 3.1** and **3.2**. The proportions of the concrete mixtures are provided in **Table 3.3.**

3.3.2 Curing Conditions

All concrete cylinders were cured for 28 days in a moist room with RH $\geq$ 95% and T = 20°C [68°F] before exposure to the sulphate environment. The curing was carried out according to ASTM C511 (Standard Specification for Mixing Rooms, Moist Cabinets, Moist Rooms, and Water Storage Tanks Used in the Testing of Hydraulic Cements and Concretes).

3.3.3 Environmental Exposure Conditions

According to Thaulow and Sahu (2004), the most commonly found salt on scaled concrete surfaces exposed to environments conducive to physical sulphate attack is sodium sulphate. Previous studies by Aye and Oguchi (2011), and Haynes *et al.,* (2008 and 2010) found higher surface scaling for concrete partially immersed in 5% sodium sulpahte compared to that exposed to other salts such as magnesium sulphate, sodium carbonate, and sodium chloride under the same exposure conditions (i.e. similar temperature, relative humidity (RH), and sulphate concentration). In addition, Haynes *et al.,* (2008) found that surface scaling escalated drastically when the concrete was exposed to cyclic temperature and RH consisting of two weeks at temperature = 20°C [68°F] and RH = 82% followed by two weeks at temperature = 40°C [104°F] and RH = 31% . Therefore, all concrete cylinders were partially immersed in a 5% sodium sulphate solution and placed inside a walk-in environmental chamber with cycling temperature and RH. To accelerate the experiment, cycles were reduced to one week at temperature = 20°C [68°F] and RH = 82% followed by one week at temperature = 40°C [104°F] and RH = 31%.

Table 3.1: Physical and chemical properties of various binders

Components /Property	Cement Type (10)	Cement Type HS	Silica Fume	Metakaolin	Fly ash
Silicon oxide (SiO_2) (%)	19.6	22	95.3	52.2	43.39
Aluminum oxide (Al_2O_3) (%)	4.8	4.1	0.2	41	22.1
Ferric oxide (Fe_2O_3) (%)	3.3	4.4	0.1	1.8	7.7
Calcium oxide (CaO) (%)	61.50	64.90	0.49	-	15.63
Magnesium oxide (MgO) (%)	3.0	1.1	0.27	-	
Sulfur trioxide (SO_3) (%)	3.50	2.25	0.24	0.04	1.72
Loss on ignition (%)	1.90	0.70	1.99	1.1	1.17
Insoluble residue (%)	0.44	0.08	-	-	-
Equivalent alkalis (%)	0.7		-	-	-
Tricalcium silicate (C_3S) (%)	55	57	-	-	-
Dicalcium silicate (C_2S) (%)	15	20	-	-	-
Tricalcium aluminate (C_3A) (%)	7	3	-	-	-
Tetracalcium aluminoferrite (C_4AF) (%)	10	13	-	-	-
Blaine fineness (m^2/kg)	371	380	-	-	-
Autoclave expansion (%)	0.09	-0.01	-	-	-
Compressive strength 28 days (MPa)	40.9	44.8	-	-	-
Specific gravity	3.15	3.12	2.58	2.20	2.50
Time of setting (min) Vicat Initial	104	225	-	-	-

Table 3.2: Physical and chemical properties of fine and coarse aggregates

Property	Coarse aggregate	Fine aggregate
Potential alkali reactivity (Mortar-bar method) (%)	0.05	-
Absorption (%)	1.11	1.09
Crushed particles (%)	68.00	-
Flat/elongated (%)	6.00	-
Micro-deval (A) (%)	11.00	17.00
Soundness (freeze-thaw) (%)	2.20	-
Soundness (MgSO4) (%)	3.90	-
Specific gravity (apparent) (%)	2.73	2.73
Specific gravity (dry) (%)	2.65	2.65
Specific gravity (SSD) (%)	2.68	2.68
Unit weight (kg/m^3)	1734	1512
Materials finer than 75-μm (sieve # 200) (%)	0.90	2.10

Table 3.3: Proportion of tested concrete mixture

Mixture #	Binder Type	Cement Content (kg/m3)	Pozzolanic Content (kg/ m3)	Aggregate Content (kg/m3)	
				Coarse	Fine
1	OPC	350	0		689
2	OPC+25% FA	262	87.5		754
3	OPC+8% SF	322	28	1110	679
4	OPC+8% Meta	322	28		797
5	HS	350	0		689

3.3.4 Mercury Intrusion Porosimetry (MIP)

Figure 3.1 shows the MIP test apparatus. This test method covers the determination of the pore volume and the pore volume distribution of concrete by the mercury intrusion porosimetry method. Fragments were taken from the surface of concrete cylinders at age of 28 days and immediately plunged in an isopropanol solvent to stop cement hydration reactions. The samples were subsequently dried inside a desiccator until a constant mass was reached. The pore size distribution for each specimen was determined using a Micrometrics AutoPore IV 9500 Series porosimeter allowing a range of pressures from 0 to 414 MPa [60000 psi]. The assumed surface tension of

mercury was 0.484 N/m [2.76x10-3 lb/in] at 25°C [77°F] according to ASTM D 4404 (Standard Test Method for Determination of Pore Volume and Pore Volume Distribution of Soil and Rock by Mercury Intrusion Porosimetry).

Figure 3.1: Illustration of MIP test apparatus.

3.3.5 Concrete Mechanical Properties

Compressive strength according to ASTM C39 (Standard Test Method for Compressive Strength of Cylindrical Concrete Specimens) and static modulus of elasticity according to ASTM C469 (Static Modulus of Elasticity and Poisson's Ratio of Concrete in Compression) were measured for the cured concrete cylinders partly immersed in sulphate solutions.

3.3.6 SEM, EDX, and XRD Analysis

Figure 3.2 shows the SEM test apparatus. SU4500 secondary scanning electron microscopy (resolution 7 nm at 3 kV) with energy dispersive X-ray analysis (EDX) was used to investigate the nature of damage (above and below the sodium sulphate solution). Specimens for SEM analysis were dried using a desiccator and then coated with gold before testing. In addition, X-ray diffraction (XRD- Bruker D8 diffractometer) was carried out on samples taken from the deteriorated surfaces. All samples were dried and grounded to pass the 200 µm sieve before testing. Cu-Kα

radiation with a wavelength of 1.54 Å was conducted at a voltage of 40 kV. The scanning speed was 2°/min at a current of 35 mA.

Figure 3.2: Illustration of SEM test apparatus.

3.4 Results and Discussion

After two days of exposure to a temperature of 20°C [68°F] and RH of 82%, salt precipitation (efflorescence) appeared above the solution level on the drying surface of the concrete cylinders. This exposure condition is considered as an ideal environment for mirabilite formation according to previous studies (Thaulow and Sahu, 2004; Flatt, 2002; Haynes *et al.,* 2008). After one week, the exposure was switched to a temperature = 40°C [104°F] and RH = 31%, a condition conducive for thenardite formation. During the second week, the volume of the precipitated salt on the concrete surface decreased compared to that in the first week of exposure. This is related to the transformation of the formed mirabilite to thenardite, which results in a volume contraction of about 314% (Tsui *et al.,* 2003).

After one month of sulphate exposure (4 cycles of wetting and drying) scaling of concrete surfaces appeared above the sulphate solution level. The exposure was continued for up to six months (24 cycles of wetting and drying) and all concrete cylinders were inspected to diagnose the level of damage. **Figure 3.3** shows typical surface scaling above the solution level for the concrete cylinders. For all tested

cylinders, the portion of concrete immersed in the solution was found in intact condition compared with the damaged above solution part. Higher surface scaling above the solution level was found in the concrete specimens incorporating pozzolanic minerals compared to that of the specimens made with 100% OPC or 100% HS.

(a)   (b)   (c)

(d)   (e)

Figure 3.3: Concrete cylinders made with w/b = 0.60 after six months of physical sulphate exposure: (a) concrete made with OPC; (b) OPC + 25% fly ash; (c) OPC + 8% metakaolin; (d) OPC + 8% silica fume; and (e) concrete with HS.

Figure 3.4 shows MIP test results for specimens from the various concrete mixtures before exposure to physical sulphate attack. Results indicate that concrete made either with pure OPC or HS cement incorporate pores with relatively larger diameter. Partially replacing the cement with pozzolanic minerals led to a decrease in the pore size diameter due to the pore refinement effect of pozzolanic minerals.
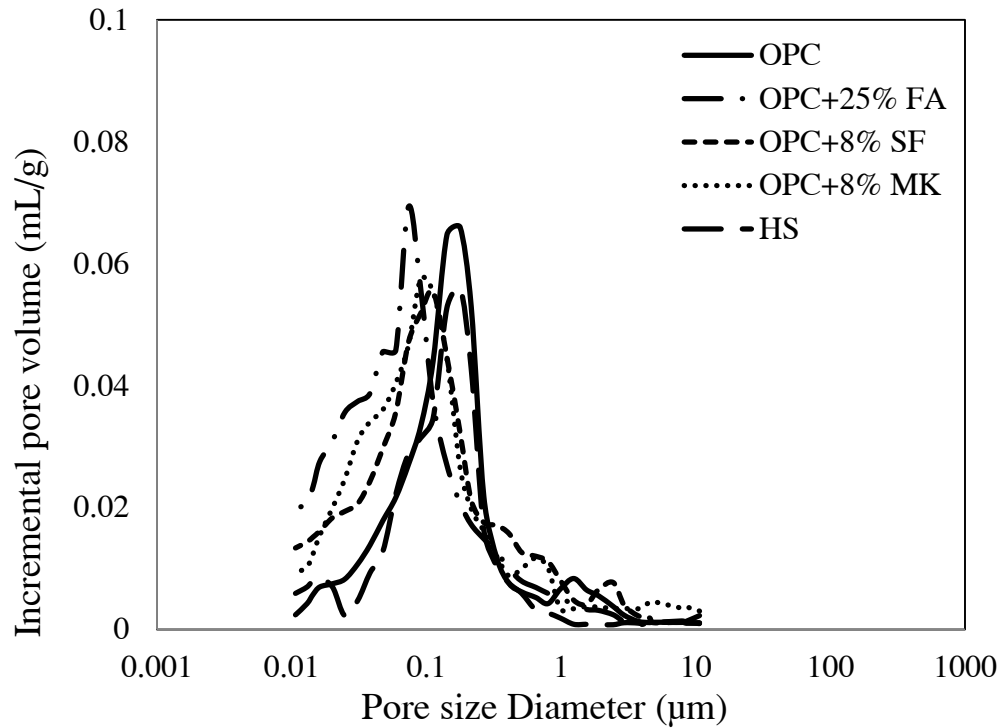
Figure 3.4: MIP results for different concrete mixtures before exposure to physical sulphate attack.

The compressive strength and static modulus of elasticity were measured for all the concrete cylinders partially immersed in the sulphate solution. Appendix B shows the results of the compressive strength and static modulus of elasticity tests. In addition, control specimens were reserved in the laboratory condition at temperature = 23°C [73.4 °F] and RH = 70% for 180 days. **Figure 3.5** shows the testing procedure. **Figures 3.6** and **3.7** show the compressive strength and static modulus of elasticity for concrete cylinders before sulpahte exposure at 28 days and partially immersed in 5% sulphate solution at 90 and 180 days.

(a)   (b)

Figure 3.5: Illustration of testing procedure: (a) compressive strength, and (b) modulus of elasticity.

For all the concrete cylinders, the compressive strength and modulus of elasticity increased regardless of their surface damage. This indicates that the concrete core was in intact condition and the concrete surface scaling did not significantly affect the mechanical properties of the concrete. According to Boyd and Mindess (2004), applying a compressive stress on deteriorated concrete tends to close up internal cracks. Hence, compressive strength may not be a sensitive indicator for internal cracks. However, at six months, a decrease by 12.5 % occurred in the modulus of elasticity of the 100% OPC concrete cylinders in comparison with the control specimen. This suggests that the decrease in modulus of elasticity may be due to the chemical sulphate attack on the submerged portion of specimen. Concrete made with 100% OPC exhibited less surface degradation above the solution level than that of the other concrete cylinders incorporating binders that can resist the chemical sulphate attack.
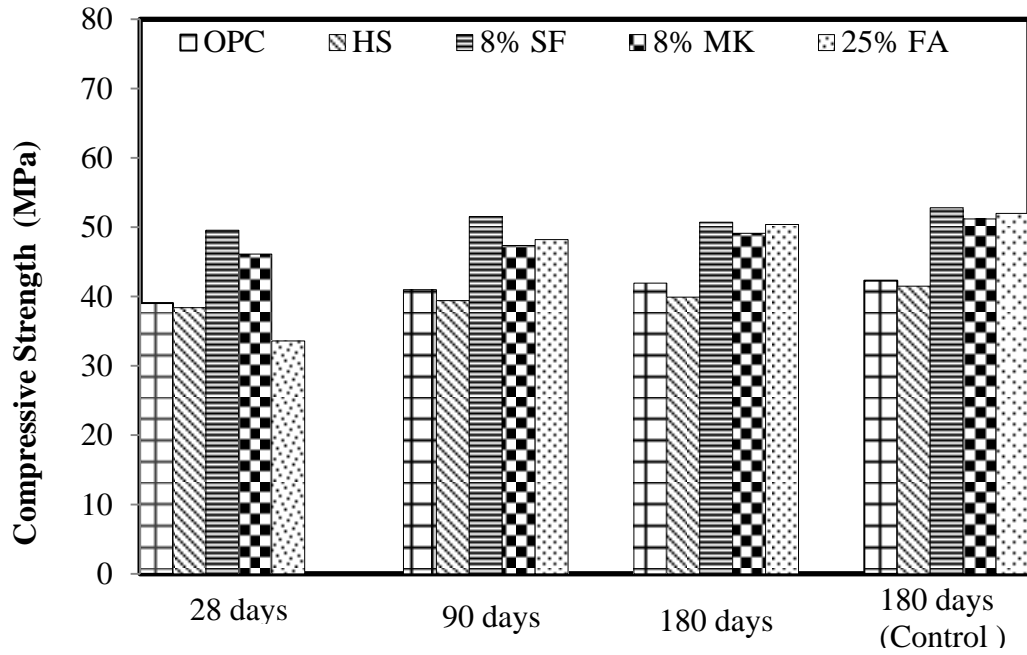
Figure 3.6: Compressive strength for concrete mixtures made with w/b = 0.60.
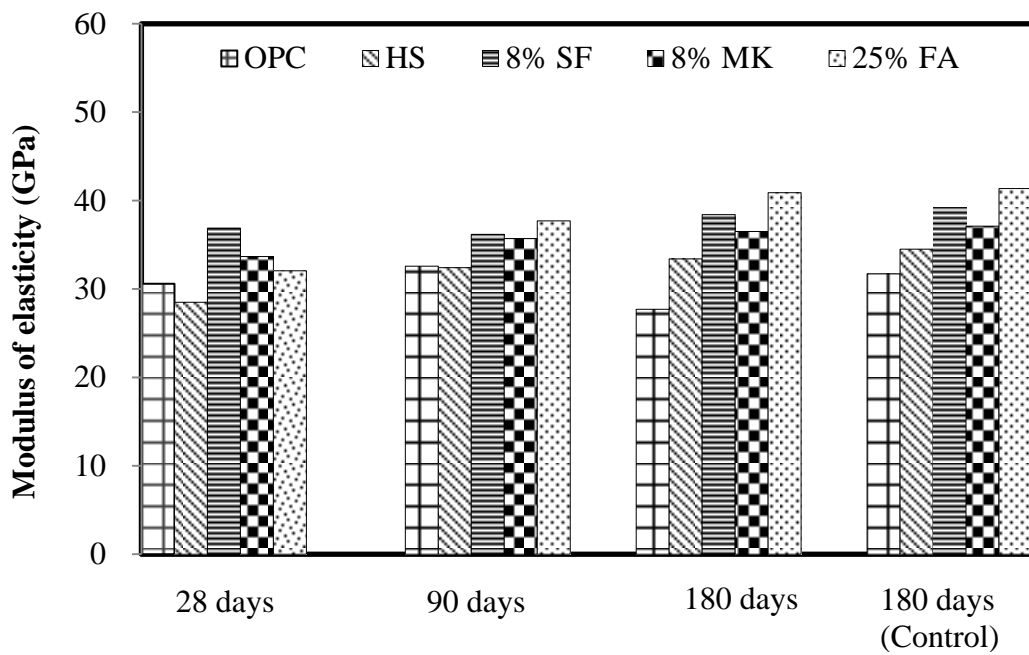
Figure 3.7: Modulus of elasticity for concrete mixtures made with w/b = 0.60.

Figure 3.8 illustrates XRD analysis for the deteriorated concrete above the solution level. For all the concrete cylinders, none of the main components responsible for chemical sulphate attack, such as gypsum and ettringite, were identified in the deteriorated parts above the solution level. Instead, some levels of thenardite were found. The presence of thenardite indicates that the damage of concrete above the solution level was mainly due to salt crystallization.

This was confirmed by SEM and EDX analysis (**Figures 3.9** and **3.10**), which identified thenardite in the damaged parts above the solution level. However, for the concrete cylinders made with 100% OPC, gypsum and ettringite were formed in concrete below the solution level. This indicates that concrete can experience dual sulphate attack. The lower portion immersed in the sodium sulphate solution can suffer from chemical sulphate attack, while the upper portion can be vulnerable to physical sulphate attack.

Previous study by Liu *et al.,* (2012) suggested that the damage above the solution level is more likely caused by the chemical sulphate attack due to formation of high sulphate concentration in the upper part. Thus, extensive chemical sulphate attack can occur according to the theory of the chemical reaction. However, their study only relied on measuring the sulphate concentration above the solution level and did not show damage or formation of gypsum or ettringite above the solution level. Damage due to the chemical sulphate attack mainly results from expansion of the concrete due to formation of gypsum or ettringite. In the current study, surface scaling was occurred instead of concrete expansion. Thus, damage due to the physical sulphate attack above the solution level is the more likely the predominant mechanism.
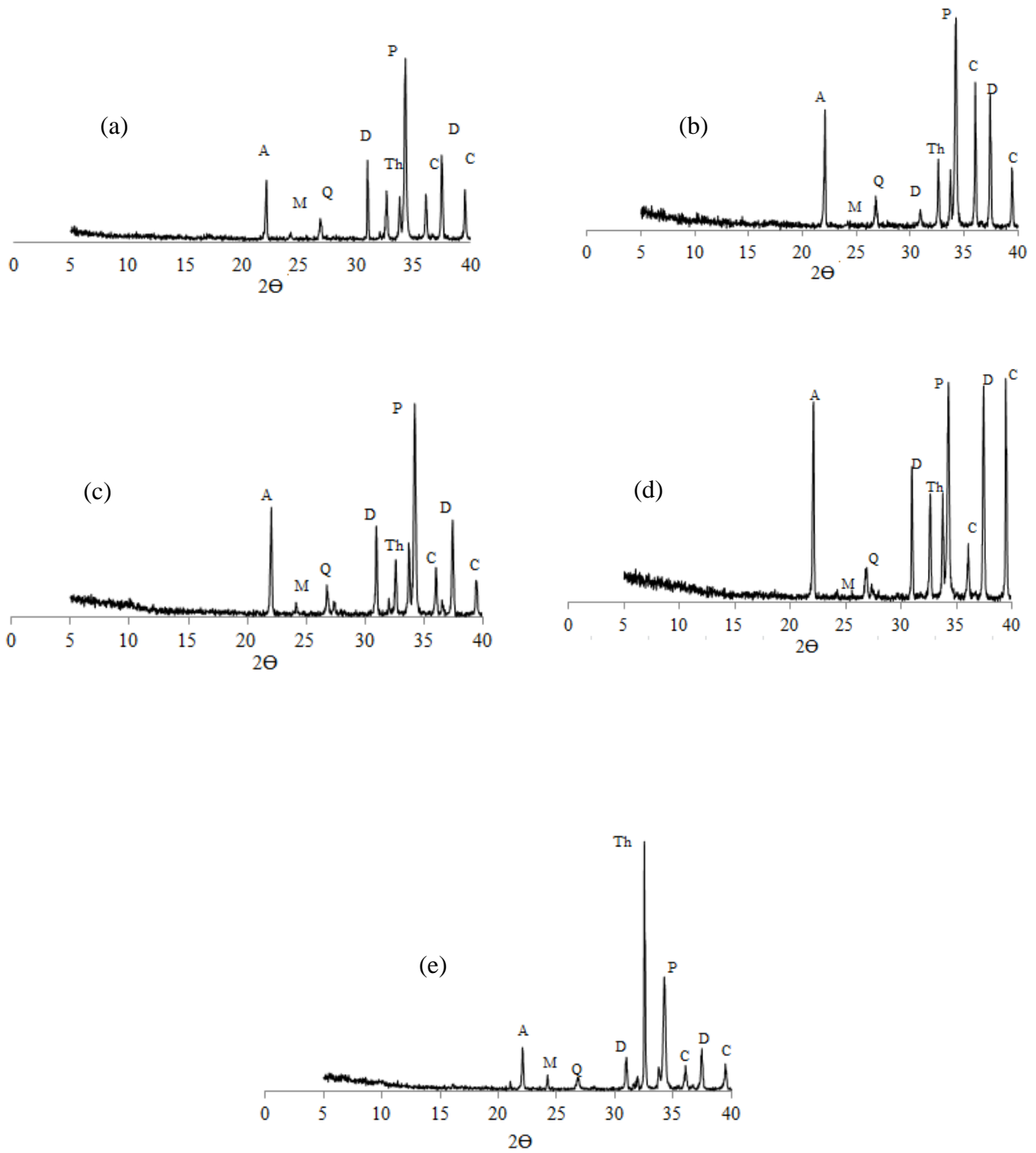
Figure 3.8: XRD results of concrete above the solution level: (a) concrete with OPC; (b) OPC +25% fly ash; (c) OPC + 8% silica fume; (d) OPC + 8% metakaolin; and (e) concrete with HS. [A: Albite, D: Dolomite, Q: Quartz, P: Portlandite, M: Monosulfate, C: Calcite, Th: Thenardite].
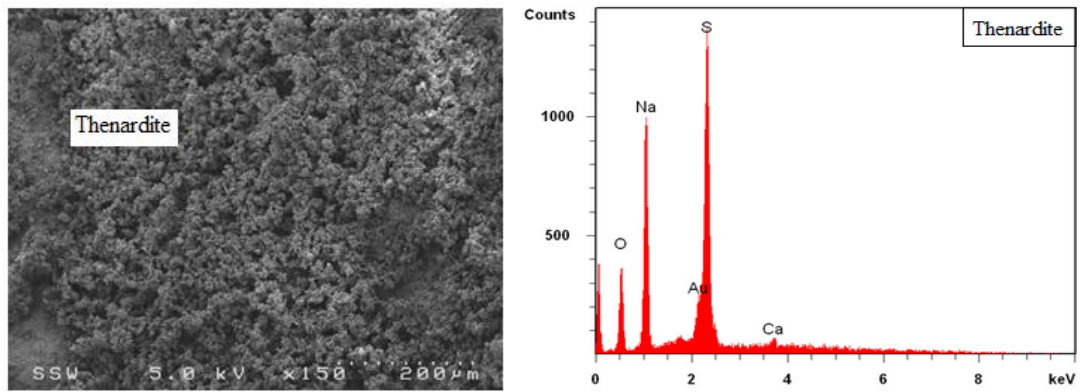
Figure 3.9: SEM and XRD analysis showing thenardite above the solution level.
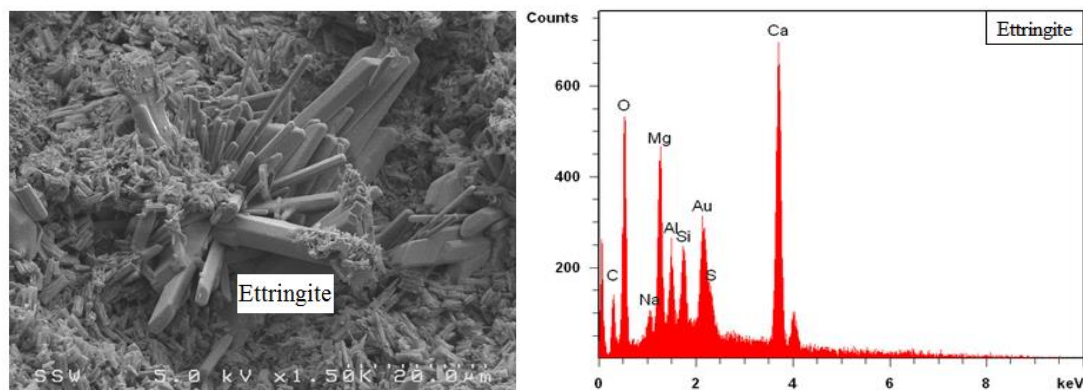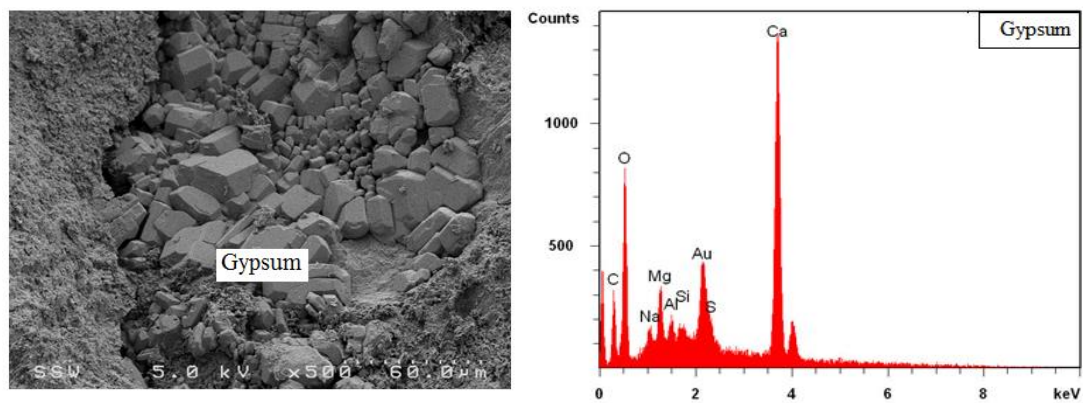
Figure 3.10: SEM and XRD analysis showing formation of gypsum and ettringite in the portion of concrete immersed in the sulphate solution.

3.5 Conclusions

In this chapter, the performance of concrete partially immersed in a 5% sodium sulphate solution was investigated under cycling temperature and relative humidity. Several conclusions can be drawn based on the experimental results:

- Concrete that is partially immersed in a sodium sulphate solution can experience dual sulphate attack. The lower portion immersed in the sodium sulphate solution can suffer from chemical sulphate attack, while the upper portion can be vulnerable to physical sulphate attack.

- High damage due to six months of exposure to physical sulphate attack did not affect both the concrete compressive strength and modulus of elasticity since the damage was only limited to the external surface of the concrete. It is however expected that long-term exposure can lead to decreased mechanical properties.

3.6   References

ASTM C511., (2009), Standard Specification for Mixing Rooms, Moist Cabinets, Moist Rooms, and Water Storage Tanks Used in the Testing of Hydraulic Cements and Concretes, *American Society for Testing and Materials* ,West Conshohocken, PA.

ASTM D4404., (2010), Standard Test Method for Determination of Pore Volume and Pore Volume Distribution of Soil and Rock by Mercury Intrusion Porosimetry, *American Society for Testing and Materials* ,West Conshohocken, PA.

Aye, T., Oguchi, C. T., (2011), "Resistance of plain and blended cement mortars exposed to severe sulfate attacks", *Construction and Building Materials,* Vol. 25, No. 6, pp. 2988-2996.

Boyd, A., Mindess, S., (2004), "The use of tension testing to investigate the effect of W/C ratio and cement type on the resistance of concrete to sulfate attack", *Cement and Concrete Research,* Vol. 34, No. 6, pp. 373-377

Haynes, H., O'Neill, R., and Mehta, P. K. (1996), "Concrete deterioration from physical attack by salts", *Concrete International*, Vol. 18, No. 1, pp. 63-68.

Haynes, H., O'Neill, R., Neff, M. and Mehta, P. K. (2008), "Salt weathering distress on concrete exposed to sodium sulfate environment", *ACI Materials Journal*, Vol. 105, No. 1, pp. 35-43.

Irassar, E. F., Di Maio, A., and Batic, O. R., (1995), "Sulfate attack on concrete with mineral admixtures", *Cement and Concrete Research,* Vol. 26, No. 1, pp. 113-123.

Santhanam, M., Cohen, MD., Olek, J., (2001), "Sulfate attack research − whither now?", *Cement and Concrete Research,* Vol. 31, No. 6, pp. 845-51.

Roziere, E., Loukili, A., Hachem R. EI, and Grondin, F., (2009) "Durability of concrete exposed to leaching and external sulphate attacks", *Cement and Concrete Research,* Vol. 39, pp. 1188-1198.

Tian, B., and Chen, M. (2000), "Expansion of Alite Paste Caused by Gypsum Formation during Sulfate Attack", *Journal of Materials in Civil Engineering*, Vol. 12, No. 1, pp. 24-25.

Yoshida, N., Matsunami, Y., Nagayama, M., and Sakai, E., (2010), "Salt weathering in residential concrete foundation exposed to sulfate-bearing ground", *Journal of Advanced Concrete Technology,* Vol. 8, No. 2, pp. 121-134.

Liu, Z., Deng, D., Schutter, G. D., and Yu, Z., (2012), "Chemical sulfate attack performance of partially exposed cement and cement + fly ash paste", *Construction and Building Materials,* Vol. 28, pp. 230-237.

CHAPTER FOUR

EFFECT OF PORE STRUCTURE ON CONCRETE DETERIORATION BY PHYSICAL SULPHATE ATTACK

4.1   Introduction

Repeated crystallisation of salt minerals has been considered as the driving force for surface scaling of concrete exposed to physical sulphate attack. This damage is initiated when stresses induced by the internal pressure created via repeated salt crystallisation exceed the tensile strength of the concrete. The degree of such damage will depend mainly on the structure and connectivity of pores, which control the penetration of sulphates into the concrete. Several factors affect the pore structure including the concrete constituents, mixture proportions and the curing process. Therefore, in this chapter, the effects of these factors on the performance of concrete exposed to physical sulphate were investigated.

4.2   Need for Research

The pore structure of concrete is an essential factor that controls the durability of concrete   exposed to physical sulphate attack since previous studies have shown that the vulnerability of stones exposed to salt weathering depends on their pore structure. Therefore, the effects of factors that control the concrete pore structure including the w/b ratio, binder type, and curing conditions on the performance of concrete exposed to severe physical sulphate attack have been investigated. The findings should demystify the role of these parameters on physical sulphate attack, allowing to gain a more fundamental understanding of the associated damage mechanisms, which could enhance the durability design of concrete in sulphate laden environments and possibly prevent some of the associated litigation.

.

4.3 Experimental Program

4.3.1 Materials and Specimen Preparation

Three groups of concrete mixtures with different w/b ratio (i.e. 0.30, 0.45, and 0.60) were tested. In each group, five binder types were used including: ordinary portland cement (OPC), high sulphate resisting cement (HS), OPC with 8% silica fume (SF), OPC with 25% class F fly ash (FA), and OPC with 8% metakaolin (MK). The proportions of the concrete mixtures are provided in **Table 4.1**. For each of the fifteen concrete mixtures, standard cylinders 100×200 mm (4×8 in.) were cast according to ASTM C192 (Standard Practice for Making and Curing Concrete Test Specimens in the Laboratory).

Table 4.1: Mixture design for tested concrete

Mixture #	Binder Type	Cement Content (kg/m^3)	Pozzolanic Content (kg/m^3)	Aggregate Content (kg/m^3)		w/b	Super-plasticizer (ml/m^3)
				Coarse	Fine		
1	OPC	450	0.000		804	0.30	2250
2	OPC + 25% FA	337.5	122.5		779	0.30	1600
3	OPC + 8% SF	414	36.00	1110	791	0.30	3200
4	OPC + 8% MK	414	36.0		797	0.30	2900
5	HS	450	0.00		804	0.30	2250
6	OPC	400	0.000		727	0.45	1570
7	OPC + 25% FA	300	100.0		705	0.45	900
8	OPC + 8% SF	368	32.00	1110	715	0.45	2100
9	OPC + 8% MK	368	32.00		720	0.45	1850
10	HS	400	0.00		727	0.45	1571
11	OPC	350	0.000		689	0.60	---
12	OPC + 25% FA	262	87.50		754	0.60	---
13	OPC + 8% SF	322	28.00	1110	679	0.60	---
14	OPC + 8% MK	322	28.00		797	0.60	---
15	HS	350	0.000		689	0.60	---

4.3.2 Curing Conditions

In general, damage of concrete structures in sulphate rich soils (e.g. foundations, retaining walls, etc.) can start at an early-age before concrete is fully cured. The volume of capillary pores is typically high in concrete at earlier age compared with that of the fully cured concrete. Hence, more sulphates can penetrate into the concrete, leading to higher damage. Therefore, in the present study, both the performance of

non-cured and cured concrete exposed to physical sulphate attack have been investigated. For the non-cured concrete, a group of cylinders from each mixture were exposed to the sulphate environment after 24 hours from casting. Another identical group of concrete cylinders from each concrete mixture was cured for 28 days in a moist room with RH ≥ 95% and T = 20°C [68°F] before exposure to the sulphate environment. The curing was carried out according to ASTM C511 (Standard Specification for Mixing Rooms, Moist Cabinets, Moist Rooms, and Water Storage Tanks Used in the Testing of Hydraulic Cements and Concretes).

4.3.3 Environmental Exposure Conditions

Figure 4.1 shows the tested specimens in the environmental chamber. According to Thaulow and Sahu (2004), the most commonly found salt on scaled concrete surfaces exposed to environments conducive to physical sulphate attack is sodium sulphate. Previous studies by Aye and Oguchi (2011), and Haynes *et al.,* (2008 and 2010) found higher surface scaling for concrete partially immersed in 5% sodium sulphate compared to that exposed to other salts such as magnesium sulphate, sodium carbonate, and sodium chloride under the same exposure conditions (i.e. similar temperature, relative humidity (RH), and sulphate concentration). In addition, Haynes *et al.,* (2008) found that surface scaling escalated drastically when the concrete was exposed to cyclic temperature and RH consisting of two weeks at temperature = 20°C [68°F] and RH = 82% followed by two weeks at temperature = 40°C [104°F] and RH = 31% . Therefore, all concrete cylinders were partially immersed in a 5% sodium sulphate solution and placed inside a walk-in environmental chamber with cycling temperature and RH. To accelerate the experiment, cycles were reduced to one week at temperature = 20°C [68°F] and RH = 82% followed by one week at temperature = 40°C [104°F] and RH = 31%.

4.3.4 Mercury Intrusion Porosimetry (MIP)

Fragments were taken from the surface of both non-cured and cured concrete cylinders at ages of 2 and 28 days, respectively and immediately plunged in an isopropanol solvent to stop cement hydration reactions. Similar testing procedure was fallowed according to section **3.3.4**

Figure 4.1: Tested specimens in the environmental chamber.

4.3.5 Mass Loss

Concrete cylinders from each mixture were transferred to the exposure condition after measuring their initial mass using a balance with an accuracy of 0.01 g [0.00035 oz.]. Before measuring the initial mass, all concrete cylinders were air-dried in the laboratory condition at temperature = 20°C-22°C and RH = [68°F-71.6°F]. The mass loss was calculated according to **Eq. 4.1:**

$$Mass\ loss\ at\ (t) = \frac{M_i - M_t}{M_i} \times 100 \tag{4.1}$$

Where t is the time,

M_i is the initial mass of the cylinder,

M_t is the mass of the cylinder at time t.

4.4   Results and Discussion

After one month of sulphate exposure (4 cycles of wetting and drying) scaling of concrete surfaces appeared above the sulphate solution level. The exposure was continued for up to six months (24 cycles of wetting and drying) and all concrete cylinders were inspected to diagnose the level of damage. **Figure 4.2** shows typical surface scaling above the solution level for the non-cured concrete cylinders made with w/b = 0.60. For all tested cylinders, the portion of concrete immersed in the solution was found relatively in intact condition compared with the damaged above solution part. Higher surface scaling above the solution level was found in the non-cured concrete specimens incorporating pozzolanic minerals compared to that of the specimens made with 100% OPC or 100% HS at a w/b = 0.60.

Figure 4.3 depicts the deterioration of the bottom surface of concrete cylinders made with w/b = 0.60. It can be observed that at the age of six months, deterioration started to appear at the bottom surface of the 100% OPC concrete cylinders, while concrete cylinders made with either HS or including pozzolanic minerals were still intact.

Figures 4.4 and 4.5 illustrate representative surface scaling above the solution level of the non-cured concrete cylinders made with w/b = 0.45 and 0.30, respectively. Concrete cylinders with w/b = 0.45 exhibited similar trend to that of cylinders made with w/b = 0.60, but with significantly less deterioration. For the non-cured concrete cylinders with w/b = 0.30, no surface scaling was observed after six months of sulphate exposure.

Figure 4.6 illustrates the typical effect of the curing regime on concrete exposed to physical sulphate attack. It can be observed that cured concrete specimens exhibited less surface scaling than that of their non-cured counterparts.
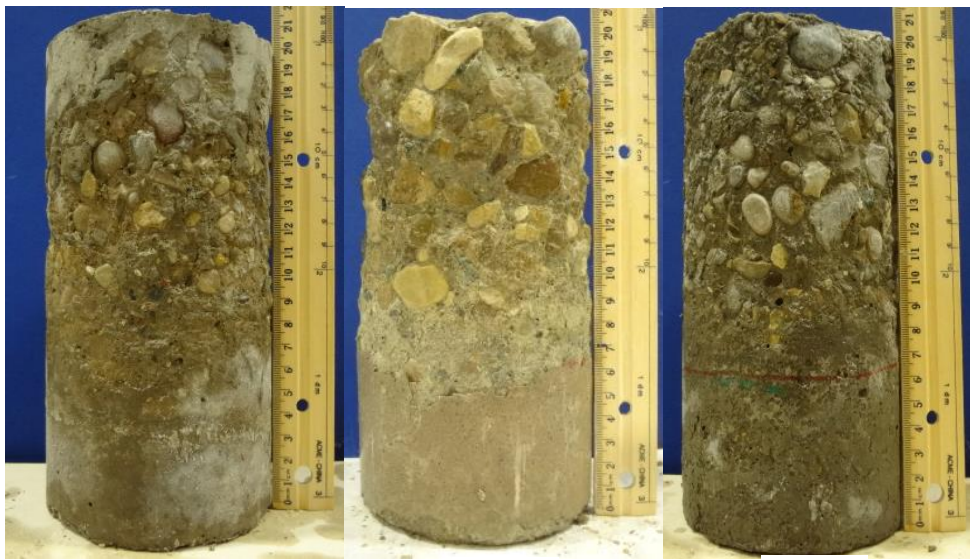
(a)　　　　　　　　(b)　　　　　　　　(c)

(d)　　　　　　　　(e)

Figure 4.2: Non-cured concrete cylinders made with w/b = 0.60 after six months of physical sulphate exposure: (a) concrete made with OPC; (b) OPC + 25% FA; (c) OPC + 8% SF; (d) OPC + 8% MK; and (e) concrete with HS.

(a) (b)

(c) (d)

(e)
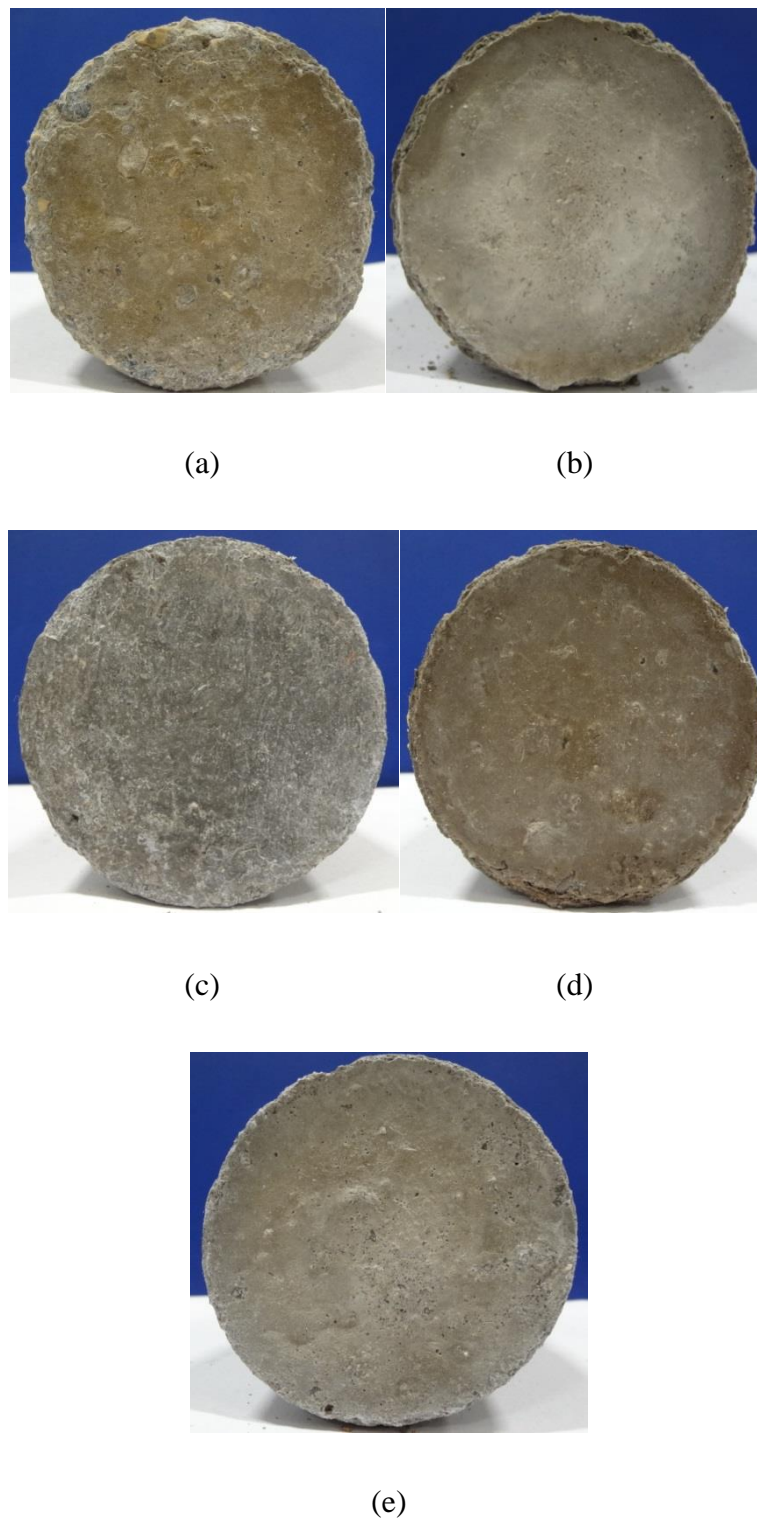
Figure 4.3: Bottom surface of concrete cylinders with w/b = 0.60 immersed in sodium sulphate solution for 6 months: (a) concrete made with OPC; (b) OPC + 25% FA; (c) OPC + 8% SF; (d) OPC + 8% MK; and (e) concrete with HS.

(a) (b) (c)
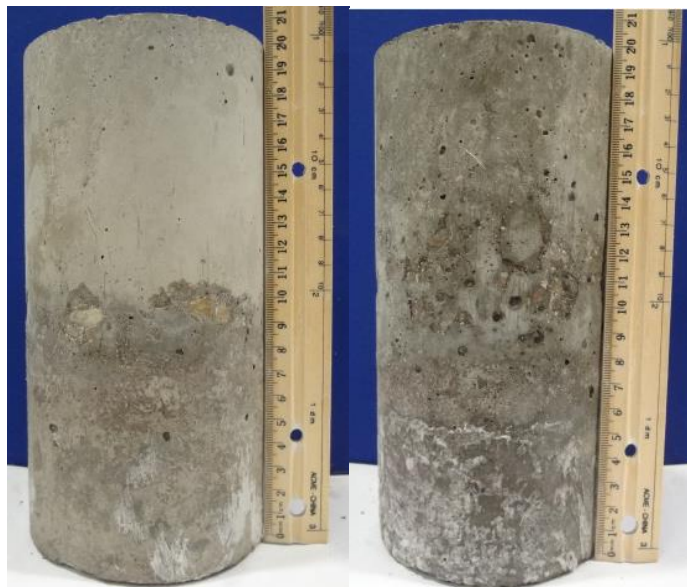
(d) (e)

Figure 4.4: Non-cured concrete cylinders made with w/b = 0.45 after six months of physical sulphate exposure: (a) concrete made with OPC; (b) OPC + 25 % FA; (c) OPC + 8 % SF; (d) OPC + 8% MK; and (e) concrete with HS.
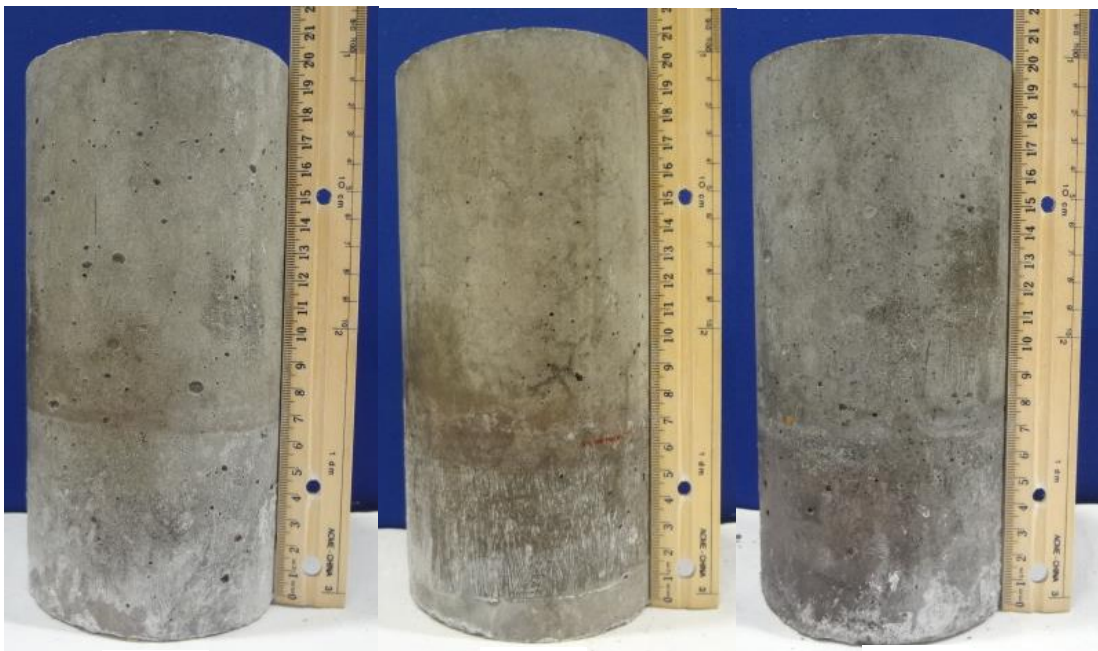
(a)   (b)   (c)

(d)   (e)

Figure 4.5: Non-cured concrete cylinders made with w/b = 0.30 after six months of physical sulphate exposure: (a) concrete with OPC; (b) OPC + 25% FA; (c) OPC + 8% SF; (d) OPC + 8% MK; and (e) concrete with HS.

(a)   (b)

Figure 4.6: Effect of curing on physical sulphate attack of concrete made with OPC +25% FA at w/b = 0.60: (a) non-cured specimen; and (b) specimen moist cured for 28 days.

Figure 4.7 to **4.9** and **Table 4.2** show MIP test results for specimens from the various concrete mixtures before exposure to physical sulphate attack. Results indicate that concrete made either with pure OPC or HS cement incorporate pores with relatively larger diameter. Partially replacing the cement with pozzolanic minerals led to a decrease in the pore size diameter due to the pore refinement effect of pozzolanic minerals.

A low w/b ratio caused a significant decrease in the total intrusion volume for the plain and blended cement concrete mixtures due to the increase in the solid volume and subsequent reduction in the total volume of pores. Moist curing the concrete also induced a decrease in the intrusion volume, which also indicates a decrease in the total porosity.
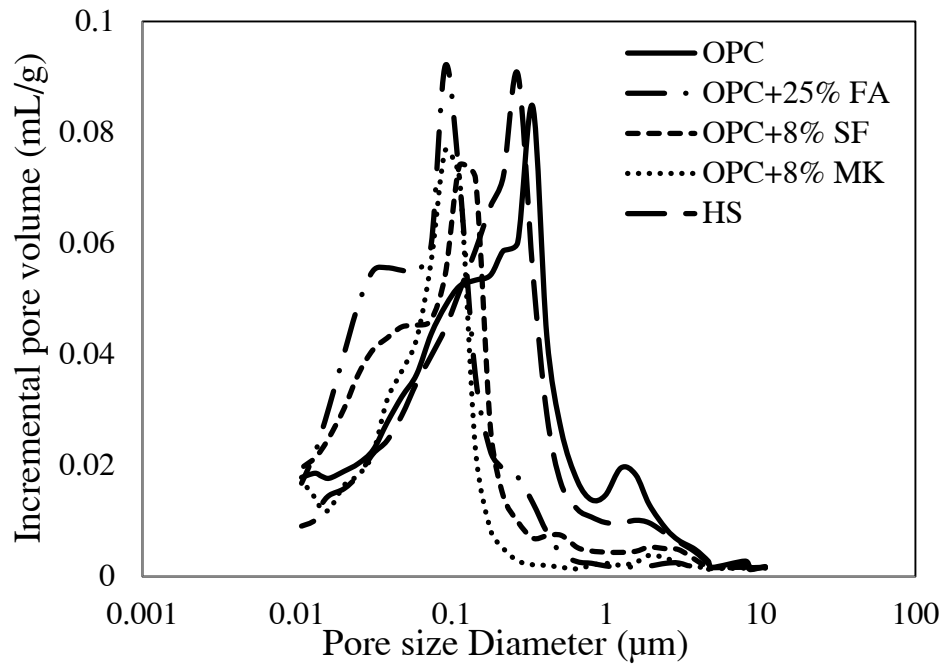
Figure 4.7: MIP results for concrete mixtures made with w/b = 0.60 before exposure to physical sulphate attack.
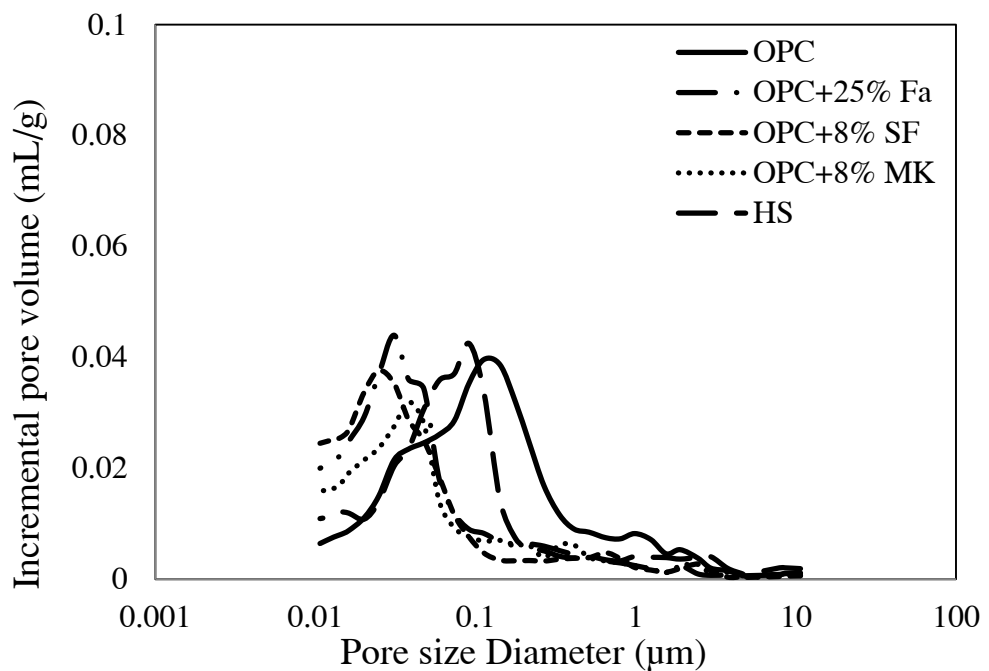
Figure 4.8: MIP results for concrete mixtures made with w/b = 0.45 before exposure to physical sulphate attack.
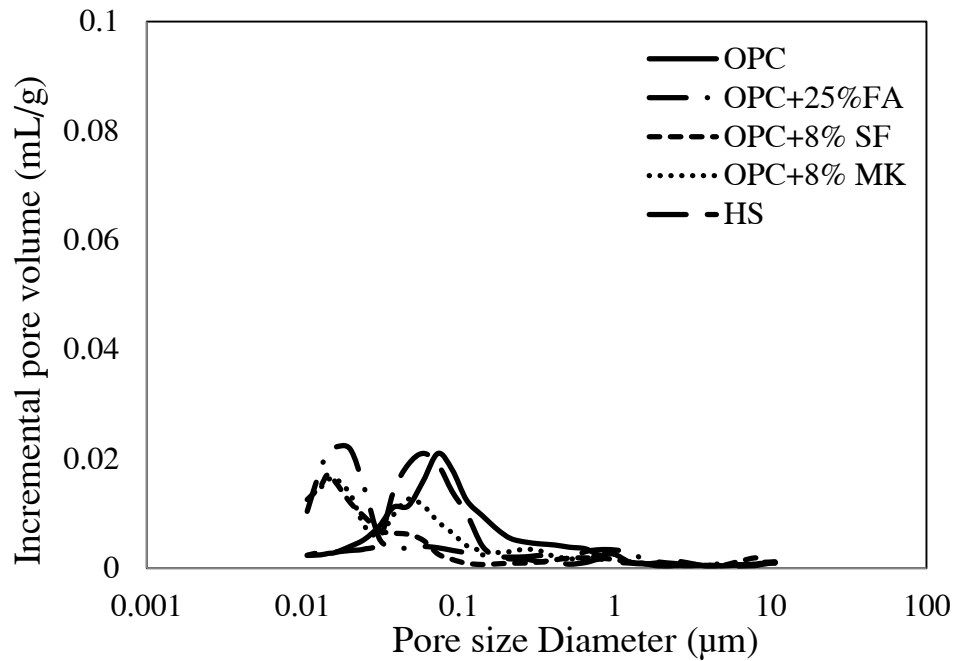
Figure 4.9: MIP results for concrete mixtures made with w/b = 0.30 before exposure
to physical sulphate attack

Table 4.2: Average pore size and total intrusion volume for the tested concrete

	w/b = 0.60*		w/b = 0.60**		w/b = 0.45*		w/b = 0.30*	
	Average Pore Diameter (μm)	Total Intrusion Volume (m/Lg)	Average Pore Diameter (μm)	Total Intrusion Volume (m/Lg)	Average Pore Diameter (μm)	Total Intrusion Volume (m/Lg)	Average Pore Diameter (μm)	Total Intrusion Volume (m/Lg)
100% OPC	0.063	0.090	0.058	0.066	0.046	0.042	0.041	0.021
OPC + 25% FA	0.049	0.092	0.045	0.069	0.031	0.043	0.023	0.023
OPC + 8% SF	0.051	0.074	0.041	0.052	0.034	0.037	0.025	0.017
OPC + 8% MK	0.054	0.076	0.043	0.055	0.037	0.032	0.027	0.016
HS	0.061	0.084	0.059	0.056	0.048	0.039	0.044	0.022

*Non-cured

**Cured

4.4.1.1 Effect of w/b ratio

The total intruded volume of mercury mainly depends on the volume of the pores and their connectivity. As expected, MIP results showed high mercury intrusion for concrete mixtures made with higher w/b compared to that of mixtures with lower w/b. For instance, the total intrusion volume of mercury dropped from 0.090 (m/Lg) to 0.042 (m/Lg) and 0.021 (m/Lg) when the w/b was lowered from 0.60 to 0.45 and 0.30, respectively. This approximately represent a 50 % decrease in the total pore volume for concrete made with w/b = 0.45 compared to that of concrete made with w/b = 0.60 and 75 % for concrete made with w/b = 0.30. Therefore, by increasing the w/b, the volume of the pores and their connectivity can be increased, leading to higher capillary rise and increased salt growth on the concrete surface, thus accelerating the damage mechanisms.

4.4.1.2 Effect of Curing

Moist curing the concrete showed relatively less surface scaling (**Figure 4.6),** since curing the concrete increase the solid volume of the concrete (Mehta and Monteiro, 2006), leading to decrease in the total volume of the pores and their connectivity. MIP results (**Table 4.2)** showed less mercury intrusion for the cured concrete compared with non-cured concrete. For all cured specimens, a decrease by more than 20 % occurred in the total intruded volume of mercury compared with that of the non-cured specimen.

4.4.1.3 Effect of Pozzolanic Minerals

At the same w/b ratio, partially replacing the cement with pozzolanic minerals showed a decrease in the average pore size as shown in the **Table 4.2**. **Figures** from **4.7** to **4.9** show that at different w/b ratio, partially replacing the cement with pozzolanic minerals shifted the curve to the smaller pore diameter portion. For instance, at different w/b ratios, the percentage of pores with diameter smaller than 0.10 μm was significantly increased when cement partially replaced with pozzolanic minerals. Pores with smaller diameter tend to increase the capillary rise on the concrete surface. Hence, it appears that the refinement of porosity due to the use of

supplementary cementing materials had caused increased capillary rise of the sulphate solution and possibly more surface area for evaporation. Consequently, concrete specimens incorporation such pozzolanic minerals exhibited higher surface damage and surface scaling at the above solution part of specimens compared with that of concrete specimens made with pure OPC.

The mass loss was monitored for all concrete cylinders that were partially immersed in the sodium sulphate solution and exposed to cyclic temperature and RH. **Figures 4.10** and **4.11**, illustrate the mass loss after 6 months of exposure to physical sulphate attack.
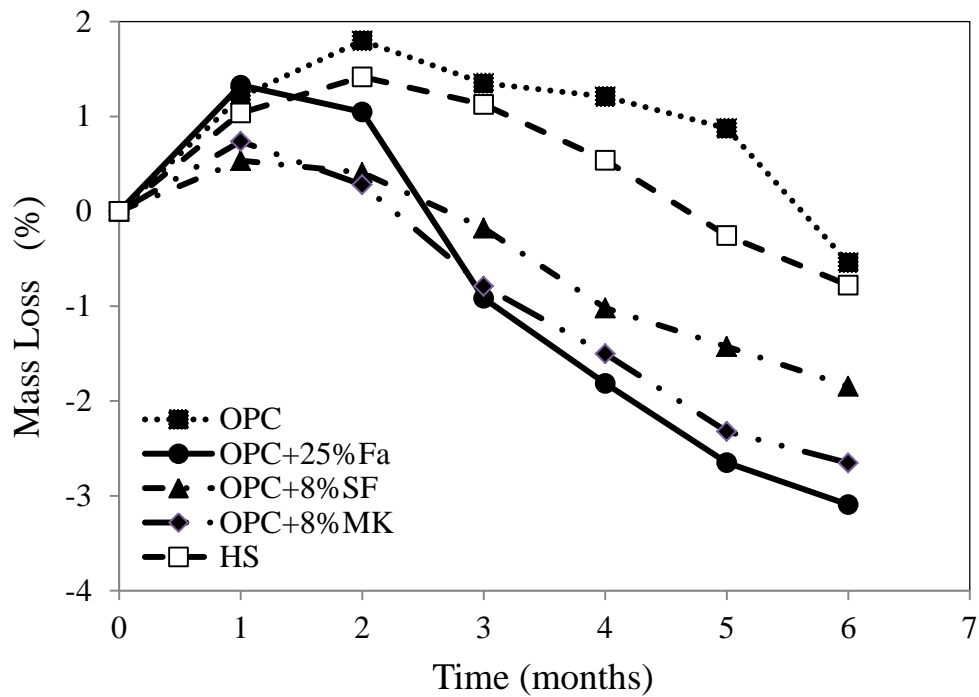
Figure 4.10: Mass loss for non-cured concrete cylinders made with w/b = 0.60
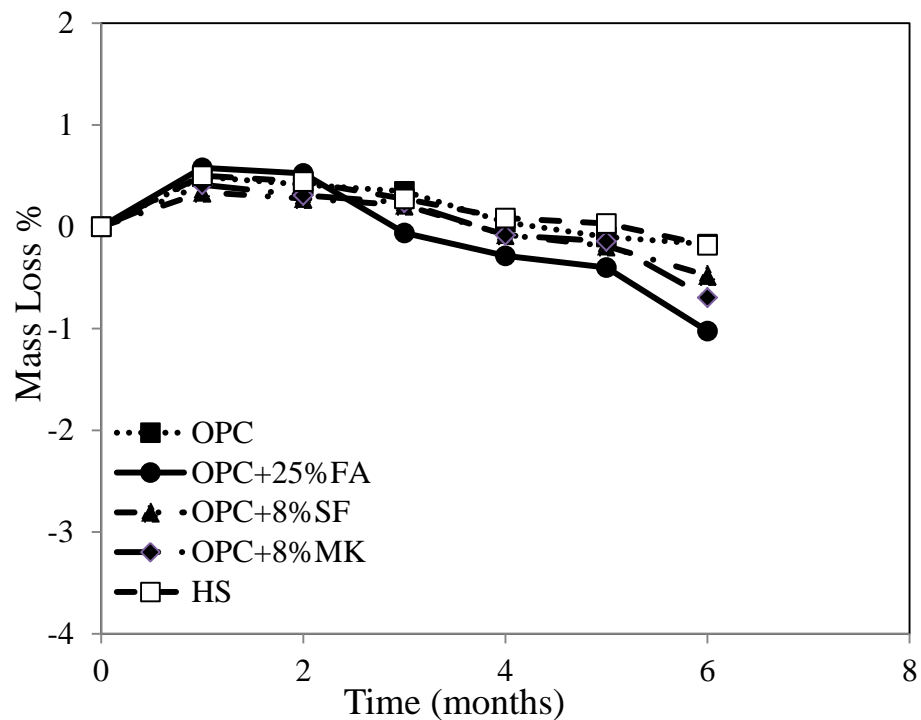
Figure 4.11: Mass loss for non-cured concrete cylinders made with w/b = 0.45.

During the first month, concrete cylinders gained mass due to water absorption, especially for those with higher porosity. For instance, concrete cylinders with w/b = 0.60 gained higher mass than that of those made with w/b = 0.45 and w/b = 0.30, respectively. In addition, at the same w/b ratio, 100% OPC or HS concrete cylinders gained higher mass than that of specimens incorporating pozzolanic minerals. At later age, the concrete cylinders started to lose mass. Highest mass loss was observed for those concrete cylinders made with w/b = 0.60 and incorporating pozzolanic minerals. Similar trend was observed for concrete cylinders made with w/b = 0.45, but with less mass loss. However, all concrete cylinders (cured and non-cured) made with w/b = 0.30 did not experience any mass loss.

The mass loss occurred due to scaling of the concrete surface above the solution level. The immersed portion of concrete into the sodium sulphate solution was mostly in intact condition. The concrete surface above the solution level was exposed to evaporation, which creates super-saturation of the sodium sulphate solution. Therefore, crystals can grow from the supersaturated solution and exert high tensile stress, leading to damage and mass loss of the concrete above the solution level. In addition, cycling both the temperature and RH accelerated the damage since thenardite dissolves during the wetting cycle and generates high super-saturation with

respect to mirabilite that exerts high crystallisation pressure (Tsui, *et al,.* 2003; Flatt, 2002). According to Flatt (2002), the expected crystallisation pressure generated in this process ranges from 10-20 MPa, which is higher than the typical tensile strength of concrete.

4.5   Conclusions

In this chapter, the effect of the pore structure on concrete deterioration by physical sulphate attack was investigated. Several factors that control the concrete pore structure including the w/c ratio, pozzolanic minerals, and the curing regime were explored under environments prone to physical sulphate attack. Several conclusions can be drawn based on the experimental results:

- The durability of concrete against physical sulfate attack depends significantly on the concrete pore structure, and is less dependent on the chemical composition and nature of the binder.
- Using low w/b ratio can significantly improve the durability of concrete under physical sulphate attack since it reduces the total volume of the pores and their connectivity, leading to less capillary rise and surface scaling.
- Moist curing the concrete for 28-days before exposure to physical sulphate attack led to reduced surface scaling due to an increase in the solid volume and decreased porosity of the cementitious matrix.
- At the same w/b ratio, although partially replacing ordinary portland cement with pozzolanic minerals also reduced the total porosity of the concrete, it was found that the surface scaling was escalated due to an increase in the proportion of the pores with very small diameter, which caused an increase of capillary rise and more surface area for evaporation.

4.6   References

ASTM C511., (2009), Standard Specification for Mixing Rooms, Moist Cabinets, Moist Rooms, and Water Storage Tanks Used in the Testing of Hydraulic Cements and Concretes, American Society for Testing and Materials ,West Conshohocken, PA.

ASTM D4404., (2010), Standard Test Method for Determination of Pore Volume and Pore Volume Distribution of Soil and Rock by Mercury Intrusion Porosimetry, American Society for Testing and Materials ,West Conshohocken, PA.

Aye, T., Oguchi, C. T., (2011), "Resistance of plain and blended cement mortars exposed to severe sulfate attacks", Construction and Building Materials, Vol. 25, No. 6, pp. 2988-2996..

Flatt, R. J., (2002), "Salt damage in porous materials: how high supersaturations are generated", Journal of Crystal Growth, Vol. 242, No. 3-4, pp. 435-454.

Haynes, H., O'Neill, R., and Mehta, P. K. (1996), "Concrete deterioration from physical attack by salts", Concrete International, Vol. 18, No. 1, pp. 63-68.

Haynes, H., O'Neill, R., Neff, M. and Mehta, P. K. (2008), "Salt weathering distress on concrete exposed to sodium sulfate environment", ACI Materials Journal, Vol. 105, No. 1, pp. 35-43.

Haynes, H., O'Neill, R., Neff, M. and Mehta, P. K. (2010), "Salt weathering of concrete by sodium carbonate and soduim chloride", ACI Materials Journal, Vol. 107, No. 3, pp. 258-266.

Irassar, E. F., Di Maio, A., and Batic, O. R., (1995), "Sulfate attack on concrete with mineral admixtures", Cement and Concrete Research, Vol. 26, No. 1, pp. 113-123.

Mehta, P. K., and Monteiro, P. J. M., (2006), Concrete Microstructure, Properties, and Materials", McGraw-Hill, Third Edition, 659 p.

Navarroa, C. R., and Doehnea, E., (1999), "Salt weathering: influence of evaporation rate, supersaturation, and crystallization pattern", Earth Surface Processes and Landforms, Vol. 24, No. 3, pp. 191-209.

Scherer, G. W., (2004), "Stress from crystallization of salt", Cement and Concrete Research, Vol. 34, No. 9, pp. 1613– 1624.

Stark, D., (1989), "Durability of concrete in sulfate-rich soils", Research and Development Bulletin, Portland Cement Association, Vol. RD097.

Thaulow, N., Sahu, S., (2004), "Mechanism of concrete deterioration due to salt crystallization", Materials Characterization, Vol. 53, No. 2-4, pp. 123-127.

Tsui, N., Flatt, R. J., and Scherer, G. W., (2003), "Crystallization damage by sodium sulfate", Journal of Cultural Heritage, Vol. 4, No. 2, pp. 109-115.

EFFECT OF SURFACE TREATMENT ON DURABILITY OF CONCRETE EXPOSED TO PHSYICAL SULPHATE ATTACK

5.1   Introduction

Concrete surface generally includes macro-pores and micro-cracks that provide paths for the ingress of harmful substances into the concrete, often leading to deterioration (Aguiar *et al.,* 2008; Swamy *et al.,* 1998). Thus, concrete protection can be provided using surface treatment materials, such as hydrophobic and film-forming coating materials that act as a barrier to isolate the concrete from its surrounding environment (Aguiar *et al.,* 2008). However, choosing an effective type of surface treatment material is a challenge since different types and formulations are commercially available (Hawkins, 1985). In particular, only limited studies have focused on concrete exposed to physical sulphate attack (Haynes *et al.,* 2008; Aye and Oguchi, 2011; Nehdi and Hayek, 2005). Therefore, the main focus of this study is to assess the ability of different types of surface treatment materials to enhance the durability of concrete to physical sulphate attack.   .

5.2   Need for Research

Protecting the surface of concrete can be essential for improving its durability under certain exposure conditions. However, different types of surface treatment materials are commercially available, which makes it difficult to identify the appropriate type, especially in the case of concrete exposed to physical sulphate attack. Therefore, this study focuses on evaluating the effects of coating the surface of concrete with different types of commercially available surface treatment materials on its resistance to physical sulphate attack. The results could provide guidance to avoiding many law suits related to physical sulphate attack damage of concrete.

5.3 Experimental Program

Concrete cylinders 100×200 mm (4×8 in) in size were cast according to ASTM C192 (Standard Practice for Making and Curing Concrete Test Specimens in the Laboratory). **Table 5.1** summarizes the concrete mixture compositions.

Table 5.1: Proportions of tested concrete mixtures

Ingredient	Mixture 1	Mixture 2
Cement (kg)	300	263
Fly ash (kg)	100	87
Coarse Aggregate (kg)	1110	1110
Fine Aggregate (kg)	705	754
w/b	0.45	0.60
Superplasticizer (ml/ m^3)	900	-

Generally, sulphate attack on concrete structures exposed to sulphate rich-soil can start at early-age. In addition, most cast in-situ concrete structures are not cured for 28 days and are usually surface coated at early-age to accelerate the construction process. Therefore, in this study, concrete cylinders were de-molded after 24 hours from casting and divided into two groups. The first group was kept at ambient laboratory temperature (20°C [68°F] - 23°C [73°F]) for 72 hours before coating, while the other group was cured for 28 days before exposure to the sulphate environment. The curing was carried out according to ASTM C511 (Standard Specification for Mixing Rooms, Moist Cabinets, Moist Rooms, and Water Storage Tanks Used in the Testing of Hydraulic Cements and Concretes).

Table 5.2 shows the properties of the used surface treatment materials. Two application layers of four different types of surface treatment materials were tested, namely (a) silane, which is a hydrophobic penetrating sealer (water-repellent), (b) epoxy, which acts as a membrane coating, (c) bitumen modified polyurethane, which is a waterproof membrane, and (d) water-based solid acrylic polymer resin, which is a curing and surface sealer compound.

Table 5.2: Properties of the used surface treatment materials

	Epoxy	Bitumen	Silane	Acrylic
Color	Gray	Black	Clear	Milky white
Adhesion to dry or damp concrete (MPa)	2.4	-	-	-
Moisture retention, (kg/m^2)	-	-	-	0.53
Comparative abrasion resistance, mg lost	-	-	-	100
Flash point, (° C)	-	-	62.7	-
Water weight gain reduction (%)	-	-	90	-
Absorbed chloride reduction (%)	-	-	96	-
Tensile strength (MPa)	20.7	1	-	-
Compressive strength(MPa)	58.6	-	-	-
Tensile elongation (%)	3	600	-	-
Flexural strength (MPa)	29.6	-	-	-

Figure 5.1 illustrates a schematic of concrete surface pore structure and the proposed protection mechanism provided by each of the four surface treatment materials. **Figure 5.2** shows SEM images of the different coating surfaces. After coatings have dried, cylinders were partially immersed in a 5% sodium sulphate solution and placed inside a walk-in environmental chamber with cycling temperature and relative humidity. Previous study by Haynes *et al.,* (2008) found that the surface scaling escalated drastically when the concrete was exposed to cyclic temperature and RH consisting of two weeks at temperature = 20°C [68°F] and RH = 82% followed by two weeks at temperature = 40°C [104°F] and RH = 31%. Therefore, to accelerate the experiment, cycles were reduced to one week at temperature = 20°C [68°F] and RH = 82% followed by one week at temperature = 40°C [104°F] and RH = 31%.

<div align="center">(a)   (b)   (c)   (d)</div>
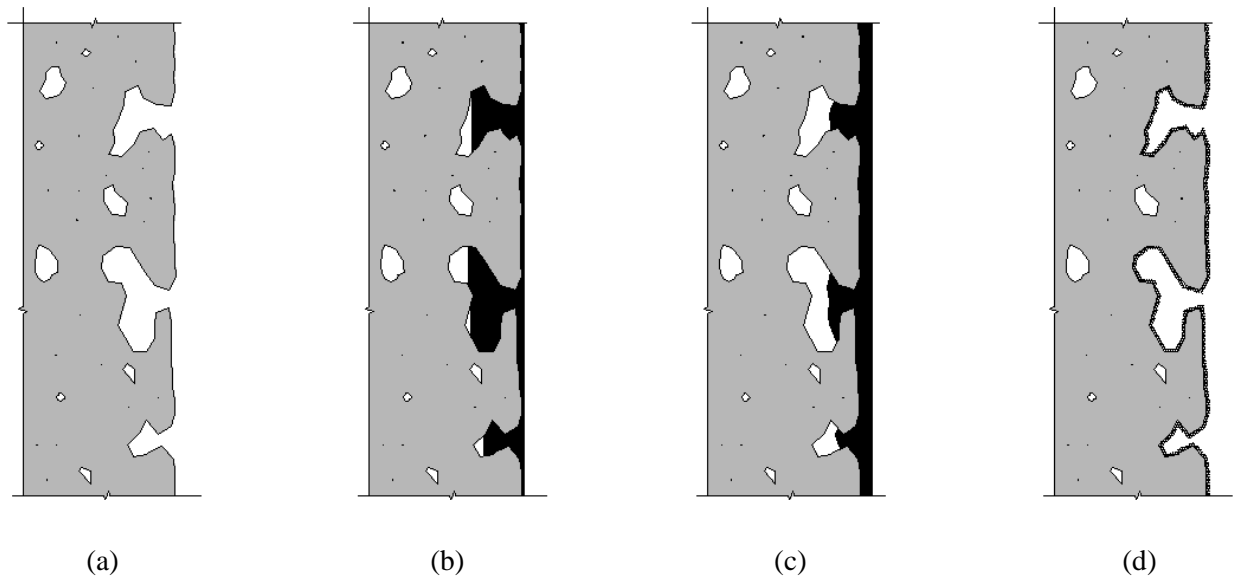
Figure 5.1: Schematic illustration of concrete surface pores and protection mechanism provided by various surface treatment materials: (a) non-coated concrete; (b) concrete surface coated with acrylic sealer; (c) concrete surface coated with epoxy or bitumen that provides an impervious membrane; and (d) concrete coated with silane water repellent.
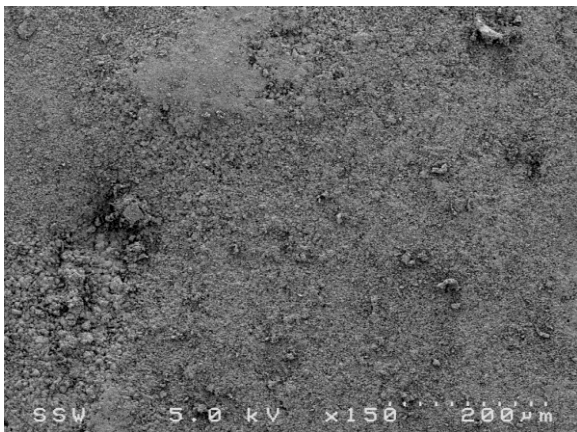
(a)
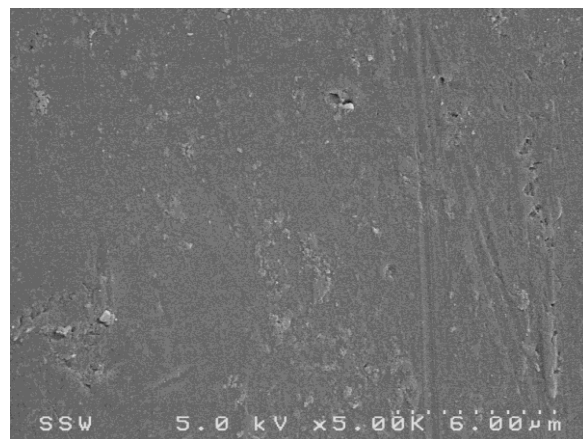
(b)
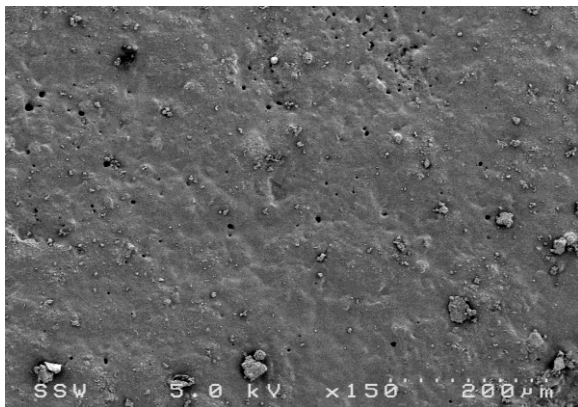
(c)
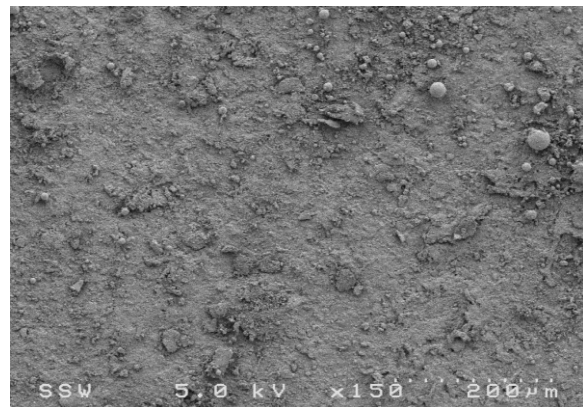
(d)
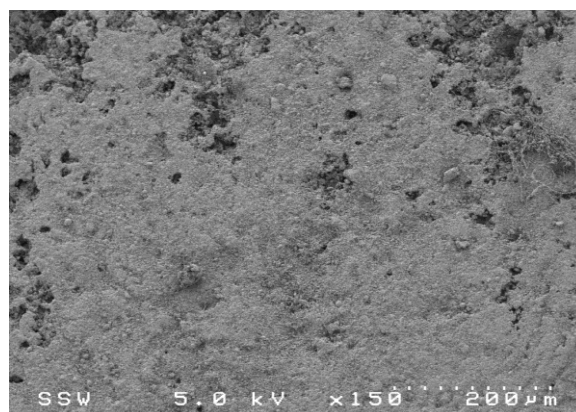
(e)

Figure 5.2: SEM images for surface of: (a) non-coated concrete; (b) concrete coated with epoxy; (c) coated with acrylic; (d) coated with bitumen; and (e) coated with silane.

5.3.1 Visual Inspection

Concrete cylinders were visually monitored for up to six months of sulphate exposure. The visual rating of concrete surface degradation was conducted based on the proposed rating system by Malhotra *et al.,* (1987). In this system, concrete can be rated on a scale of ten based on its surface scaling and mass loss as shown in **Table 5.2**.

Table 5.2: Visual rating system for the degraded concrete (Adapted from Malhotra *et al*., 1987). (*Reproduced with permission from the American Concrete Institute*)

Rating Grade	Rating Description
0	Less than 15% of surface aggregates are exposed
1	More than 15% of surface aggregates are exposed
2	50% of surface aggregates immediately below the surface are exposed
3	80% of surface aggregates are exposed
4	Surface aggregates are exposed over 20% of their perimeter
5	90% of the surface aggregates are exposed over one half of their perimeter
6	95% of volume of specimen remaining
7	80% of volume of specimen remaining
8	60% of volume of specimen remaining
9	20% of volume of specimen remaining
10	Specimen disintegrated

5.4   Experimental Results

Figure. 5.3 and **Table 5.3** show MIP results for the non-coated concrete surfaces before exposure to physical sulphate attack. As expected, results showed higher content of larger pores (1μm-0.1μm) and mercury intrusion for concrete specimens made with w/b = 0.60 compared with that of those made with w/b = 0.45. The total intrusion volume of mercury dropped from 0.069 (m/Lg) to 0.038 (m/Lg) when the w/b was lowered from 0.60 to 0.45. Approximately 50 % decrease in pore volume was observed for concrete made with w/b = 0.45 compared to that of concrete made with w/b = 0.60. This difference was more pronounced for non-cured specimens. Therefore, by increasing the w/b, the volume of the pores and their connectivity can

be increased, leading to higher capillary rise and increased salt growth on the concrete surface, thus accelerating the damage mechanisms.
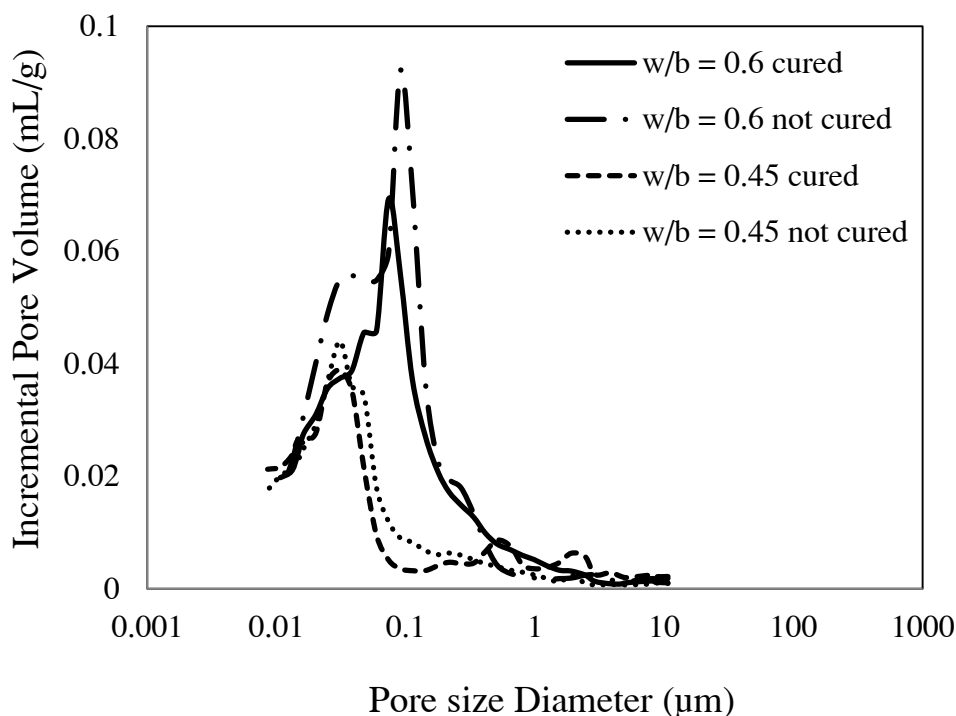
Figure 5.3: MIP test results for concrete specimens before coating and exposure to physical sulphate attack.

Table 5.3: Average pore size and total intrusion volume for the tested concrete

	Average Pore Diameter (µm)	Total Intrusion Volume (m/Lg)
w/c = 0.60	0.049	0.092
w/c = 0.60 cured	0.045	0.069
w/c = 0.45	0.031	0.043
w/c = 0.45 cured	0.029	0.038

Table 5.4 shows the visual rating for each concrete cylinder after six months of physical sulphate exposure using the Malhotra *et al.,* (1987) rating system. After one month of exposure (i.e. four cycles of wetting and drying), surface scaling appeared

on the drying surfaces of the non-coated cylinders (both cured and non-cured) made with w/c = 0.60, with more substantial degradation for the non-cured cylinders. However, no deterioration was observed on the coated cylinders. After six cycles, damage appeared on the acrylic coated specimens (for both the cured and non-cured cylinders) as shown in **Figure 5.4**. In addition, it was observed that the bitumen coating layer had separated from the non-cured cylinders. Conversely, no deterioration was observed for the cylinders coated with epoxy and silane. Furthermore, at lower w/c = 0.45, less degradation was observed for the non-coated cylinders and those coated with acrylic. No separation of the bitumen layer occurred for the non-cured concrete cylinders made with w/c = 0.45.

Table 5.4 Visual rating for concrete cylinders after six months of exposure to physical sulphate attack

	w/c = 0.60 cured	w/c = 0.60 non-cured	w/c = 0.45 cured	w/c = 0.45 non-cured
Non-coated	5	5.5	1	1.8
Coated with epoxy	0	0	0	0
Coated with bitumen	0	0.8	0	0
Coated with silane	0	0	0	0
Coated with acrylic	4.4	4.8	0.5	1.2

Figure 5.5, 5.6, 5.7, and **5.8** show cured and non-cured and coated and non-coated concrete cylinders after six months of sulphate exposure. It can be observed that damage was confined to the concrete surface above the solution level. Most extensive damage was observed for the non-cured and cured concrete cylinders, respectively made with w/b = 0.60. Severe damage was also observed for cylinders made with w/b = 0.60 and coated with acrylic. Concrete cylinders that were coated with epoxy and silane were in intact condition. For specimens coated with bitumen, only those made with w/b = 0.60 have shown damage.

A similar trend was observed for the non-coated cylinders (both cured and non-cured) made with w/b = 0.45, but with significantly less deterioration. Again, no

deterioration was observed for the cylinders coated either with epoxy, silane, or bitumen, except for cylinders coated with acrylic.

Figure 5.4: Damage of the acrylic layer of coated non-cured concrete made with w/b = 0.60 after two months of physical sulphate exposure.
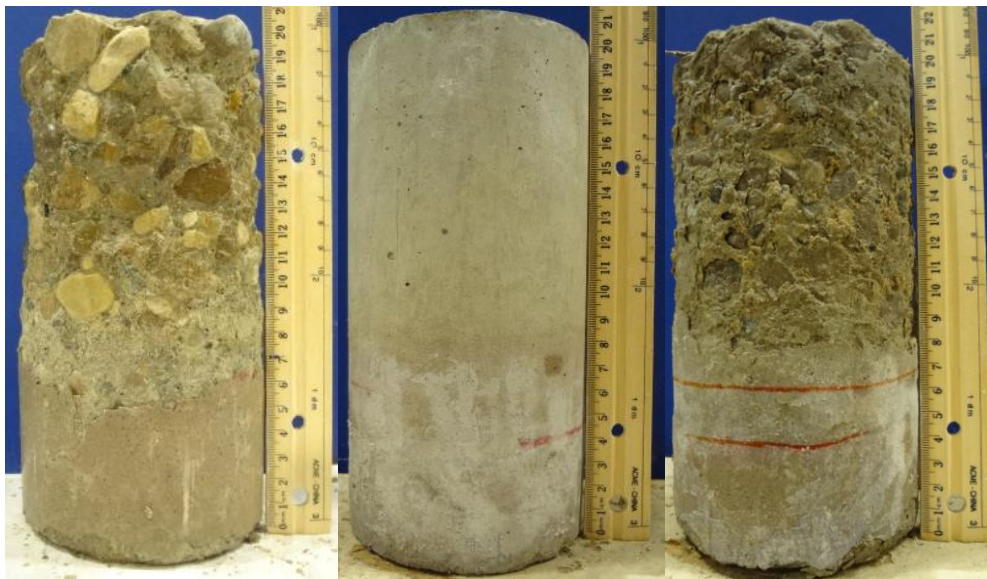
(a) (b) (c)

(d) (e)

Figure 5.5: Non-cured concrete cylinders made with w/b = 0.60 after 6 months of physical sulphate exposure: (a) non-coated and coated with; (b) silane (water-repellent); (c) acrylic solution (curing and sealer); (d) epoxy (membrane); and (e) bitumen (membrane).
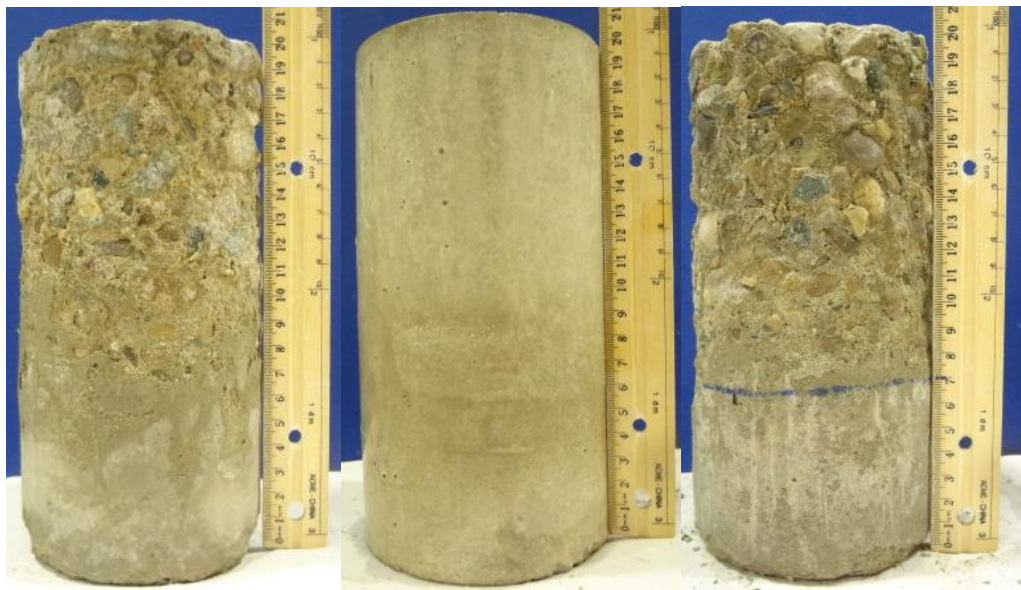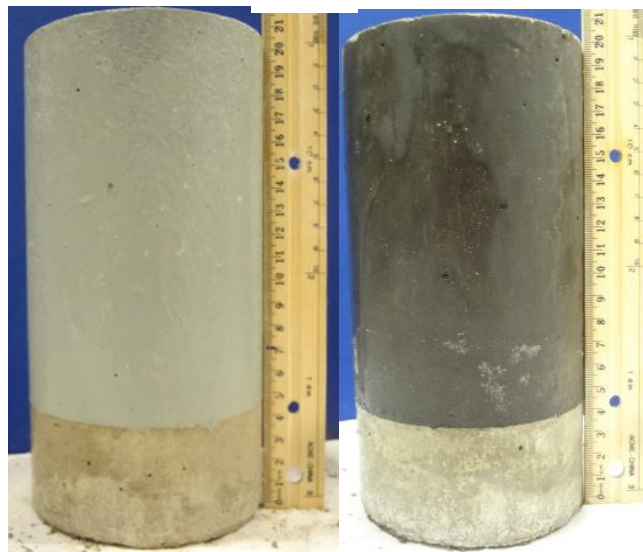
Figure 5.6: Cured cylinders made with w/b = 0.60 after 6 months of physical sulphate exposure (a) non-coated and coated with; (b) silane (water-repellent); (c) acrylic solution (curing and sealer); (d) epoxy (membrane); and (e) bitumen (membrane).
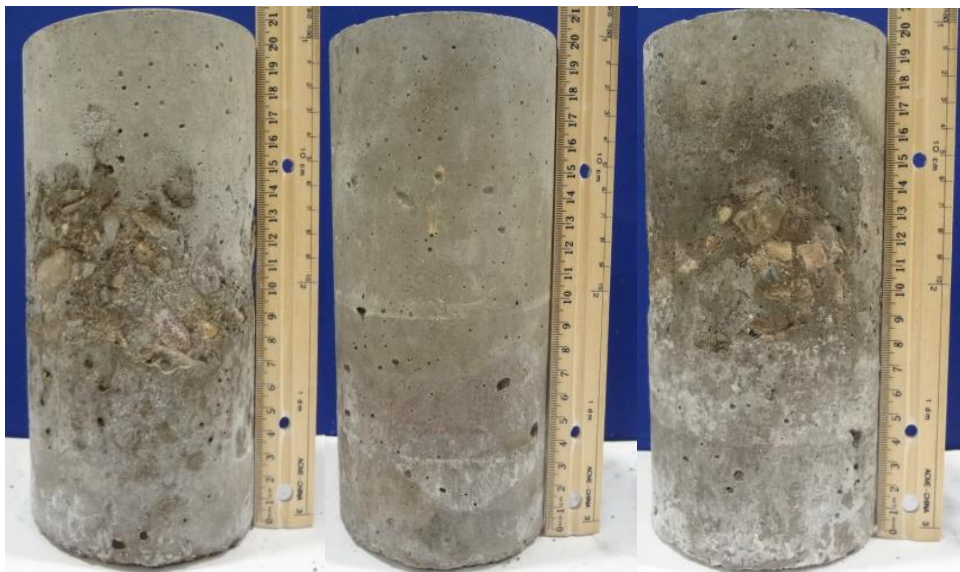
(a)   (b)   (c)

(d)   (e)

Figure 5.7: Non-cured concrete cylinders made wıtn w/b = 0.45 after 6 months of exposure (a) Non-coated, and coated with; (b) silane (water-repellent); (c) acrylic solution (curing and sealer); (d) epoxy (membrane); and (e) bitumen (membrane).
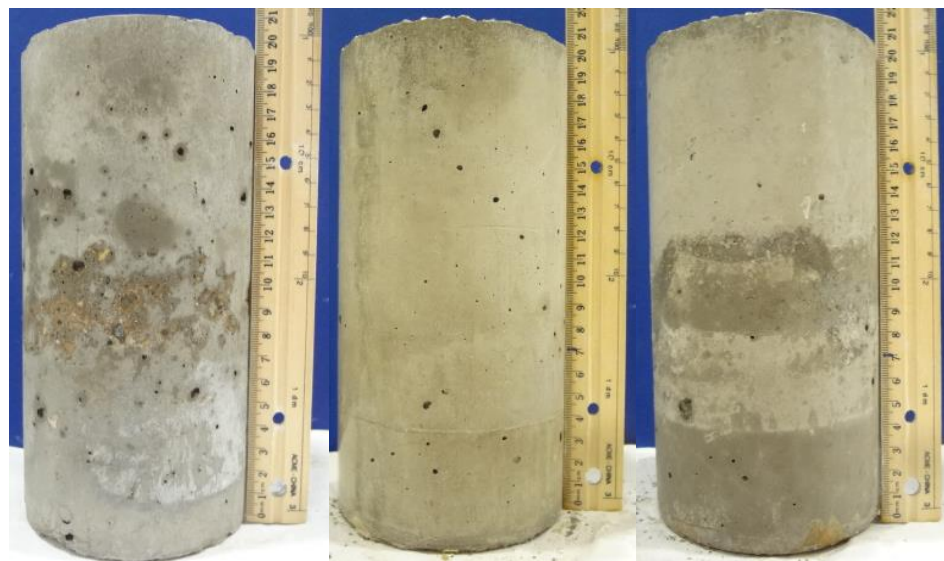
(a)   (b)   (c)
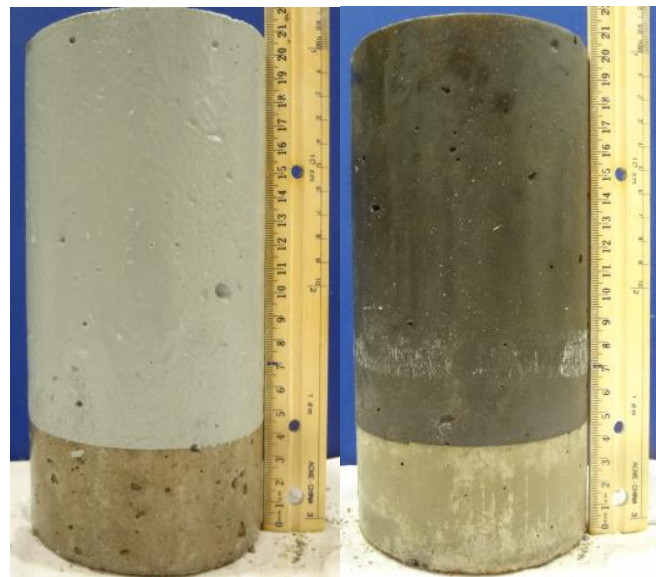
(d)   (e)

Figure 5.8: Cured concrete cylinders made with w/b = 0.45 after 6 months of physical sulphate exposure: (a) Non-coated and coated with; (b) silane (water-repellent); (c) acrylic solution (curing and sealer); (d) epoxy (membrane); and (e) bitumen (membrane).

The mass loss of concrete cylinders partially immersed in the 5 % sodium sulphate solution was monitored on a monthly basis. **Figures 5.8**; **5.9**; **5.10**; and **5.11** illustrate the mass loss for both coated and non-coated concrete cylinders after six months of exposure to physical sulphate attack.
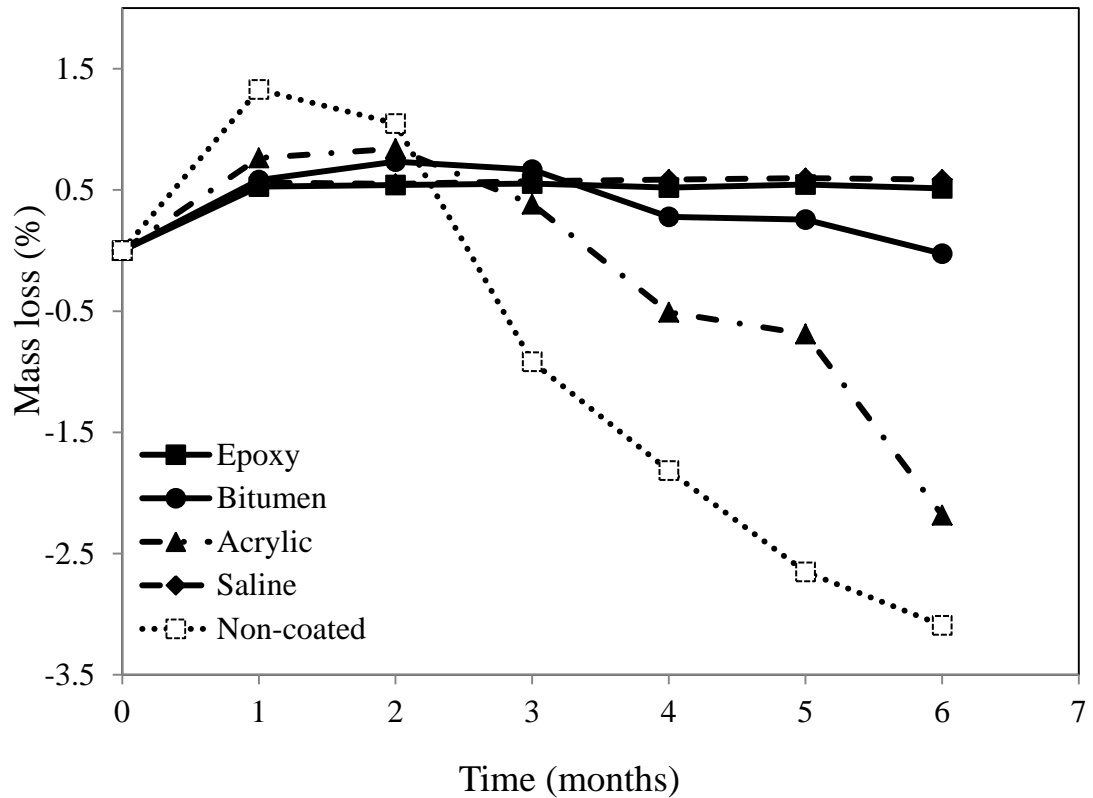
Figure 5.9: Mass loss of non-cured concrete cylinders made with w/b = 0.60.
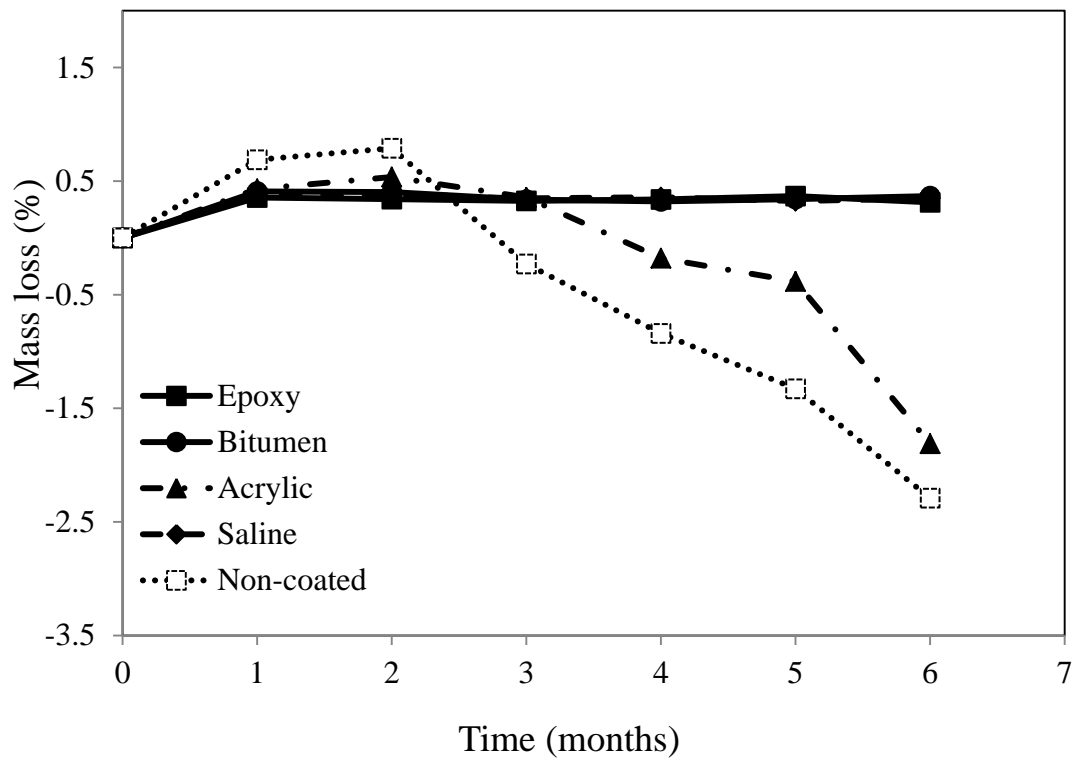
Figure 5.10: Mass loss of cured concrete cylinders made with w/b = 0.60.
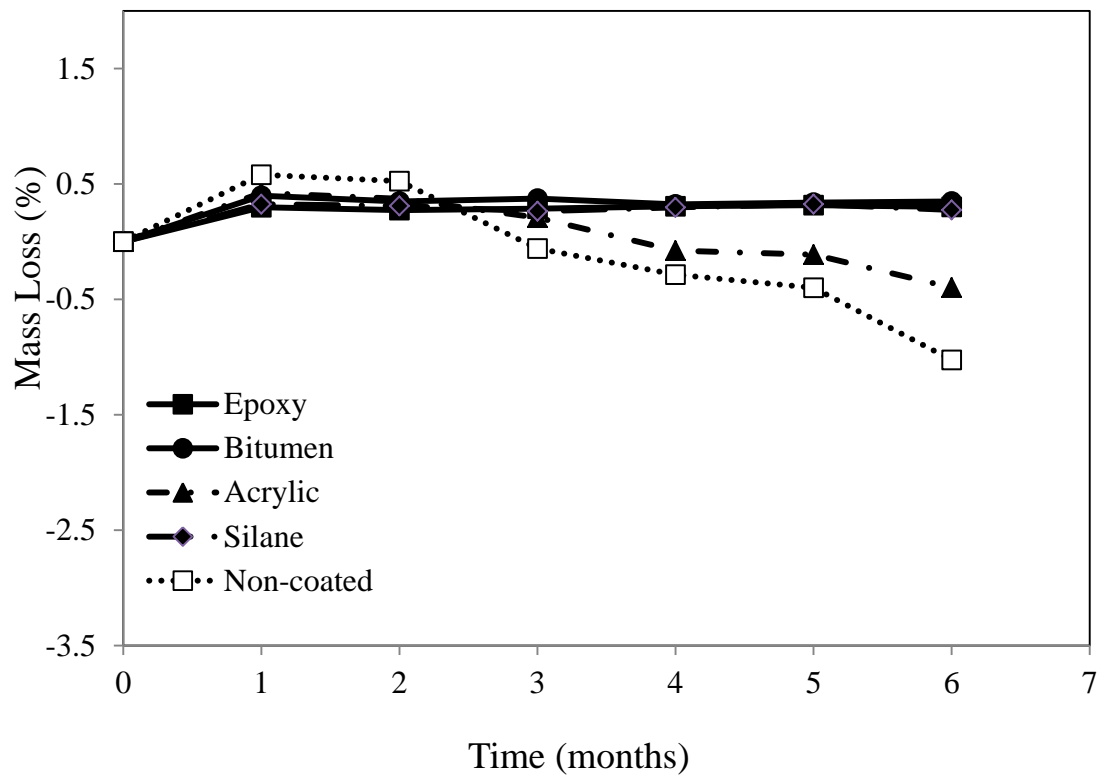
Figure 5.11: Mass loss of non-cured concrete cylinders made with w/b = 0.45.
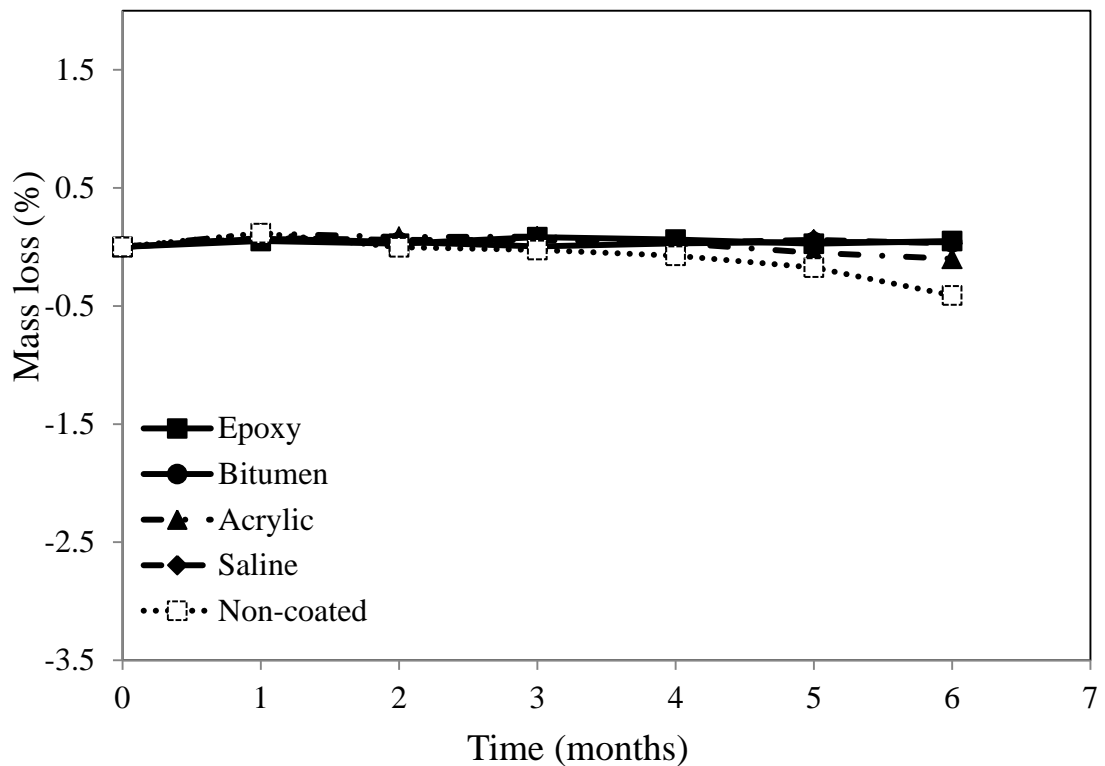
Figure 5.12: Mass loss of cured concrete cylinders made with w/b = 0.45.

During the first month, the concrete cylinders gained mass due to water absorption, especially for the non-coated high w/b cylinders having higher porosity. At later age, concrete cylinders started to lose mass. The highest mass loss occurred for the non-coated non-cured concrete cylinders made with w/b = 0.60, followed by the cured cylinders with the same w/b ratio. None of the cylinders made with w/b = 0.60 and coated with epoxy or silane experienced mass loss. Only those concrete cylinders coated with acrylic and those non-cured and coated with bitumen have experienced mass loss. For non-coated concrete cylinders made with w/b = 0.45, a similar trend was observed, but with significantly less mass loss. Moreover, none of the coated cylinders made with w/b = 0.45 experienced mass loss, except for those coated with the acrylic solution.

Mass loss occurred due to the degradation and surface scaling of the concrete above the solution level. The concrete portion immersed into the sodium sulphate solution was mostly in intact condition for all cylinders. **Figure. 5.11** shows SEM

image and XRD for the precipitated salt (thenardite) filling the pores on the concrete surface above the solution level. The concrete surface above the solution level was exposed to evaporation, which created supersaturation of the sodium sulphate solution. Hence crystals could grow from the supersaturated solution and exert high tensile pressure, thus leading to damage and mass loss of the concrete above the solution level. Therefore, monitoring the mass loss seems to be a useful indication of the performance of concrete exposed to physical sulphate attack.
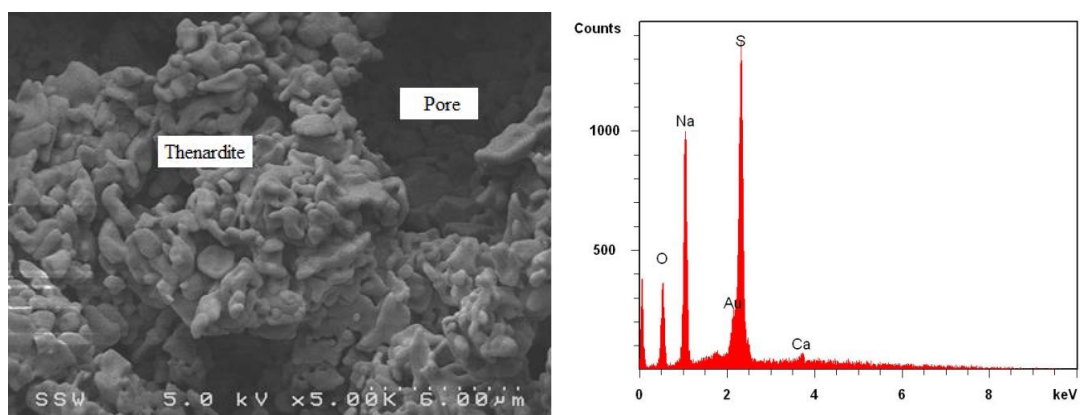
Figure 5.13: SEM and XRD analysis showing thenardite above the solution level.

5.4.1 Discussion

Using surface treatment materials has been a practical solution to improve the durability of concrete since most harmful agents penetrate into concrete through its surface. However, several studies have shown that the effectiveness of different types of surface treatment materials can vary depending on exposure conditions. For instance, a study by Aguiar *et al.,* (2008) showed poor performance under sulphate attack of concrete protected by a silicon agent compared with that of concrete coated with a water based acrylic. Conversely, under a chloride penetration test, the silicon agent better improved the performance of the concrete compared with the water based acrylic. Another study by Ibrahim, *et al.,* (1999) showed that using silane as a surface treatment material enhanced the durability of concrete that was fully immersed in a

sulphate solution compared to sodium silicate. However, the sodium silicate was found to provide better protection against carbonation. Therefore, caution is required to select the appropriate concrete coating material for different exposure conditions.

In the present study, since there is a lack of data on concrete exposed to physical sulphate attack, the effectiveness of various surface treatment materials was investigated for concrete partially immersed in a sulphate solution, an exposure that is conducive to damage by physical sulphate attack. The difference in the results observed can be mainly attributed to the different protection mechanisms provided by each of the surface treatment materials and the condition of the corresponding concrete substrate. For example, the epoxy coating provides a thick membrane on the concrete surface, which can be hardly penetrated by sulphates. Moreover, it eliminates the capillary water rise on the concrete surface. Therefore, salt crystals cannot precipitate in the sub-efflorescence zone where they can exert pressure within the concrete pores, thus eliminating damage. In addition, the used epoxy has adequate bond and mechanical properties that can enhance the concrete surface. For instance, the tensile strength of the epoxy is 20.7 MPa according to ASTM D638 (Standard Test Method for Tensile Properties of Plastic) and the flexural strength is 29.6 MPa according to ASTM C580 (Standard Test Method for Flexural Strength and Modulus of Elasticity of Chemical-Resistant Mortars, Grouts, Monolithic Surfacing, and Polymer Concretes).

Regarding the bitumen base coating, it provides similar protection for concrete to that of epoxy since it forms a thick membrane on the concrete surface. Moreover, it has a high tensile elongation (600%) according to ASTM D412 (Standard Test Methods for Vulcanized Rubber and Thermoplastic Elastomers-Tension), which can accommodate the strains exerted by salt crystals. However, in the case of the non-cured concrete with a high w/b = 0.60, the bitumen layer had separated from the concrete surface. Generally, in hydrated cement paste, water can exist in capillary pores as absorbed water, interlayer water, and chemically combined water (Mehta and Monteiro, 2006). The amount of free water increases with increasing w/b. In addition, at early age, the amount of free water is high compared with that in lower porosity fully hydrated concrete. Such capillary pores are typically interconnected with the surface. Thus, when high porosity concrete is coated at early-age, water molecules

may entrap between the bitumen coating layer and the substrate, leading to emulsification of the bitumen and its separation. This did not occur for the epoxy based coating which provides a similar protection mechanism, but has much stronger adhesion to the substrate than the bitumen base coating and is not vulnerable to emulsification. Previous investigation by Price (1989) on different types of water proofing systems showed excellent adhesion and bond of epoxy based coating systems to concrete surface compared to that of bitumen based systems.

Concrete cylinders coated with the water-based acrylic coating exhibited slightly less damage than that of the non-coated cylinders. This can be attributed to the fact that the acrylic solution acts as a curing and sealing compound, thus, protecting the concrete against its surrounding environment by partially filling the concrete surface pores and creating a thin membrane (Vipulanandan *et al.,* 2011; Al-Gahtani *et al.,* 1999; Radlinska *et al.,* 2012). However, the acrylic solution did not provide an adequate protection to concrete since it was completely damaged after 2 months of exposure to physical sulphate attack, as shown in **Figure 5.3**. Previous study by Moreira *et al.,* (2006) showed poor performance of water-based acrylic resin under capillary absorption compared with other types of surface treatment materials. This agrees with findings of the present study since concrete cylinders coated with acrylic gained more mass in the beginning of the experiment than the other coated cylinders. It is also possible that the acrylic solution partially fill the concrete surface pores, allowing salt crystals to grow and damage the acrylic film. In addition, acrylic is a relatively brittle material (Zhu and Chai, 2010; Radlinska *et al.,* 2012) and may not sustain the strains due to salt crystallization.

The silane water-repellent agent achieved excellent protection of the concrete against physical sulphate attack since none of the cylinders (cured and non-cured) coated with silane have experienced surface scaling or mass loss. The protection mechanism of silane is different from that of the other coating materials tested in this study as it penetrates the concrete surface and chemically reacts within the concrete pores, providing molecules that perform as a water repellent (Vipulanandan *et al.,* 2011; Henry, 2004). Thus, it can prevent the water that contains sulphates from entering into the concrete pores, mitigating capillary rise and salt crystallisation. However, previous studies have shown that the performance of water repellant agents

can vary depending on their formulation and type of application. For instance, Villegas and Vale (1993) showed that under a salt weathering test, organosilicic (water-repellent) products provide better protection to limestone used in historical monuments than other water-repellent products of different formulations. Another study by Zhu *et al.* (2013) found that using surface water-repellent agents is more effective to reduce capillary absorption than using integral water-repellent agents added to the concrete mixtures. Thus, choosing the appropriate water-repelling agent for a certain environmental exposure requires past experience and knowledge of its performance under similar exposure.

5.5 Conclusions

The resistance to physical sulphate attack of concrete cylinders made with w/c = 0.45 and 0.60, both cured and non-cured, and coated with different types of surface treatment materials has been investigated in this chapter. The following conclusions can be drawn based on the experimental results.

- Reducing the w/c ratio improved the performance of concrete exposed to physical sulphate attack since less salt growth can form through the concrete pore space leading to less damage.

- Epoxy- and silane-based surface treatment materials were found to be adequate for protecting both cured and non-cured concrete exposed to physical sulphate attack. Epoxy provides a thick protective membrane on the concrete surface, which can be hardly penetrated by sulphates, thus mitigating capillary rise on the concrete. Conversely, silane penetrates the concrete surface and chemically reacts within the concrete pores, providing molecules that perform as a water repellent.

- For the surface treatment material based on bitumen, it was found that adequate curing of the concrete before coating is important to eliminate the separation of the bitumen and enhance the resistance of concrete to physical sulphate attack.

- Using a water-based solid acrylic polymer resin did not provide an adequate protection of concrete against physical sulphate attack.

- Designing concrete that is durable to both chemical and physical sulphate attack should entail lowering the w/c ratio and/or creating a barrier between the ground water and the above ground portion of concrete exposed to capillary rise and evaporation.

5.6 References

Aguiar, J. B., Camoes, A., and Moreira, P. M., (2008), "Performance of concrete in aggressive environment" , *Concrete Structures and Materials*, Vol. 2, No. 1, pp. 21-25.

Al-Gahtani, A., Ibrahim, M., Maslehuddin, M., and Almusallam, A. A., (1999), "Performance of concrete surface treatment systems", *Concrete International,* Vol. 21, No. 1, pp. 64-68.

ASTM C192 (2012), "Standard Practice for Making and Curing Concrete Test specimens in the Laboratory", American Society for Testing and Materials ,West Conshohocken, PA.

ASTM C511, (2009), "Standard Specification for Mixing Rooms, Moist Cabinets, Moist Rooms, and Water Storage Tanks Used in the Testing of Hydraulic Cements and Concretes", American Society for Testing and Materials ,West Conshohocken, PA.

ASTM C580, (2012), "Standard Test Method for Flexural Strength and Modulus of Elasticity of Chemical-Resistant Mortars, Grouts, Monolithic Surfacing, and Polymer Concretes", American Society for Testing and Materials ,West Conshohocken, PA.

ASTM D4404, (2010), "Standard Test Method for Determination of Pore Volume and Pore Volume Distribution of Soil and Rock by Mercury Intrusion Porosimetry", American Society for Testing and Materials ,West Conshohocken, PA.

ASTM D638, (2010), "Standard Test Method for Tensile Properties of Plastics", *American Society for Testing and Materials* ,West Conshohocken, PA.

ASTM D412, (2013), "Standard Test Methods for Vulcanized Rubber and Thermoplastic Elastomers-Tension", American Society for Testing and Materials ,West Conshohocken, PA.

Aye, T., Oguchi, C. T., (2011), "Resistance of plain and blended cement mortars exposed to severe sulfate attacks", *Construction and Building Materials,* Vol. 25, No. 6, pp. 2988-2996.

Haynes, H., O'Neill, R., and Mehta, P. K. (1996), "Concrete deterioration from physical attack by salts", *Concrete international*, Vol. 18, No. 1, pp. 63-68.

Haynes, H., (2002), "Sulfate attack on concrete: Laboratory versus field experience", *Concrete International,* Vol. 24, No. 7, pp. 64-70.

Haynes, H., O'Neill, R., Neff, M. and Mehta, P. K., (2008), "Salt weathering distress on concrete exposed to sodium sulfate environment", *ACI Materials Journal*, Vol. 105, No. 1, pp. 35-43.

Hawkins, P. J., (1985), "The use of surface coating to minimize carbonation in the middle east" *Proceedings of 1ˢᵗ International Conference on Deterioration and Repair of Reinforced Concrete in the Arabian Gul,* Bahrain, pp. 273-285.

Henry, G., (2004), "Pentrating water-repplent sealers", *Concrete International,* Vol. 26, No. 5, pp. 81– 83.

Hime, W. G., Martinek, R. A., Backus, L. A., and Marusin, S. L., (2001), "Salt hydration distress", *Concrete International* , Vol. 23, No. 10, pp. 43-50.

Ibrahim, M., Al-Gahtani, A., Maslehuddin, M., and Dakhil, F., (1999), "Use of surface treatment materials to improve concrete durability", *Journal of Materials in Civil Engineering,* Vol. 11, No. 1, pp. 36-40.

Irassar, E. F., Di Maio, A., and Batic, O. R., (1995), "Sulfate attack on concrete with mineral admixtures", *Cement and Concrete Research,* Vol. 26, No. 1, pp. 113-123.

Malhotra, V. M, Carette, G., and Bremner, T., (1987), "Durability of concrete containing supplementary cementing materials in marine environment" SP-100-63, pp. 1227-1258..

Moreira, P. M., Aguiar, J. B., and Camoes, A., (2006), "Systems for superficial protection of concretes", *International Symposium Polymers in Concrete*, University of Minho, Portugal pp. 225– 236.

Nehdi, M., and Hayek, M., (2005), "Behavior of blended and cement mortars exposed to sulfate solutions cycling in relative humidity", *Cement and Concrete Research,* Vol. 35, No. 4, pp. 731-742.

Radlinska, A., McCarthy, L., Yost, J., Matzke, J. and Nagel, F. (2012), " Coatings and treatments for beam ends," Final Technical Report, FHWA-PA-2012-002-100402, Pennsylvania Department of Transportation, 134 p.

Scherer, G. W., (2004), "Stress from crystallization of salt", *Cement and Concrete Research*, Vol. 34, No. 9, pp.1613– 1624.

Stark, D., (1989), "Durability of concrete is sulfate-rich soils", *Research and Development Bulletin*, Portland Cement Association, Vol. RD097, 19p.

Swamy, R. N., Suryavanshi, A. K. and Tanikawa, S., (1998), "Protective ability of an acrylic-based surface coating system against chloride and carbonation penetration into concrete", *ACI Materials Journal*, Vol. 95, No. 2, pp.101– 112.

Tsui, N., Flatt, R. J., and Scherer, G. W., (2003), "Crystallization damage by sodium sulfate", *Journal of Cultural Heritage,* Vol. 4, No. 2, pp. 109-115.

Villegas, R., Vale, J. F., (1993), "Evaluation of water repellent treatments applied to stones used in andalusian cathedrals. II. Salt crystallization test", *Materials De Construction ,* Vol. 43, No. 230, pp. 5-13.

Vipulanandan, M., Parihar, A., Issac, M., (2011), "Testing and modeling composite coatings with silanes for protecting reinforced concrete in saltwater Environment", *Jouranl of Materials in Civil Engineering,* Vol. 23, No. 12, pp.1602– 1608.

Yoshida, N., Matsunami, Y., Nagayama, M., and Sakai, E., (2010), "Salt weathering in residential concrete foundation exposed to sulfate-bearing ground", *Journal of Advanced Concrete,* Vol. 8, No. 2, pp. 121-134.

Zhu, S., Chai, G. B., (2010), "Ductile and brittle material failures in low-velocity impact", *Journal of Materials Design and Applications,* Vol. 224, No. 4, pp. 162-172.

Zhu, Y., Kou, S., Poon, C., Dai, J., and Li, Q., (2013), "Influence of silane-based water repellent on the durability properties of recycled aggregate concrete ", *Cement and Concrete Composites,* Vol. 35, No. 1, pp. 32-38.

EFFECT OF SUPPLEMENTARY CEMENTITIOUS MATERIALS ON DURABILITY OF CONCRETE EXPOSED TO PHYSICAL SULPHATE ATTACK

6.1 Introduction

Several studies have shown that partially replacing Portland cement with supplementary cementitious materials (SCMs) significantly improved the durability of concrete under chemical sulphate attack (Al-Amoudi, 2002; Hooton, 1993; Al-Akhras, 2006; Nehdi and Hayek, 2005; Ramezanianpour and Jovein, 2012). For instance Al-Akhras, (2006) studied the effect of cement replacement with metakaolin and found that the sulphate resistance of concrete fully immersed in a sulphate solution increased with increasing the cement replacement level. Another study by Hooton (1993) showed that partially replacing cement with silica fume provided an excellent resistance to sulphate attack under ASTM C1012 (Standard Test Method for Length Change of Hydraulic-Cement Mortars Exposed to a Sulphate Solution). In addition, design specifications including ACI 318 recommend using pozzolanic materials for concrete exposed to severe sulphate exposure since SCMs decrease the porosity of concrete and reduce permeability and the ingress of sulphate ions into concrete.

Sulphate ions chemically interact with the cement paste components leading to expansion, cracking and loss of adhesion of the cement hydration products due formation of ettringite, gypsum, and thaumasite (Mehta, 2000). When cement partially replaced with pozzolanic minerals, concrete durability can be improved since pozzolanic minerals consume the products that are to chemical sulphate attack (e.g. calcium hydroxide) through pozzolanic reactions and reduce the total amount of tricalcium aluminate (Mehta and Monteiro, 2006).

However, the effect of SCMs in concrete exposed to physical sulphate attack is controversial. Indeed, there are only limited studies which investigated the performance of concrete when exposed to an environment prone to physical sulphate attack. Therefore, in the present chapter, the influence of using different types and percentages of pozzolanic minerals on the deterioration of concrete due to physical sulphate attack was explored.

6.2 Experimental Program

6.2.1 Materials and Specimen Preparation

Thirteen concrete mixtures were prepared according to ACI 211.1 to investigate the influence of cement replacement with pozzolanic minerals on the physical sulphate attack. The proportions of the concrete mixtures are provided in **Table 6.1**.

Table 6.1: Proportions of tested concrete mixtures.

Mixture #	Binder	Cement Content (kg/m3)	Pozzolanic Content (kg/m3)	Aggregate Content (kg/m3)	
				Coarse	Fine
1	OPC	350	0	1110	804
2		332.5	17.5		784
3	OPC + FA	315.0	35.0	1110	763
4		297.5	52.5		745
5		280.0	70.0		780
6		332.5	17.5		779
7	OPC + SF	315.0	35.0	1110	750
8		297.5	52.5		740
9		280.0	70.0		735
10		332.5	17.5		791
11	OPC + MK	315.0	35.0	1110	740
12		297.5	52.5		730
13		280.0	70.0		719

For each of the thirteen concrete mixtures, standard cylinders 100×200 mm (4×8 in.) were cast according to ASTM C192 (Standard Practice for Making and Curing Concrete Test Specimens in the Laboratory). Concrete cylinders from each concrete mixture were cured for 28 days in a moist room at RH ≥ 95% and T = 20°C [68°F]

before exposure to the sulfate environment.. The curing was carried out according to ASTM C511 (Standard Specification for Mixing Rooms, Moist Cabinets, Moist Rooms, and Water Storage Tanks Used in the Testing of Hydraulic Cements and Concretes).

6.2.2 Environmental Exposure Conditions

Concrete specimens were exposed to a similar environment condition that used in Chapter 3.

6.3 Results and Discussion

After two days of exposure to a temperature of 20°C [68°F] and RH of 82%, salt precipitation (efflorescence) appeared above the solution level on the drying surface of the concrete cylinders as shown in **Figures 6.2** to **6.5**. This exposure condition is considered as an ideal environment for mirabilite formation according to previous studies (Thaulow and Sahu, 2004; Flatt, 2002; Haynes, *et al.*, 2008). After one week, the exposure was switched to a temperature = 40°C [104°F] and RH = 31%, a condition conducive for thenardite formation. During the second week, the volume of the precipitated salt on the concrete surface decreased compared to that in the first week of exposure. This is related to the transformation of the formed mirabilite to thenardite which results in a volume contraction of about 314% (Tsui *et al.*, 2003).
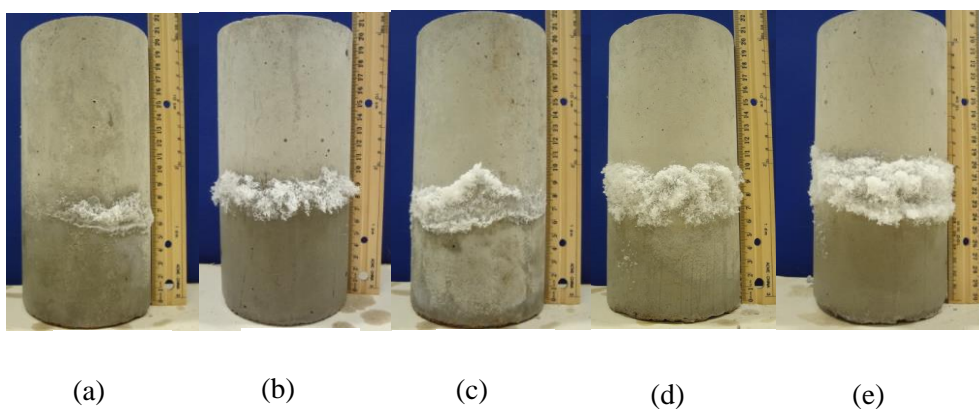
(a)   (b)   (c)   (d)   (e)

Figure 6.1: Salt crystallisation for concrete made with: (a) OPC; (b) OPC + 5% FA; (c) OPC + 10% FA; (d) OPC + 15% FA; and (e) OPC + 20% FA.

<div align="center">(a)   (b)   (c)   (d)   (e)</div>

Figure 6.2: Salt crystallisation for concrete made with: (a) OPC; (b) OPC + 5% MK; (c) OPC + 10% MK; (d) OPC + 15% MK; and (e) OPC + 20% MK.
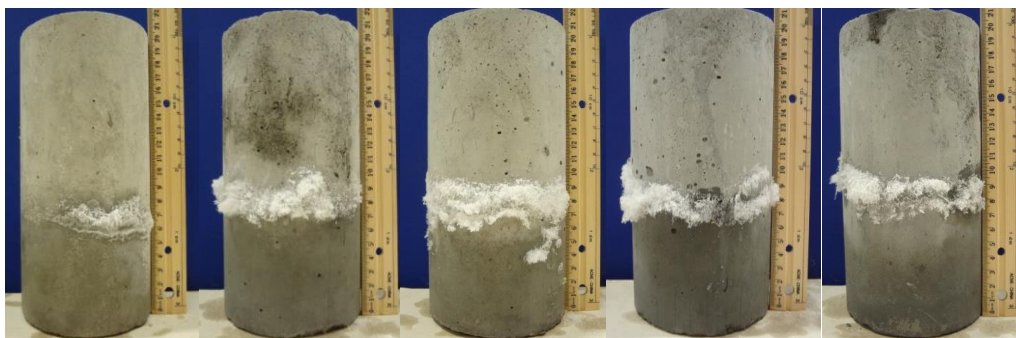
<div align="center">(a)   (b)   (c)   (d)   (e)</div>

Figure 6.3: Salt crystallisation for concrete made with: (a) OPC; (b) OPC + 5% SF; (c) OPC + 10% SF; (d) OPC + 15% SF; and (e) OPC + 20% SF.

The exposure was continued for up to six months (24 cycles of wetting and drying) and all concrete cylinders were inspected to diagnose the level of damage. For all tested cylinders, the portion of concrete immersed in the sulphate solution was found in intact condition compared with the damaged above solution part. **Figures 6.5**, **6.6**, and **6.7** show the typical concrete damage above the solution level.

(a)　　　(b)　　　(c)　　　(d)　　　(e)

Figure 6.4: Damage due to salt crystallisation for concrete made with:
(a) OPC; (b) OPC + 5% FA; (c) OPC + 10% FA; (d) OPC + 15% FA;
and (e) OPC + 20% FA.

(a)　　　(b)　　　(c)　　　(d)　　　(e)

Figure 6.5: Damage due to salt crystallisation for concrete made with:
(a) OPC; (b) OPC + 5% MK; (c) OPC + 10% MK; (d) OPC + 15% MK;
and (e) OPC + 20% MK.

<div align="center">(a)   (b)   (c)   (d)   (e)</div>
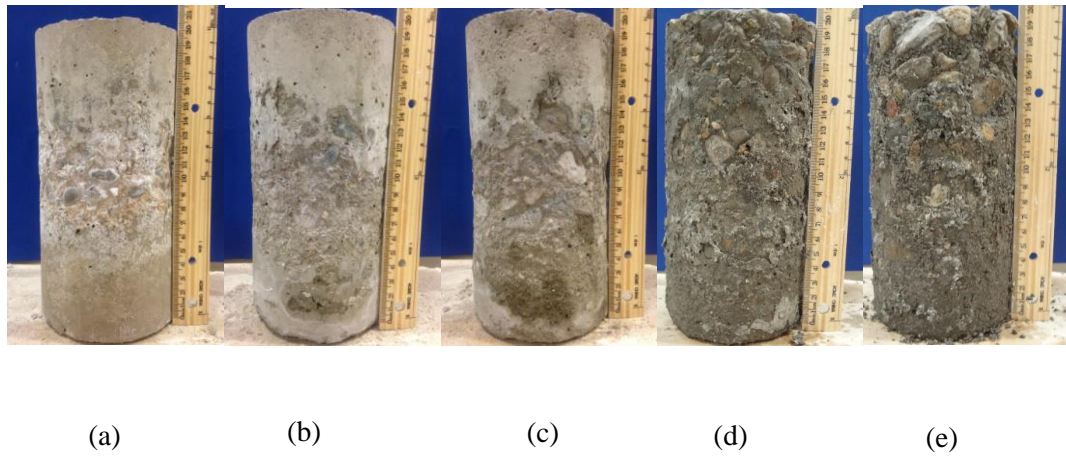
Figure 6.6: Damage due to salt crystallisation for concrete made with: (a) OPC; (b) OPC + 5% SF; (c) OPC + 10% SF; (d) OPC + 15% SF; and (e) OPC + 20% SF.

The mass loss was monitored for all concrete cylinders that have been partially immersed in the sodium sulphate solution and exposed to cyclic temperature and RH. **Figures 6.8**, **6.9**, and **6.10**, illustrate the mass loss after 6 months of exposure to physical sulphate attack. The mass loss occurred due to scaling of the concrete surface above the solution level. The immersed portion of concrete into the sodium sulphate solution was mostly in intact condition. Both the surface scaling and mass loss increased with increasing the partial replacement level of cement by pozzolanic minerals.
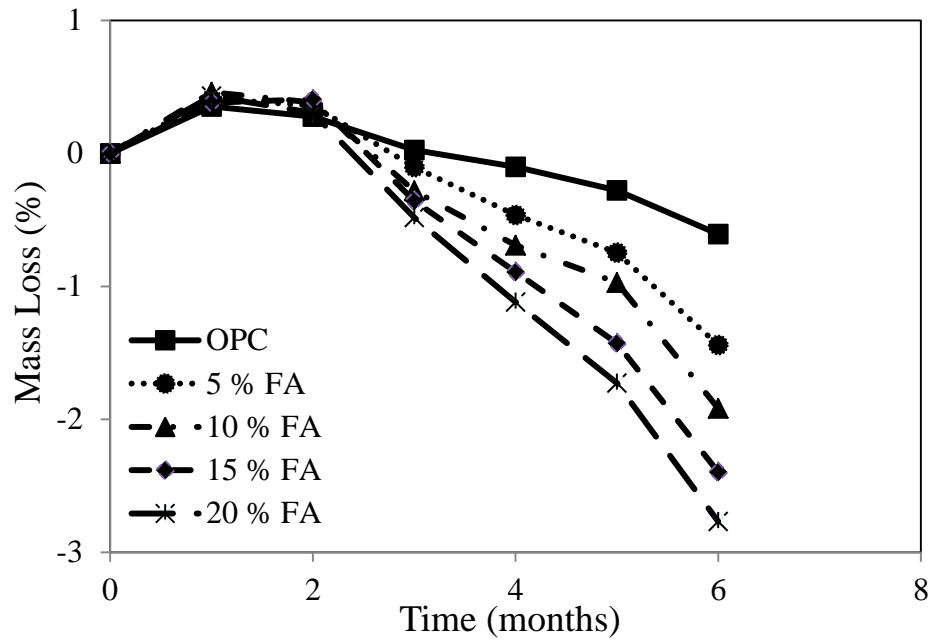
Figure 6.7: Mass loss for concrete cylinders (cement partially replaced with FA).
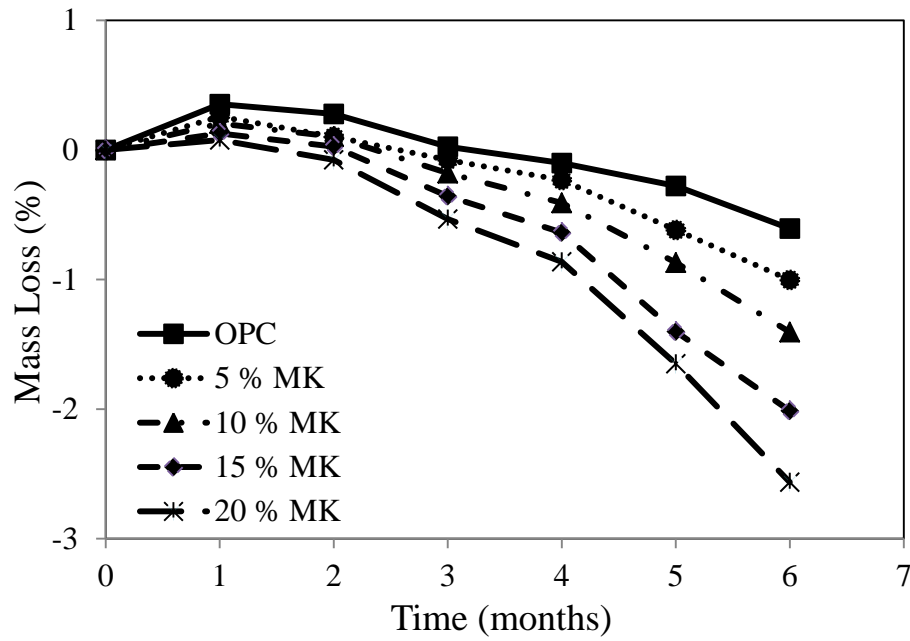
Figure 6.8: Mass loss for concrete cylinders (cement partially replaced with MK).
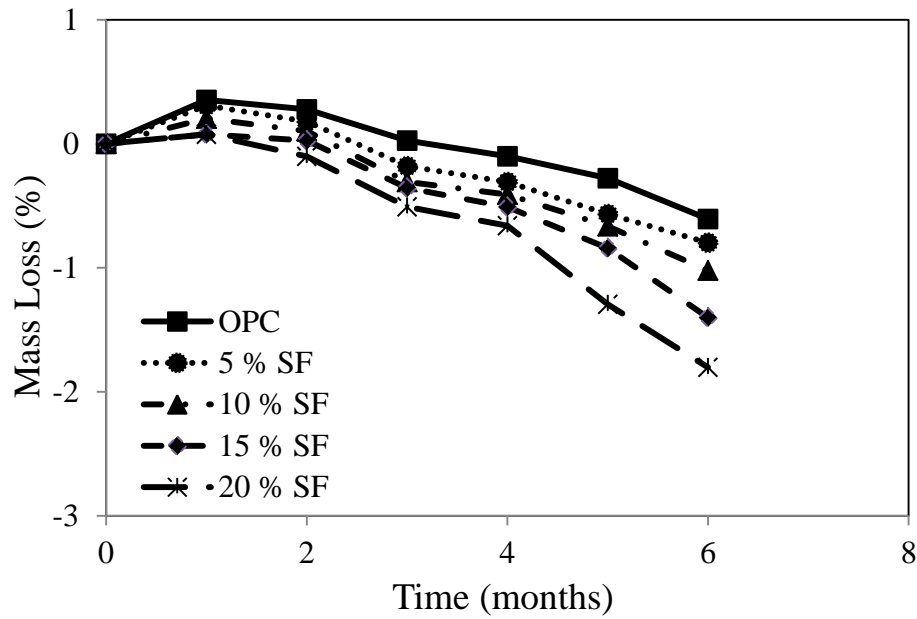
Figure 6.9: Mass loss for concrete cylinders (cement partially replaced with SF).

Figures 6.10 to 6.13 show the MIP results for different concrete mixtures. **Table 6.2** shows the average pore size and mercury intrusion for the concrete specimens. Results indicate that concrete made with 100% OPC incorporated pores with relatively larger diameter. Partially replacing the cement with pozzolanic minerals led to a decrease in the average pore size diameter due to the pore refinement effect of pozzolanic minerals. For instance, the average pore size decreased from 0.058 in the case of 100 % OPC to 0.048, 0.410, and 0.038 when 20 % of cement partially replaced by FA, MK, and SF respectively. In addition, **Figures 6.10 to 6.13** show that the percentage of pores with diameter smaller than 0.10 μm was significantly increased by increasing the replacement level of cement by SCMS. This can lead to higher capillary rise since according to **Eq. 6** (Young *et al.,* 2006) the capillary rise on the concrete surface is inversely proportional to the size of the pores on the concrete surface.

$$h = \frac{2\gamma_{LV} \, Cos\theta}{rg\rho} \qquad (6.1)$$

Where; γ_{LV} is the liquid/vapor interfacial energy,

Θ is the contact angle,

r is the pore radius,

g is the gravitational acceleration, and ρ is the density of the solution.

The surface of concrete above the solution level is exposed to evaporation, which creates super-saturation of the sodium sulphate solution (Scherer, 2004). By increasing the capillary height, a larger amount of the solution can be exposed to evaporation, leading to higher supersaturation. Therefore, crystals can exert higher stress than in the case of less capillary rise, leading to larger damage and mass loss of the concrete above the solution level. According to Thaulow and Sahu (2004), crystals that grow from only a saturated condition cannot exert sufficient pressure to disrupt the concrete pores. However, in the case of supersaturation, crystals can grow and exert higher pressure, leading to greater damage. The degree of the supersaturation depends on several factors including evaporation, the rate of solution supply, and the type of salt (Scherer, 2004). Evaporation can increase the degree of the supersaturation since more crystals can grow compared with the saturated condition.

Higher damage occurred in the case of partially replacing Portland cement with fly ash than in the case of using metakaolin and silica fume, respectively. According to Uchikawa (1986), partially replacing cement with fly ash can delay cement hydration reactions since fly ash absorbs calcium Ca^{2+} ions; unlike silica fume, which accelerates the hydration and increases the concrete solid volume at early-age. Therefore, higher pores connectivity can be expected for the concrete incorporating fly ash at the beginning of the exposure, thus leading to higher capillary rise. This is demonstrated by MIP results, which showed higher intrusion volume of mercury in the case of concrete incorporating fly ash than in the case of concrete made with silica fume or metakaolin.
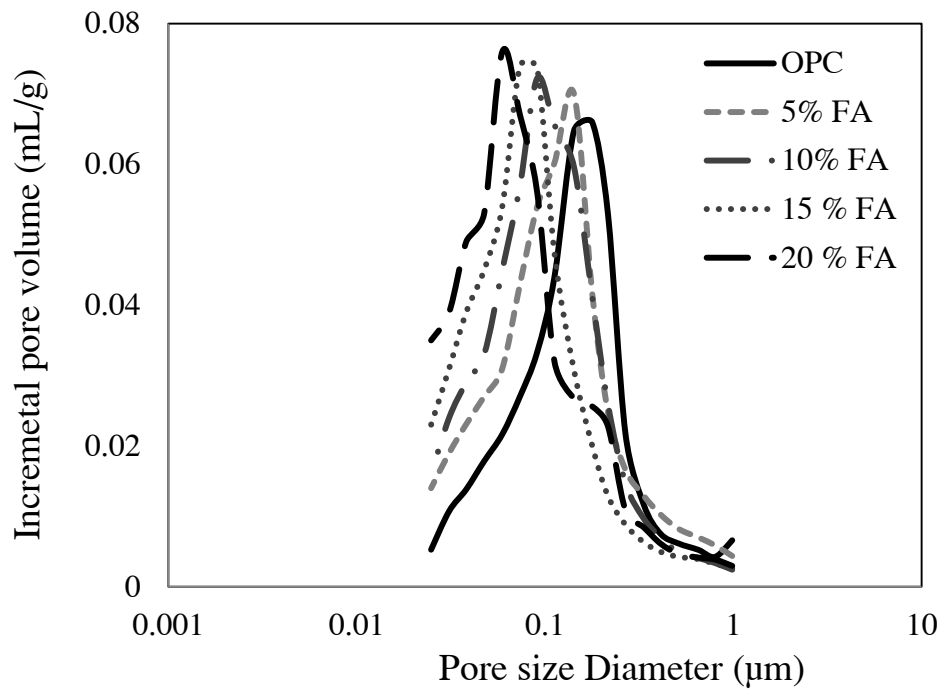
Figure 6.10: MIP results for concrete mixtures before exposure to physical sulphate attack (OPC and OPC + FA).
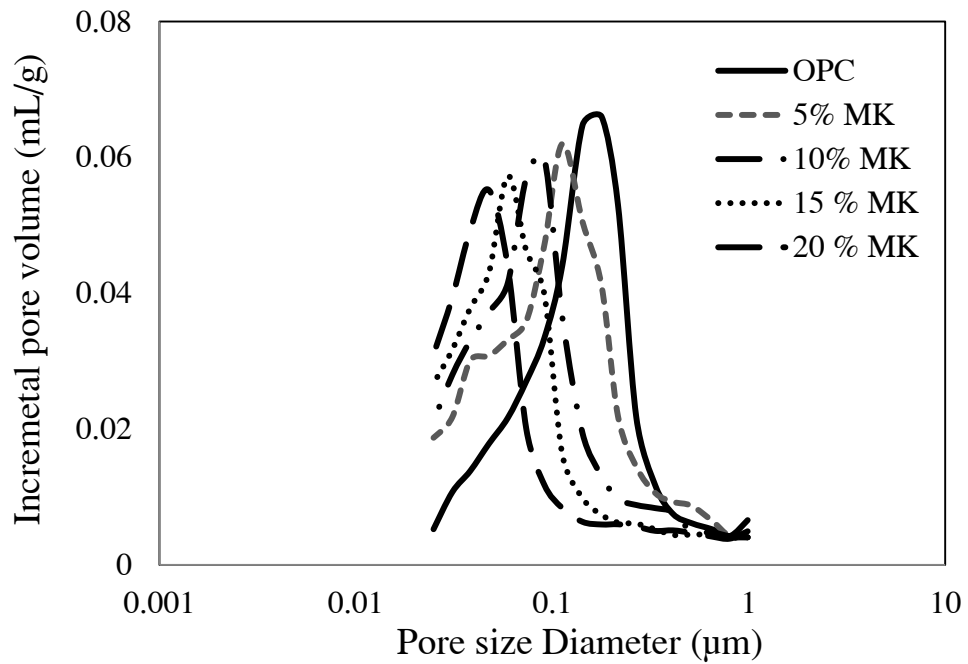
Figure 6.11: MIP results for concrete mixtures before exposure to physical sulphate attack (OPC and OPC + MK).
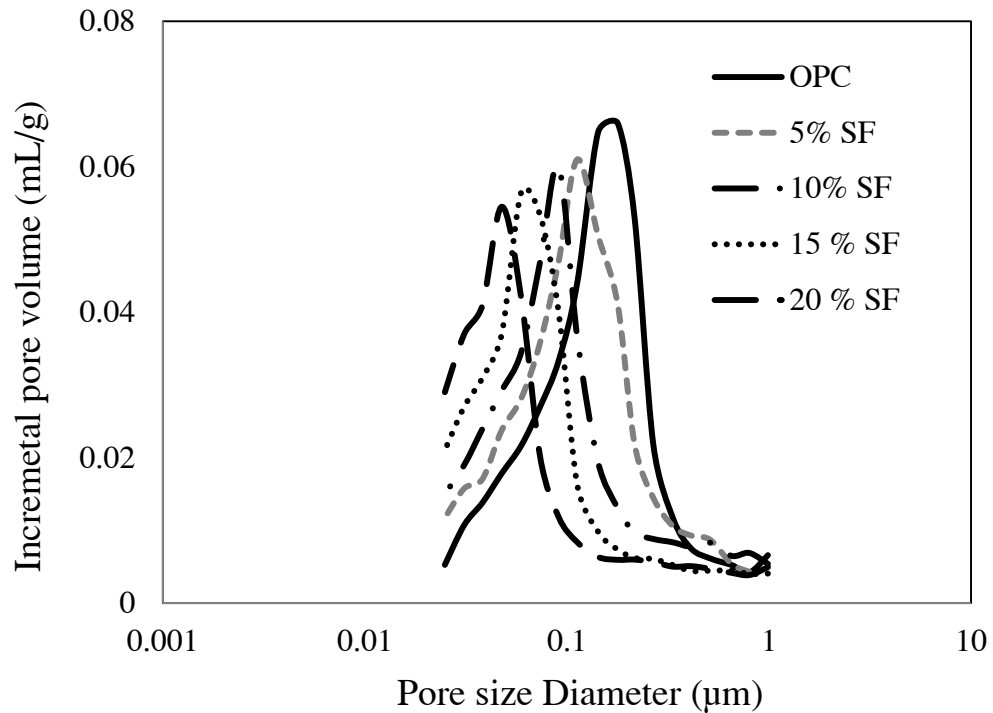
Figure 6.12: MIP results for concrete mixtures before exposure to physical sulphate attack (OPC and OPC + SF).

Table 6.2 shows the average pore size and mercury intrusion for the concrete specimens

	Average Pore Diameter (μm)	Total Intrusion Volume (m/Lg)
OPC	0.058	0.066
5% FA	0.056	0.070
10% FA	0.054	0.072
15 % FA	0.051	0.075
20 % FA	0.048	0.078
5% MK	0.051	0.062
10% MK	0.047	0.059
15% MK	0.043	0.057
20% MK	0.410	0.052
5% SF	0.049	0.061
10% SF	0.045	0.059
15% SF	0.041	0.056
20% SF	0.038	0.054

The results show that the vulnerability of concrete to damage by physical salt weathering depends on its pore structure, which is similar to stones. Previous studies have shown that stones with higher volume of connected small pores are the most vulnerable to damage by salt crystallization (Wellman and Wilson, 1965; Angeli *et al,* 2008; Navarro and Doehne, 1999). The presence of small pores increases the capillary rise and the surface area of evaporation, leading to higher supersaturation of the pore solution and subsequently more damage (Navarro and Doehne, 1999).

6.4   Conclusions

This experimental study shows that partially replacing portland cement with pozzolanic minerals can be a disadvantage under physical sulphate attack since the damage was intensified by increasing the percentage of cement replacement, unlike in the case of concrete exposed to chemical sulphate attack. Therefore, current standards and specifications should reconsider the use of the pozzolanic minerals in concrete exposed to severe sulphate environments characterized by cycling temperature and relative humidity and prone to physical sulphate attack.

6.5 References

Al-Amoudi, O. S. B., (2002), "Attack on plain and blended cement exposed to aggressive sulfate environment", *Cement and Concrete Composites*, Vol. 24, No. 3, pp. 305-316.

Angeli, M., Benavente, D., Bigas, J., Menendez, B., Hebert, R., David, C., (2008), "Modification of the porous network by salt crystallization in experimentally weathered sedimentary stones", *Materials and Structures*, Vol. 41, No. 6, pp. 1091-1108.

Al-Akhras, N. M., (2006), "Durability of metakaolin concrete to sulfate attack ," *Cement and Concrete Research*, Vol. 36, No. 9, pp. 1727-1734.

ASTM C511., (2009), Standard Specification for Mixing Rooms, Moist Cabinets, Moist Rooms, and Water Storage Tanks Used in the Testing of Hydraulic Cements and Concretes, *American Society for Testing and Materials* ,West Conshohocken, PA.

ASTM D4404., (2010), Standard Test Method for Determination of Pore Volume and Pore Volume Distribution of Soil and Rock by Mercury Intrusion Porosimetry, *American Society for Testing and Materials* ,West Conshohocken, PA.

ASTM C1012, (2009), Standard Test Method for Length Change of Hydraulic-Cement Mortars Exposed to a Sulfate Solution, *American Society for Testing and Materials*, West Conshohocken, PA.

ASTM C192, (2009), Standard Practice for Making and Curing Concrete Test Specimens in the Laboratory, *American Society for Testing and Materials*, West Conshohocken, PA.

Buj, O., and Gisbert, J., (2010), "Influence of pore morphology on the durability of sedimentary building stones from Aragon (Spain) subjected to standard salt decay tests", *Environment Health Sicence,* Vol. 61, No. 7, pp. 1327-1336.

Flatt, R. J., (2002), "Salt damage in porous materials: how high supersaturations are generated", *Journal of Crystal Growth,* Vol. 242, No. 3-4, pp. 435-454.

Haynes, H., O'Neill, R., and Mehta, P. K. (1996), "Concrete deterioration from physical attack by salts", *Concrete International*, Vol. 18, No. 1, pp. 63-68.

Haynes, H., O'Neill, R., Neff, M. and Mehta, P. K. (2008), "Salt weathering distress on concrete exposed to sodium sulfate environment", *ACI Materials Journal*, Vol. 105, No. 1, pp. 35-43.

Haynes, H., O'Neill, R., Neff, M. and Mehta, P. K. (2010), "Salt weathering of concrete by sodium carbonate and soduim chloride", *ACI Materials Journal*, Vol. 107, No. 3, pp. 258-266.

Hooton, R. D. (1993) " Influence of silica fume replacement of cement on physical properties and resistance of sulfate attack, freezing and thawing, and alkali-silica reactivity", *ACI Materials Journal*, Vol. 90, No. 2, pp. 143-151.

Mehta, P. K., (2000), "Sulfate attack on concrete: Separating myths from reality", *Concrete International,* Vol. 22, No. 8, pp. 57-61.

Mehta, P. K., and Monteiro, P. J. M., (2006), Concrete Microstructure, Properties, and Materials", *McGraw-Hill,* Third Edition, 659 p.

Navarroa, C. R., and Doehnea, E., (1999), "Salt weathering: influence of evaporation rate, supersaturation, and crystallization pattern", *Earth Surface Processes and Landforms,* Vol. 24, No. 3, pp. 191-209.

Nehdi, M., and Hayek, M., (2005), "Behavior of blended cement mortars exposed to sulfate solutions cycling in relative humidity", *Cement and Concrete Research,* Vol. 35, No. 4, pp. 731-742.

Duan, P., Shui, Z., Chen, W., and Shen, C., (2013), "Effects of metakaolin, silica fume and slag on pore structure, interfacialtransition zone and compressive strength of concrete", *Construction and Building Material,* Vol. 44, pp. 1-6.

Ramezanianpour, A. A, and Jovein, H. B., (2012), "Influence of metakaolin as supplementary cementing material on strength and durability of concretes", *Construction and Building materials ,* Vol. 30, pp. 470-479.

Santhanam, M., Cohen, MD., Olek, J., (2001), "Sulfate attack research − whither now?", *Cement and Concrete Research,* Vol. 31, No. 6, pp. 845-51

Scherer, G. W., (2004), "Stress from crystallization of salt", *Cement and Concrete Research*, Vol. 34, No. 9, pp. 1613– 1624.

Thaulow, N., Sahu, S., (2004), "Mechanism of concrete deterioration due to salt crystallization", *Materials Characterization,* Vol. 53, No. 2-4, pp. 123-127.

Tsui, N., Flatt, R. J., and Scherer, G. W., (2003), "Crystallization damage by sodium sulfate", *Journal of Cultural Heritage,* Vol. 4, No. 2, pp. 109-115.

Uchikawa, H. (1989), "Similarities and discrepancies of hardened cement paste, mortar and concrete for concrete from the standpoint of composition and structure", *Advances in Cement Manufacture and Use*, Engineering Foundation, N. Y., pp.271-294.

Wellman, H. W., and Wilson, A. T., (1965), "Salt weathering, a neglected geological erosive agent in coastal and arid environments", *Nature*, Vol. 205, pp.1097-1098.

Young, F. J., Sidney, M., Robert, G., and Arnon, B., (2006), "The science and technology of civil engineering materials", *Chinese Architecture and Building Press*. 384p.

CHAPTER SEVEN

CONCLUSIONS AND RECOMMENDATIONS

7.1   Summary and Conclusions

Since the last century, several studies and investigations have focused on the performance of concrete under chemical sulphate attack. This has led to establishing specifications and standards that mainly address the behaviour of concrete when exposed to chemical sulphate attack. However, the durability of concrete exposed to physical sulphate attack has been generally ignored and confused, in some occasions, with chemical sulphate attack.

Chapter 2 of the current thesis showed that the lack of information regarding the deterioration of concrete due to physical sulphate attack has led to confusion and contradictory views. In addition, previous studies have recommended further research to understand the real distress mechanisms associated with physical sulphate attack and how it is affected by the w/cm, mineral additions, and other mixture parameters of concrete, especially under field conditions.

Chapters 3 and 4 showed that concrete partially immersed in a sodium sulphate solution can experience dual sulphate attack. The lower portion immersed in the sodium sulphate solution can suffer from chemical sulphate attack, while the upper portion can be vulnerable to physical sulphate attack. In addition, relatively high damage due to physical sulphate attack did not affect both the concrete compressive strength and modulus of elasticity since the damage was limited to the external surface of the concrete specimens. The damage was mainly controlled by the pore structure of the concrete surface. It was found that lowering the w/b ratio and better curing the concrete reduced the surface scaling above the solution level since the volume of the pores was decreased. Although, partially replacing portland cement with pozzolanic minerals also led to decreased porosity, surface scaling in concrete

incorporating pozzolanic minerals was increased due to the increase in the volume of pores having a very small diameter.

In Chapter 5, the effectiveness of different commercially available surface treatment materials in mitigating physical sulphate attack on concrete was investigated. It was found that using epoxy or silane based surface treatment materials provided adequate protection for both cured and non-cured concrete exposed to physical sulphate attack. Epoxy coating provides a thick membrane on the concrete surface that mitigates capillary suction and prevents salt crystals from precipitating in the subefflorescence zone where they can exert pressure within the concrete pores, thus reducing damage. Conversely, silane coating penetrates the concrete surface and chemically reacts within the concrete pores, providing molecules that perform as a water repellent, which reduces capillary suction and salt crystallization.

Using bitumen based coating provided protection for the cured concrete specimens. However, in the case of non-cured concrete specimens with high w/c, the bitumen layer separated from the concrete surface since water molecules were entrapped between the bitumen coating layer and the substrate, leading to emulsification of the bitumen and its separation. Moreover, using a water-based acrylic coating did not provide protection to both the cured and non-cured concrete specimens exposed to physical sulphate attack since the acrylic solution partially filled the concrete surface pores, allowing salt crystals to grow and damage the acrylic film. In addition, acrylic is a relatively brittle material, which compromises its ability to withstand strains generated by salt crystallization.

Previous studies have shown that increasing the level of cement replacement by pozzolanic minerals can improve the overall concrete performance when exposed to harsh environments. However, chapter six showed that under physical sulphate attack, increasing the dosage of pozzolanic minerals can intensify the damage of concrete under physical sulphate attack due to the refinement of the concrete pore structure. Thus, higher capillary rise and salt crystallization can occur on the concrete surface leading to greater damage.

7.2   Recommendations for Future Work

1- The current thesis showed that the damage of the concrete surface due to physical sulphate attack is a result of capillary rise and salt crystallization, which applies tensile pressures, thus disrupting the concrete pores and leading to damage. It is believed that using steel or carbon fibres may improve the performance of concrete under physical sulphate attack since fibers increase the tensile strength of concrete. Therefore, the effect of fiber reinforcement of concrete should be explored.

2- It is recommended for future study to investigate the effect of using air entrainment in concrete exposed to physical sulphate attack since previous studies have shown that it is beneficial when used in concrete exposed to freezing and thawing conditions.

3- It is believed that laboratory studies on physical sulphate attack may not fully replicate in-situ behaviours and capture the actual performance of various concrete mixtures under different temperature and relative humidity scenarios. Therefore, it is recommended to validate the results of this study in actual field exposure, particularly with regards to the effects of various surface treatment materials.

APPENDIX A

Table A.1 : MIP for concrete made with OPC, w/b = 0.60 non-cured specimen

Pore size Diameter (µm)	Cumulative Intrusion (mL/g)
10.68962656	0.001641069
8.5482875	0.00184754
8.127660156	0.00235651
5.122174609	0.002674321
4.558923047	0.002976581
3.759320313	0.004478132
3.00187793	0.00625155
2.439073047	0.007708288
1.904393359	0.009677779
1.555443164	0.010131542
1.238558594	0.009608595
0.987314258	0.009741948
0.799874316	0.010730909
0.653170166	0.012120355
0.511439209	0.016663613
0.411512012	0.029229445
0.33495249	0.054995898
0.267418921	0.090622787
0.216033008	0.072033927
0.178204993	0.066675864
0.142486438	0.058773965
0.112441699	0.051391393
0.090922711	0.044718858
0.073667346	0.039750367
0.05935365	0.034933951
0.04755047	0.029048335
0.038201419	0.024494478
0.030993152	0.022124218
0.024871104	0.018220557
0.020159554	0.015850034
0.016188129	0.01465017
0.014435521	0.013012164
0.013030496	0.010179879
0.010681042	0.009094027

Table A.2 : MIP for concrete made with 25% fly Ash, w/b = 0.60 non-cured specimen

Pore size Diameter (µm)	Cumulative Intrusion (mL/g)
10.68962656	0.00181025
8.5482875	0.00125426
8.127660156	0.00193468
5.122174609	0.00128487
4.558923047	0.00134407
3.759320313	0.00158424
3.00187793	0.002441147
2.439073047	0.002400236
1.904393359	0.001894118
1.555443164	0.001799629
1.238558594	0.001663517
0.987314258	0.001929845
0.799874316	0.002399094
0.653170166	0.002673026
0.511439209	0.004155803
0.411512012	0.00801967
0.33495249	0.013307532
0.267418921	0.01793614
0.216033008	0.019428909
0.178204993	0.022554897
0.142486438	0.036276177
0.112441699	0.071235843
0.090922711	0.092067221
0.073667346	0.059727982
0.05935365	0.054845877
0.04755047	0.05517073
0.038201419	0.055633962
0.030993152	0.055086631
0.024871104	0.04892052
0.020159554	0.040186539
0.016188129	0.030749338
0.014435521	0.026129704
0.013030496	0.022271624
0.010681042	0.016812073

Table A.3: MIP for concrete made with 8% silica fume, w/b = 0.60 non-cured specimen

Pore size Diameter (μm)	Cumulative Intrusion (mL/g)
10.68962656	0.001688
8.5482875	0.001599
8.127660156	0.001688
5.122174609	0.001599
4.558923047	0.001611
3.759320313	0.003094
3.00187793	0.004848
2.439073047	0.005009
1.904393359	0.005286
1.555443164	0.004549
1.238558594	0.004357
0.987314258	0.004415
0.799874316	0.004676
0.653170166	0.005218
0.511439209	0.007431
0.411512012	0.007343
0.33495249	0.006931
0.267418921	0.009911
0.216033008	0.014528
0.178204993	0.026675
0.142486438	0.071808
0.112441699	0.074141
0.090922711	0.054453
0.073667346	0.04624
0.05935365	0.045286
0.04755047	0.044982
0.038201419	0.042965
0.030993152	0.040875
0.024871104	0.03641
0.020159554	0.030299
0.016188129	0.025153

Table A.4: MIP for concrete made with 8% metakaolin w/b = 0.60 non-cured specimen

Pore size Diameter (µm)	Cumulative Intrusion (mL/g)
10.68962656	0.001525
8.5482875	0.001437
8.127660156	0.001525
5.122174609	0.001437
4.558923047	0.001508
3.759320313	0.001833
3.00187793	0.002202
2.439073047	0.003331
1.904393359	0.003817
1.555443164	0.002533
1.238558594	0.002053
0.987314258	0.002399
0.799874316	0.002045
0.653170166	0.001397
0.511439209	0.001666
0.411512012	0.002008
0.33495249	0.002134
0.267418921	0.002833
0.216033008	0.005075
0.178204993	0.008419
0.142486438	0.023071
0.112441699	0.071655
0.090922711	0.076789
0.073667346	0.056769
0.05935365	0.042856
0.04755047	0.037024
0.038201419	0.031818
0.030993152	0.022169
0.024871104	0.018283
0.020159554	0.016478
0.016188129	0.012078

Table A.5: MIP for concrete made with HS, w/b = 0.60 non-cured specimen

Pore size Diameter (µm)	Cumulative Intrusion (mL/g)
10.68962656	0.001657
8.5482875	0.001657
8.127660156	0.002787
5.122174609	0.001657
4.558923047	0.002787
3.759320313	0.004926
3.00187793	0.00651
2.439073047	0.008578
1.904393359	0.012981
1.555443164	0.018359
1.238558594	0.019562
0.987314258	0.014646
0.799874316	0.013829
0.653170166	0.017208
0.511439209	0.0264
0.411512012	0.043302
0.33495249	0.084699
0.267418921	0.060203
0.216033008	0.058677
0.178204993	0.054298
0.142486438	0.053398
0.112441699	0.052329
0.090922711	0.048732
0.073667346	0.0437
0.05935365	0.036447
0.04755047	0.032394
0.038201419	0.02772
0.030993152	0.022793
0.024871104	0.020352
0.020159554	0.018982
0.016188129	0.017718

Table A.6 : MIP for concrete made with OPC w/b = 0.60 cured specimen

Pore size Diameter (µm)	Cumulative Intrusion (mL/g)
10.68962656	0.001098
8.5482875	0.001025
8.127660156	0.001178
5.122174609	0.001174
4.558923047	0.001129
3.759320313	0.001325
3.00187793	0.002344
2.439073047	0.003778
1.904393359	0.005541
1.555443164	0.006482
1.238558594	0.008358
0.987314258	0.006687
0.799874316	0.004241
0.653170166	0.00524
0.511439209	0.006154
0.411512012	0.007511
0.33495249	0.011646
0.267418921	0.021808
0.216033008	0.052972
0.178204993	0.066436
0.142486438	0.064734
0.112441699	0.044085
0.090922711	0.03334
0.073667346	0.027041
0.05935365	0.021657
0.04755047	0.017838
0.038201419	0.01383
0.030993152	0.01074
0.024871104	0.008263
0.020159554	0.007505
0.016188129	0.006969

Table A.7: MIP for concrete made with 25% fly Ash w/b = 0.60 cured specimen

Pore size Diameter (µm)	Cumulative Intrusion (mL/g)
10.68962656	0.001058
8.5482875	0.001151
8.127660156	0.001393
5.122174609	0.001066
4.558923047	0.000837
3.759320313	0.000877
3.00187793	0.001315
2.439073047	0.002416
1.904393359	0.003135
1.555443164	0.00328
1.238558594	0.004091
0.987314258	0.005182
0.799874316	0.005913
0.653170166	0.006893
0.511439209	0.007924
0.411512012	0.009886
0.33495249	0.012706
0.267418921	0.014863
0.216033008	0.017219
0.178204993	0.020706
0.142486438	0.026947
0.112441699	0.037225
0.090922711	0.055848
0.073667346	0.0693
0.05935365	0.04581
0.04755047	0.045552
0.038201419	0.038731
0.030993152	0.037416
0.024871104	0.035616
0.020159554	0.030971
0.016188129	0.027546

Table A.8: MIP for concrete made with 8% silica fume, w/b = 0.60 cured specimen

Pore size Diameter (µm)	Cumulative Intrusion (mL/g)
10.68962656	0.000964
8.5482875	0.001172
8.127660156	0.00122
5.122174609	0.001116
4.558923047	0.001871
3.759320313	0.002237
3.00187793	0.00402
2.439073047	0.007705
1.904393359	0.006499
1.555443164	0.004151
1.238558594	0.0048
0.987314258	0.008123
0.799874316	0.011163
0.653170166	0.012005
0.511439209	0.012635
0.411512012	0.0157
0.33495249	0.017069
0.267418921	0.017543
0.216033008	0.021205
0.178204993	0.032276
0.142486438	0.04466
0.112441699	0.055353
0.090922711	0.051865
0.073667346	0.047066
0.05935365	0.035627
0.04755047	0.029715
0.038201419	0.024304
0.030993152	0.020655
0.024871104	0.019372
0.020159554	0.018352
0.016188129	0.016148

Table A.9 : MIP for 8% metakaolin w/b = 0.60 cured specimen

Pore size Diameter (µm)	Cumulative Intrusion (mL/g)
10.68962656	0.003017
8.5482875	0.003694
8.127660156	0.003493
5.122174609	0.00458
4.558923047	0.004467
3.759320313	0.0034
3.00187793	0.00345
2.439073047	0.003445
1.904393359	0.00367
1.555443164	0.00375
1.238558594	0.0034
0.987314258	0.00344
0.799874316	0.01009
0.653170166	0.011722
0.511439209	0.00999
0.411512012	0.008751
0.33495249	0.011906
0.267418921	0.016151
0.216033008	0.019807
0.178204993	0.026537
0.142486438	0.044459
0.112441699	0.055343
0.090922711	0.05756
0.073667346	0.046571
0.05935365	0.04041
0.04755047	0.03603
0.038201419	0.034066
0.030993152	0.03102
0.024871104	0.024716
0.020159554	0.020002
0.016188129	0.01546

Table A.10 : MIP for HS w/b = 0.60 cured specimen

Pore size Diameter (µm)	Cumulative Intrusion (mL/g)
10.68962656	0.002269
8.5482875	0.001345
8.127660156	0.00116
5.122174609	0.001154
4.558923047	0.000748
3.759320313	0.001041
3.00187793	0.001104
2.439073047	0.000775
1.904393359	0.000804
1.555443164	0.000853
1.238558594	0.000853
0.987314258	0.001882
0.799874316	0.002692
0.653170166	0.003181
0.511439209	0.005916
0.411512012	0.007574
0.33495249	0.010333
0.267418921	0.016359
0.216033008	0.042807
0.178204993	0.056
0.142486438	0.052774
0.112441699	0.034677
0.090922711	0.031436
0.073667346	0.028798
0.05935365	0.02217
0.04755047	0.012788
0.038201419	0.009285
0.030993152	0.004767
0.024871104	0.002241
0.020159554	0.006927
0.016188129	0.008428

Table A. 11 : MIP for OPC w/b = 0.45 non-cured specimen

Pore size Diameter (µm)	Cumulative Intrusion (mL/g)
10.68962656	0.0019
8.5482875	0.00205
8.127660156	0.002048006
5.122174609	0.000867889
4.558923047	0.001038434
3.759320313	0.001961501
3.00187793	0.004045492
2.439073047	0.00393797
1.904393359	0.003626897
1.555443164	0.00390071
1.238558594	0.003956364
0.987314258	0.004101209
0.799874316	0.003302854
0.653170166	0.003491011
0.511439209	0.004107641
0.411512012	0.003840031
0.33495249	0.004131624
0.267418921	0.005116111
0.216033008	0.005616861
0.178204993	0.007277626
0.142486438	0.014183062
0.112441699	0.033846319
0.090922711	0.042518302
0.073667346	0.037067465
0.05935365	0.035856787
0.04755047	0.030694595
0.038201419	0.023555538
0.030993152	0.020395411
0.024871104	0.013960091
0.020159554	0.010828318
0.016188129	0.011901265

Table A.12 MIP for 8% fly Ash w/b = 0.45 non-cured specimen

Pore size Diameter (µm)	Cumulative Intrusion (mL/g)
10.68962656	0.000938
8.5482875	0.001017
8.127660156	0.000859
5.122174609	0.000674
4.558923047	0.000728
3.759320313	0.000754
3.00187793	0.000697
2.439073047	0.000954
1.904393359	0.002383
1.555443164	0.0012
1.238558594	0.001839
0.987314258	0.002455
0.799874316	0.002935
0.653170166	0.003282
0.511439209	0.003921
0.411512012	0.004462
0.33495249	0.005147
0.267418921	0.005959
0.216033008	0.006341
0.178204993	0.006063
0.142486438	0.006742
0.112441699	0.008262
0.090922711	0.009001
0.073667346	0.011925
0.05935365	0.017976
0.04755047	0.034306
0.038201419	0.036019
0.030993152	0.043995
0.024871104	0.036906
0.020159554	0.029287
0.016188129	0.024926

Table A.13 MIP for 8% silica fume w/b = 0.45 non-cured specimen

Pore size Diameter (μm)	Cumulative Intrusion (mL/g)
10.68962656	0.000612
8.5482875	0.000553
8.127660156	0.000492
5.122174609	0.000321
4.558923047	0.000409
3.759320313	0.000376
3.00187793	0.001479
2.439073047	0.002728
1.904393359	0.001917
1.555443164	0.001284
1.238558594	0.001649
0.987314258	0.002109
0.799874316	0.003695
0.653170166	0.004755
0.511439209	0.003878
0.411512012	0.003773
0.33495249	0.003607
0.267418921	0.003268
0.216033008	0.003368
0.178204993	0.003322
0.142486438	0.003425
0.112441699	0.004737
0.090922711	0.007632
0.073667346	0.011592
0.05935365	0.018431
0.04755047	0.024964
0.038201419	0.028721
0.030993152	0.035294
0.024871104	0.037582
0.020159554	0.033721
0.016188129	0.026954

Table A.14 MIP for 8% metakaolin w/b = 0.45 non-cured specimen

Pore size Diameter (µm)	Cumulative Intrusion (mL/g)
10.68962656	0.0006573
8.5482875	0.0009793
8.127660156	0.0006501
5.122174609	0.0003823
4.558923047	0.0010575
3.759320313	0.0012551
3.00187793	0.0010266
2.439073047	0.0027099
1.904393359	0.0023832
1.555443164	0.0011996
1.238558594	0.0018386
0.987314258	0.0024552
0.799874316	0.0029345
0.653170166	0.0032823
0.511439209	0.0039214
0.411512012	0.0061422
0.33495249	0.0061601
0.267418921	0.0039214
0.216033008	0.0061422
0.178204993	0.0061601
0.142486438	0.0072532
0.112441699	0.0068584
0.090922711	0.0076918
0.073667346	0.0092479
0.05935365	0.0140215
0.04755047	0.0280213
0.038201419	0.032003
0.030993152	0.0275369
0.024871104	0.0236393
0.020159554	0.0215028
0.016188129	0.0191767

Table A.15 MIP for HS w/b = 0.45 non-cured specimen

Pore size Diameter (µm)	Cumulative Intrusion (mL/g)
10.68962656	0.001132
8.5482875	0.001032
8.127660156	0.000817
5.122174609	0.000619
4.558923047	0.000697
3.759320313	0.001527
3.00187793	0.001994
2.439073047	0.0038
1.904393359	0.005315
1.555443164	0.004576
1.238558594	0.007143
0.987314258	0.008226
0.799874316	0.007281
0.653170166	0.007471
0.511439209	0.008475
0.411512012	0.009035
0.33495249	0.011602
0.267418921	0.016849
0.216033008	0.024755
0.178204993	0.0318
0.142486438	0.038638
0.112441699	0.039603
0.090922711	0.0353
0.073667346	0.028575
0.05935365	0.026095
0.04755047	0.024593
0.038201419	0.023466
0.030993152	0.021507
0.024871104	0.014986
0.020159554	0.011095
0.016188129	0.00879

Table A. 16 MIP for OPC w/b = 0.30 non-cured specimen

Pore size Diameter (µm)	Cumulative Intrusion (mL/g)
10.68962656	0.0010416
8.5482875	0.00063906
8.127660156	0.00047285
5.122174609	0.00033588
4.558923047	0.00041998
3.759320313	0.00044925
3.00187793	0.00098079
2.439073047	0.00129546
1.904393359	0.00098637
1.555443164	0.00078008
1.238558594	0.00094311
0.987314258	0.00113409
0.799874316	0.00164931
0.653170166	0.00103543
0.511439209	0.00073304
0.411512012	0.0012083
0.33495249	0.00116853
0.267418921	0.00167781
0.216033008	0.0017
0.178204993	0.0021
0.142486438	0.004
0.112441699	0.01
0.090922711	0.014
0.073667346	0.019
0.05935365	0.021
0.04755047	0.019
0.038201419	0.014
0.030993152	0.00478012
0.024871104	0.00349819
0.020159554	0.00323645
0.016188129	0.00293803

Table A. 17 MIP for 25% fly Ash w/b = 0.30 non-cured specimen

Pore size Diameter (µm)	Cumulative Intrusion (mL/g)
10.68962656	0.00112
8.5482875	0.000777
8.127660156	0.000618
5.122174609	0.000718
4.558923047	0.000764
3.759320313	0.00067
3.00187793	0.000716
2.439073047	0.000856
1.904393359	0.001148
1.555443164	0.001602
1.238558594	0.002889
0.987314258	0.003346
0.799874316	0.003381
0.653170166	0.003033
0.511439209	0.001822
0.411512012	0.002085
0.33495249	0.002316
0.267418921	0.002077
0.216033008	0.002029
0.178204993	0.002092
0.142486438	0.002436
0.112441699	0.002832
0.090922711	0.003261
0.073667346	0.003732
0.05935365	0.003971
0.04755047	0.003723
0.038201419	0.003658
0.030993152	0.005414
0.024871104	0.014648
0.020159554	0.021781
0.016188129	0.022143

Table A. 18 MIP for 8% silica fume w/b = 0.30 non-cured specimen

Pore size Diameter (µm)	Cumulative Intrusion (mL/g)
10.68962656	0.001157
8.5482875	0.001133
8.127660156	0.001889
5.122174609	0.000421
4.558923047	0.000492
3.759320313	0.000496
3.00187793	0.00048
2.439073047	0.000475
1.904393359	0.000528
1.555443164	0.00086
1.238558594	0.00114
0.987314258	0.001585
0.799874316	0.001844
0.653170166	0.001882
0.511439209	0.001842
0.411512012	0.001518
0.33495249	0.001147
0.267418921	0.000943
0.216033008	0.000909
0.178204993	0.000801
0.142486438	0.000671
0.112441699	0.000893
0.090922711	0.001597
0.073667346	0.002594
0.05935365	0.005091
0.04755047	0.006185
0.038201419	0.006428
0.030993152	0.006897
0.024871104	0.009411
0.020159554	0.012006
0.016188129	0.015773

Table A. 19 MIP for 8% metakaolin w/b = 0.30 non-cured specimen

Pore size Diameter (µm)	Cumulative Intrusion (mL/g)
10.68962656	0.000952
8.5482875	0.000881
8.127660156	0.000743
5.122174609	0.000484
4.558923047	0.00052
3.759320313	0.000546
3.00187793	0.00056
2.439073047	0.000565
1.904393359	0.000628
1.555443164	0.00086
1.238558594	0.00114
0.987314258	0.002587
0.799874316	0.002386
0.653170166	0.001629
0.511439209	0.001748
0.411512012	0.00212
0.33495249	0.003151
0.267418921	0.003483
0.216033008	0.00305
0.178204993	0.002876
0.142486438	0.003189
0.112441699	0.004122
0.090922711	0.006455
0.073667346	0.008526
0.05935365	0.011441
0.04755047	0.012642
0.038201419	0.009753
0.030993152	0.005944
0.024871104	0.007716
0.020159554	0.013559
0.016188129	0.01641

Table A. 20 MIP for HS w/b = 0.30 non-cured specimen

Pore size Diameter (µm)	Cumulative Intrusion (mL/g)
10.68962656	0.000942
8.5482875	0.000865
8.127660156	0.000723
5.122174609	0.000421
4.558923047	0.000492
3.759320313	0.000496
3.00187793	0.00048
2.439073047	0.000475
1.904393359	0.000428
1.555443164	0.00086
1.238558594	0.00114
0.987314258	0.002587
0.799874316	0.002386
0.653170166	0.003539
0.511439209	0.003843
0.411512012	0.004247
0.33495249	0.004442
0.267418921	0.004784
0.216033008	0.00543
0.178204993	0.007019
0.142486438	0.009567
0.112441699	0.012425
0.090922711	0.018
0.073667346	0.021
0.05935365	0.016
0.04755047	0.0114
0.038201419	0.011145
0.030993152	0.007698
0.024871104	0.005266
0.020159554	0.00399
0.016188129	0.002881

Table B.1 : Compressive strength of concrete w/b = 0.60 (28dyas)

	OPC			*Fly Ash*			*Silica-Fume*			*Metakaolin*			*HS*		
Sample number	1	2	3	1	2	3	1	2	3	1	2	3	1	2	3
Compressive strength (Mpa)	40.50	39.30	37.40	32.00	33.80	35.00	51.40	48.30	49.00	45.00	47.40	46.00	38.50	39.30	37.40
Average	39.07			33.60			49.57			46.13			38.40		
Coefficient of variation	0.032			0.037			0.025			0.018			0.021		

Table B.2 : Compressive strength of concrete w/b = 0.60 (90dyas)

	OPC			*Fly Ash*			*Silica-Fume*			*Metakaolin*			*HS*		
Sample Number	1	2	3	1	2	3	1	2	3	1	2	3	1	2	3
Compressive strength (Mpa)	42.40	40.32	40.26	48.21	47.26	49.18	52.40	50.43	51.72	48.11	47.17	46.83	39.38	40.12	38.75
Average	40.99			48.22			51.52			47.37			39.42		
Coefficient of variation	0.023			0.017			0.016			0.017			0.021		

Table B.3 : Compressive strength of concrete w/b = 0.60 (180dyas)

	OPC			*Fly Ash*			*Silica-Fume*			*Metakaolin*			*HS*		
Sample Number	1	2	3	1	2	3	1	2	3	1	2	3	1	2	3
Compressive strength (Mpa)	43.40	41.87	40.56	52.37	52.35	54.89	50.25	52.36	51.57	48.53	47.95	49.92	39.21	41.24	38.43
Average	41.94			53.20			51.33			49.13			39.92		
Coefficient of variation	0.030			0.018			0.016			0.017			0.032		

Table B.4 : Compressive strength of concrete w/b = 0.45 (28dyas)

	OPC			*Fly Ash*			*Silica-Fume*			*Metakaolin*			*HS*		
Sample Number	1	2	3	1	2	3	1	2	3	1	2	3	1	2	3
Compressive strength (Mpa)	55.32	56.21	57.42	47.36	49.32	48.25	69.47	68.94	66.23	63.56	64.45	62.13	52.84	51.94	53.76
Average	56.32			48.31			67.9			63.38			52.85		
Coefficient of variation	0.015			0.017			0.018			0.013			0.016		

Table B.5 : Compressive strength of concrete w/b = 0.45 (90dyas)

	OPC			*Fly Ash*			*Silica-Fume*			*Metakaolin*			*HS*		
Sample Number	1	2	3	1	2	3	1	2	3	1	2	3	1	2	3
Compressive strength (Mpa)	55.43	54.26	56.46	61.46	63.25	62.20	71.14	70.03	72.60	67.14	65.21	66.32	53.86	52.79	54.93
Average	55.38			62.30			70.92			66.22			53.86		
Coefficient of variation	0.015			0.013			0.011			0.012			0.015		

Table B.6 Compressive strength of concrete w/b = 0.45 (180dyas)

	OPC			*Fly Ash*			*Silica-Fume*			*Metakaolin*			*HS*		
Sample Number	1	2	3	1	2	3	1	2	3	1	2	3	1	2	3
Compressive strength (Mpa)	57.88	55.75	56.96	71.4	68.3	69.5	72.4	70.1	69.3	67.43	68.93	66.5	54.34	56.49	55.04
Average	56.86			69.08			71.20			67.40			55.29		
Coefficient of variation	0.015			0.018			0.018			0.012			0.015		

Table B.7 : Compressive strength of concrete w/b = 0.30 (28dyas)

	OPC			*Fly Ash*			*Silica-Fume*			*Metakaolin*			*HS*		
Sample Number	1	2	3	1	2	3	1	2	3	1	2	3	1	2	3
Compressive strength (Mpa)	71.45	73.35	72.67	66.56	68.35	68.13	85.21	84.37	86.25	81.35	83.14	82.37	70.23	71.84	69.89
Average	72.49			67.68			85.28			82.29			70.32		
Coefficient of variation	0.011			0.014			0.010			0.010			0.012		

Table B.8 : Compressive strength of concrete made with w/b = 0.30 (90dyas)

	OPC			*Fly Ash*			*Silica-Fume*			*Metakaolin*			*HS*		
Sample Number	1	2	3	1	2	3	1	2	3	1	2	3	1	2	3
Compressive strength (Mpa)	73.56	74.92	75.82	79.13	78.31	77.15	88.67	87.35	89.00	82.56	83.16	81.62	72.42	71.70	73.43
Average	74.10			78.20			89.01			83.11			72.52		
Coefficient of variation	0.011			0.010			0.009			0.010			0.011		

Table B.9 : Compressive strength of concrete made with w/b = 0.30 (180days)

	OPC			*Fly Ash*			*Silica-Fume*			*Metakaolin*			*HS*		
Sample Number	1	2	3	1	2	3	1	2	3	1	2	3	1	2	3
Compressive strength (Mpa)	74.14	76.12	75.32	89.57	90.24	88.67	87.45	86.43	85.67	84.20	86.14	85.53	76.95	75.32	74.66
Average	75.19			89.49			86.52			85.29			75.64		
Coefficient of variation	0.011			0.009			0.008			0.010			0.011		

CURRICULUM VITAE

Name: Ahmed Ramadan Suleiman

Degrees: BSc (2000-2004)

Post-secondary Education   University of Garyounis, Benghazi-Libya
Western University
MESc (2011-2013)
London, Ontario, Canada

Honours and Awards: Libyan-North American Scholarship (2010)
First Dean's List Honor, University of Garyounis, (2004)

Related Work Experience: Graduate Teaching Assistant, Western University, (2012-2013)
QA-QC Engineer (MAN Enterprise, 2008-2009)
Designer Engineer (Gama Consultant Engineers 2007-2008)
Supervisor and Designer Engineer, (Alemaad 2004-2007)

Publications:

1-Suleiman, A. R., Soliman, A., and Nehdi, M. "Investigation of concrete exposed to dual sulphate attack." submitted to *ACI Materials Journal*.

2-Suleiman, A. R., Soliman, A., and Nehdi, M. "Effect of surface treatment materials on durability of concrete exposed to physical sulfate attack." submitted to *Cement and Concrete Research*.

3-Suleiman, A. R., Soliman, A., and Nehdi, M. "Effect of supplementary cementitious materilas on durability of concrete exposed to physical sulphate attack." To be submitted for peer review.